

Identification of Surrogate Anatomic Identifiers of Disease Progression in Age-Related Macular Degeneration

Ali A. Ali Lamin

UCL-Institute of Ophthalmology

Thesis submitted for the degree of Doctor of Philosophy

Thesis Declaration

I, Ali A. Ali Lamin confirm that the work presented in this thesis is my own. Where information has been derived from other sources, I confirm that this has been indicated in the thesis.

Ali Lamin

Acknowledgments

I would like to express my deepest gratitude to Professor Sobha Sivaprasad who has been my primary supervisor. It was a privilege to be supervised by her academically, learn from her clinically and to be with her team. I want to thank her for understanding my limitations, for her never-ending support, and for encouraging in assisting me with this thesis and the research work underlying it. Also, a special thanks goes to my secondary supervisor Professor Susan Lightman for accepting me as a PhD student allowing me to fulfil this ambition of mine. She has always been there to support me over the past four years.

My sincere appreciation goes to my country **Libya** for the scholarship.

Nothing will be the same without my loving wife Eman who has supported me with help, suggestions and assistance while doing my PhD. This moment is much more precious with my beautiful children Lamar, Abdellha, Jore, Omar and Raghad who have been patient and understood my time away from them.

My deepest gratitude goes to my parents, whom without their nurture; I might not be the person I am today.

I am also grateful and thankful to the cofounders of the Voxeleron LLC, Jonathan Oakley and Daniel Russakoff, for developing the deep learning model we used in this thesis, and for their help and guidance. Also to Adam Dubis who has helped me to contact Voxeleron.

Last but certainly not least, to Omar Mahroo, Zakaria Jarar, Kate Williams and Professor Chris Hammond who have helped with the heritability part of this thesis.

Abstract

Age-related macular degeneration (AMD) is the leading cause of vision loss in patients over 50 in the developed world. The visual impairment is due to either choroidal neovascularisation (wet AMD) or geographic atrophy (GA). Drusen is the hallmark of AMD but the presence of drusen does not inform progression to wet AMD. Although the disease is mostly bilateral, the rate of progression of disease in both eyes may not be simultaneous. If one eye is affected by wet AMD, the risk of progression of the fellow eye to wet AMD increases by 10% every year. However, there are no markers that inform the time of conversion to wet AMD. For this reason, there is an unmet need to identify biomarkers that can fully predict the progression to wet AMD in order to allow early intervention before permanent damage. My thesis aimed to assess whether changes in imaging characteristics can more precisely explain conversion. I studied various cohorts including (a) normal aging eyes (b) eyes with early/ intermediate AMD and (c) fellow eyes of unilateral wet AMD to study the conversion to wet AMD.

Firstly, I evaluated longitudinally volume changes in inner and outer retinal layers of 71 eyes with early/intermediate AMD using optical coherence tomography (OCT). Our results showed that inner and outer retina layer volumes may differentiate AMD eyes from healthy eyes. When comparing those who progressed to wet AMD at year 2 to those who did not, we found that baseline volume of GCIPL may differentiate between the 2 groups.

As it is an inner retinal change, I hypothesized that heritability of the retinal layers may influence the rate of retinal layer changes and that may in turn help understand the changes seen in aging and AMD. I worked with the TWIN Study database, in which OCT was done in eyes of twins of different age groups and OCT data were available on 364 eyes of 184 (92 pair) twins. I evaluated whether heritability was responsible for ageing changes of the retinal layers. I found that total retinal volume and inner retinal layer volumes may be affected by genetic factors.

I also assessed the rate of change in macular drusen load in fellow eyes of 248 patients with unilateral wet AMD using OCT. I found that patients who progressed to wet AMD (n= 69) at year 2 had increased significantly in drusen volume and area in the preceding year compared to those who did not progress (n = 179).

In addition, I explored correlations between prior drusen load and retinal layer volumes of 51 AMD eyes and the subsequent CNV subtype to evaluate whether drusen load and/or retinal layer volumes are responsible for a certain type of CNV. I found that eyes that progressed to occult CNVs at year 2 had increased significantly in drusen volume and area, and decreased in ONL volume in the 2nd year compared to eyes that progressed to classic CNV type. I also investigated, in the same cohort, agreement between CNV type in second eyes developing CNV and the first eye CNV and found that there was high agreement suggesting that these changes in drusen volume and ONL changes may inform type of CNV. However, validation in a larger cohort is required.

To evaluate these results further, I labeled OCT-based biomarkers for deep learning classifier to help predict which layers of the outer retina is most affected preceding the development of CNV. The choroid was found to be most prominent structure affected prior to conversion to CNV.

In conclusion, drusen load increases and retinal layer volumes changes before conversion to wet AMD and automated drusen and retinal layer volumes measurement tools may be used to monitor eyes for conversion to wet AMD. However, further investigations of the choroid is necessary to evaluate the observations made using deep learning techniques.

Impact Statement

This thesis has various impacts.

1. Impact on patients: The ability to predict conversion to wet AMD more precisely is very useful for patients as it reduces their apprehension. At present we advise that there is a 10% chance per year for conversion. So out of 100 patients, only 10 converts and we are unable to predict who among the 100 will convert. My thesis shows that monitoring of drusen volume using automated software will enable us to inform patients to be more vigilant of conversion when volume increases. Although this is more applicable to occult CNV, 80% of CNVs are occult. So, we can provide more accurate information on time to conversion. One may argue that there is no treatment even if a patient is found to have an asymptomatic CNV in the fellow eye. However, there are several novel agents that are being investigated in the form of eye drops and long acting agents that may in the future be useful to avert or prevent progression to symptomatic CNV
2. Impact on design of clinical trials: Current clinical trials in the stage of intermediate drusen take about 5-6 years to complete as the end points are conversion to advanced AMD. This thesis shows that we can shorten these trials by better defining the inclusion criteria. Instead of including all fellow eyes with drusen, including only those with increasing drusen volume will increase the event rates at a shorter time.
3. Clinical utility: Our approach was purely based on computational analysis of diagnostic retinal images such as optical coherence tomography (OCT), which allows fully automated, reliable, and fast detection of a wide range of several

features from the neurosensory layer, retinal pigment epithelium (RPE) to the choroid. Therefore, these findings can be easily used in clinics.

4. New research areas: my thesis adds valuable information to AMD literature. Firstly, the OCT finding of inner layer volumes thinning in early AMD stages suggests pathological process affecting particularly ganglion cell-inner plexiform layer and inner nuclear layer very early in the AMD disease process. I also show that heritability may account for these changes. Therefore, researchers can now focus their attention on complement genotype changes on inner retina. Secondly, outer nuclear layer thinning at early AMD stage may occur mainly in eyes that convert to CNV type. This concept better explains why dark adaptation is affected early in AMD. Further structure-function studies should be directed to this field. Thirdly, the deep learning predictive model shows that the predictive hallmark for CNV conversion is at the sub-RPE choroidal region in eyes that progressed to wet AMD. Although imaging of the choroid remains challenging, this thesis directs the focus of future research to the choroid.
5. Although most of my studies in this thesis are exploratory, the findings have thrown light to novel areas of investigations to better phenotype this heterogeneous disease

Table of Contents

1	Chapter 1: Introduction	22
1.1	Age-related macular degeneration (AMD).....	22
1.2	Risk factors for AMD	24
1.2.1	Sociodemographic factors	24
1.2.2	Systemic factors	27
1.2.3	Genetic factors	28
1.2.4	Environmental factors.....	30
1.3	AMD classification.....	32
1.4	Ageing versus AMD	35
1.4.1	Drusen formation	36
1.4.2	Bruch's membrane thickening	37
1.4.3	Cell loss.....	38
1.4.4	Intracellular debris	40
1.4.5	Para-inflammation and Immunity	41
1.4.6	Epigenetics	42
1.5	Optical coherence tomography (OCT)	43
1.5.1	The development of OCT in ophthalmology	43
1.5.2	Comparison between TD-OCT, SD-OCT and SS-OCT	45
1.5.3	OCT image interpretation	46
1.5.4	Automated image analysis.....	49

1.5.5	Retinal segmentation	49
1.5.6	Topcon 3D OCT	51
1.5.7	OCT in AMD	53
1.6	Changes in retinal layers with age, gender, ethnicity and axial length	56
1.6.1	Introduction.....	56
1.6.2	Age impact on macular layer thicknesses and volumes	58
1.6.3	Gender impact on macular layer thicknesses and volumes.....	61
1.6.4	Ethnicity impact on macular layer thicknesses and volumes	62
1.6.5	Axial length impact on macular layer thicknesses and volumes	62
1.7	Heritability of retina and AMD.....	63
1.7.1	Definitions.....	63
1.7.2	Estimations	64
1.7.3	Heritability studies of retina.....	65
1.7.4	Heritability of AMD.....	69
1.8	Drusen quantification	70
1.8.1	Introduction.....	70
1.8.2	Drusen quantification using colour fundus photography	71
1.8.3	Drusen quantification using OCT	72
1.8.4	Comparing drusen quantification by OCT with colour fundus photography.....	74
1.8.5	Recent clinical studies based on OCT drusen quantification	75
1.9	Overall hypothesis of this thesis.....	77

1.10	Aims and objectives of this thesis	77
2	Chapter 2: Methodology	78
2.1	General methods.....	78
2.1.1	Study population.....	78
2.1.2	Data collection	78
2.1.3	Inclusion criteria.....	79
2.1.4	Exclusion criteria	79
2.1.5	Ethical approval	79
2.2	Retinal imaging, drusen measurements and retinal layer segmentation	80
2.3	Statistical Analysis	81
3	Chapter 3: Changes in volume of various retinal layers over time in early and intermediate AMD.....	83
3.1	Introduction	83
3.2	Aims	84
3.3	Methods	85
3.4	Results	85
3.4.1	Demographics of Participants.....	85
3.4.2	AMD versus Control	87
3.4.3	Progressors versus Non- Progressors.....	92
3.5	Discussion.....	95
4	Chapter 4: Retinal layer volumes: age associations and heritability (Twin Study)	

4.1	Introduction	101
4.2	Aims	102
4.3	Methods	102
4.3.1	Participants.....	102
4.3.2	Calculating correlations	103
4.3.3	Calculating heritability.....	103
4.4	Results	104
4.4.1	Mean values and correlations with age.....	104
4.4.2	Inter-eye correlations	105
4.4.3	Correlations in MZ and DZ twins and estimates of heritability	108
4.5	Discussion.....	112
5	Chapter 5: Changes in number, area and volume of drusen in fellow eye of patients with neovascular AMD	115
5.1	Introduction	115
5.2	Aims	117
5.3	Methods	118
5.4	Results	118
5.4.1	Patients.....	118
5.4.2	Baseline drusen count, area and volume measurements	119
5.4.3	Prediction of progression to CNV based on baseline drusen measurements	120

5.4.4	Change in drusen measurements over two time points (year 1 and year 2)	121
5.5	Discussion	124
6	Chapter 6: Predictor of CNV type based on drusen load and retinal layer volumes	128
6.1	Introduction	128
6.2	Aims	130
6.3	Methods	130
6.4	Results	131
6.4.1	Demographic features of participants	131
6.4.2	Drusen load in occult and classic CNV	133
6.4.3	Retinal layer volumes in occult and classic CNV	133
6.4.4	Correlation in CNV type between the two eyes	137
6.5	Discussion	137
7	Chapter 7: Deep learning for prediction of AMD progression	142
7.1	Introduction	142
7.2	Aims	145
7.3	Methods	145
7.3.1	Traditional image processing	145
7.3.2	Deep Learning-based Analysis	149
7.3.3	Feature analysis	154
7.4	Results	154

7.4.1	Traditional image processing.....	154
7.4.2	Deep Learning.....	155
7.5	Discussion.....	159
8	Chapter 8: Summary, conclusion and future directions	163
8.1	Changes in volume of various retinal layers over time in early and intermediate AMD	163
8.2	Retinal layers volumes: age association and heritability	167
8.3	Changes in numbers, area and volume of drusen in fellow eye of patients with neovascular AMD	168
8.4	Predictor of CNV type based on drusen load and retinal layer volumes ...	170
8.5	Deep learning for prediction of AMD progression.....	172
8.6	Conclusion	173
8.7	Future directions	174
9	References from websites	176
10	References.....	177

List of Figures

Figure 1. Timeline showing the development of OCT in ophthalmology. (Ref. (Bhende et al., 2018))	45
Figure 2. SD-OCT image of a normal right eye. Adapted from Optical Coherence Tomography Scans Website, (http://www.octscans.com).	47
Figure 3. An illustration of hyper-reflective and hypo-reflective bands at the outer retina. (Adapted from (Cuenca et al., 2018)).....	48
Figure 4. A screenshot of display options of the Orion segmentation software.	50
Figure 5. Retinal layer segmentation with detectable layer boundaries in a normal healthy eye as analysed automatically by the Orion software. Layers 1-2 = Retinal Nerve Fiber Layer (RNFL); Layers 2-3 = Ganglion Cell Ganglion Cell and Inner Plexiform Layer (GCIPL); Layers 3-4 = Inner Nuclear Layer (INL); Layers 4-5 = Outer Plexiform Layer (OPL); Layers 5-6 = Outer Nuclear Layer (ONL); Layers 6-7 = Photoreceptor complex (PR); Layers 7-8 = Retinal Pigment Epithelium-Bruch’s Membrane complex (RPE-BM); Layers 1-8 = Total Retinal Layers.	51
Figure 6. Topcon OCT scan of right eye with AMD showing drusen count, area and volume as illustrated on the top right.	52
Figure 7. Illustrative images depicting the 9 ETDRS subfields. A, Macular image showing 1 mm, 3 mm and 6 mm circular areas. B, Macular image showing fovea, inner macula and outer macula.	58
Figure 8. Illustrative images depicting the age-associated changes in macular layer thicknesses. Light yellow colour represents thickness increase and dark orange represents thickness decrease. Ageing results in an overall thickening of the fovea (CFT) and a thinning of the inner and outer macula. (Adapted from ref. ((Subhi et al., 2016)).....	61
Figure 9. Retinal layer segmentation with detectable layer boundaries in a normal eye as analysed automatically by the Orion software. Layers 1-2 = Retinal Nerve Fiber Layer (RNFL); Layers 2-3 = Ganglion Cell Ganglion Cell and Inner Plexiform Layer (GCIPL); Layers 3-4 = Inner Nuclear Layer (INL); Layers 4-5 = Outer Plexiform Layer (OPL); Layers 5-6 = Outer Nuclear Layer (ONL); Layers 6-7 = Photoreceptor complex (PR); Layers 7-8 = Retinal Pigment Epithelium-Bruch’s Membrane complex (RPE-BM); Layers 1-8 = Total Retinal Layers	81
Figure 10. Flow chart of the study participants of Chapter 3	86
Figure 11. Box plots showing longitudinal volume change of AMD and control eyes in total retinal volume (TRV), Retinal Nerve Fiber Layer (RNFL), Ganglion Cell Ganglion Cell and Inner Plexiform Layer (GCIPL), Inner	

<i>Nuclear Layer (INL), Outer Plexiform Layer (OPL), Outer Nuclear Layer (ONL), Photoreceptors (PR), and Retinal Pigment Epithelium-Bruch's Membrane complex (RPE-BM). AMD = age-related macular degeneration.</i>	<i>91</i>
<i>Figure 12. Flow chart of the study participants of Chapter 4.</i>	<i>103</i>
<i>Figure 13. Selected layer volumes plotted as function of age. Points average both twins from each pair. Dashed lines show linear fits. A, GCIPL volume in 3 mm diameter central circle. Linear fit declines by 0.022 mm³ per decade. B, GCIPL volume in 6 mm diameter circle. Linear fit declines by 0.067 mm³ per decade. C, PR volume in 6 mm diameter circle. Linear fit increases by 0.033 mm³ per decade.....</i>	<i>107</i>
<i>Figure 14. Selected layer volumes plotted for twin pairs (twin 2 is plotted against twin 1). Left-hand panels are for monozygotic pairs; right-hand panels show dizygotic pairs. A and B, points plot total retinal volume for the 6 mm diameter circle. C and D, Ganglion cell-inner plexiform layer volume for the 6 mm diameter circle.</i>	<i>109</i>
<i>Figure 15. Coefficients for intra-pair correlation for monozygotic and dizygotic pairs for segmented layer volumes. For RPE, Spearman coefficients are plotted as these volumes deviated from a normal distribution; Pearson coefficients are plotted for all other layers.</i>	<i>111</i>
<i>Figure 16. Flow chart for study participant selection. Retrospective analysis of 1671 patients yielded 248 patients who were included in this trial.....</i>	<i>119</i>
<i>Figure 17. Change in drusen volume from baseline to 2 years. Shown here are the foveal scans for the subjects with the greatest and least change from baseline to year 2 for each cohort. The yellow is what the Topcon OCT designated as drusen volume for the scan. Note that least change could also be a decrease in volume (top set).</i>	<i>122</i>
<i>Figure 18. Mean volume and change from baseline to year 2 in those with and without CNV. (A) Shows the mean drusen volume, error bars or SEM. (B) shows the distributions of drusen volumes. While on average that with CNV had more drusen volume this was not absolute with the ranges overlapping nearly entirely. (C) On average those who went on to develop CNV had a greater increase in drusen volume, however again there was considerable overlap with those who did not.</i>	<i>123</i>
<i>Figure 19. Flow chart of the present study of Chapter 6.</i>	<i>132</i>
<i>Figure 20. The left-hand side shows segmentations in both the progressor (top, bottom) and non-progressor (middle) groups. The right hand side shows their corresponding total retinal thickness maps in microns.</i>	<i>146</i>
<i>Figure 21. The left-hand side shows segmentations in both the progressor (top, bottom) and non-progressor (middle) groups. The right hand side shows their corresponding drusen thickness maps in microns.</i>	<i>147</i>

Figure 22. The above compares the performance of the SVM classifier (left) with the same data + instrument type added as a feature (right). This information appears to offer very little improvement in the classification. 149

Figure 23. Example B-scan showing the automated segmentation (ILM in red, RPE in blue, and Bruch’s membrane in magenta) used for the pre-processing. In this example, we clearly see signal in the choroid, albeit diminished below the drusen. 150

Figure 24 . An example of the preprocessing used to normalize the B-scans. The top row shows B-scans from a Topcon OCT scanner and the bottom row shows the corresponding images with normalization applied. The data is cropped between the ILM (red) and a fixed offset (390 μm) from Bruch’s membrane (magenta-solid), which is itself estimated as a baseline (magenta-dashed) to the retinal pigment epithelium (RPE) (blue). Normalization in this way greatly reduces the variance in the training set and allows for robust training of smaller data sets as well as better generalizability. Note that, despite this being an SD-OCT device, the signal in the choroid is apparent and strong in each case. 150

Figure 25. A schematic of the architecture of AMDnet. 153

Figure 26. A detailed breakdown of AMDnet. 153

Figure 27. An analysis of the SVM results for a specific operating point (FP rate = 0.25). The follow-up interval does not seem to have a marked effect on the results. 155

Figure 28. Per-B-scan (left) and per-patient (right) ROC and AUC results for the fine-tuned VGG16 CNN using segmentation-based preprocessing (blue) and just simple resizing (red). As expected, preprocessing to reduce the variance of the input data dramatically improves the results. 156

Figure 29 . Per-B-scan (left) and per-patient (right) ROC and AUC results for AMDnet (green) and VGG16 with preprocessing (blue). The simplified AMDnet architecture shows improvements across both sets. 157

Figure 30 . Occlusion sensitivity analysis for progressors (right) and non-progressors (middle). These images were derived by averaging the occlusion analysis outputs for all B-scans in their respective groups. The average structure for all B-scans is shown on the left and the mean location of Bruch’s membrane in all scans is plotted in magenta. This analysis shows that, in particular, pixels around the RPE have the largest impact on the final score of the classifier for non-progressors. It also suggests more sub-RPE or choroidal involvement for progressors. 158

Figure 31 . En face visualization of occlusion sensitivity analysis. The results from each B-scan's occlusion analyses were stacked into a volume and all of these volumes were averaged. An en face image of the average volume is displayed for non-progressors (left) and progressors (right). The non-progressors seems to have more relevant features in the nasal side of the volumes while the progressors show the opposite effect..... 158

List of Tables

<i>Table 1. AMD Clinical Classification (adapted from (Ferris et al., 2013))</i>	34
<i>Table 2. Summary of different AMD classification systems</i>	35
<i>Table 3. Table 1. Comparison between the three commercially available OCT technologies. (Adapted from (Gabriele et al., 2011, Bhende et al., 2018))</i>	46
<i>Table 4. Macular Mean Thickness and Standard Deviation (SD) by grid ETDRS from the normative database. (Topconmedical website, [3])</i>	53
<i>Table 5. Demographics of the Study Participants</i>	87
<i>Table 6. Mean Retinal Layer Volumes at Baseline and Year 2 in Age-Related Macular Degeneration Eyes (n = 71) and Control Eyes (n = 31)</i>	88
<i>Table 7. Longitudinal Change in Retinal Layer Volumes in Age-Related Macular Degeneration Eyes (n = 71) and Control Eyes (n = 31)</i>	90
<i>Table 8. Mean Retinal Layer Volumes at Baseline and Year 2 in Non-Progressors (n = 40) and Progressors (n = 31)</i>	93
<i>Table 9. Longitudinal Change in Retinal Layer Volumes in Non-Progressors (n = 40) and Progressors (n = 31)</i> ... 94	
<i>Table 10. Assessing predictors for AMD progression using logistic regression analysis</i>	95
<i>Table 11. Segmented layer volumes, correlations with age, and correlations between eyes. Mean (SD) values are given for the whole cohort (n=184). Correlations with age are given (with parameters from both twins averaged within each twin pair). Inter-eye correlations are given for the cohort.</i>	106
<i>Table 12. MZ and DZ coefficients of intra-pair correlation for segmented layer volumes, and age-adjusted estimates of heritability.</i>	110
<i>Table 13. Comparing baseline drusen count, area and volume between eyes that developed CNV and eyes that did not develop.</i>	120
<i>Table 14. Assessing predictors for CNV progression using logistic regression analysis</i>	120
<i>Table 15. Comparing the change in drusen count, area and volume between the two groups in the first and second year</i>	121
<i>Table 16. Drusen parameters in AMD eyes prior to convert to either occult (N=29) or classic (N=20) CNV.</i>	133

Table 17. Mean retinal layer volumes at 3 mm and 6 mm in AMD eyes prior to convert to either occult (N=10) or classic (N=7) CNV. 134

Table 18. Longitudinal Change in Retinal Layer volumes at 3 mm and 6 mm in AMD eyes prior to convert to either occult (N=10) or classic (N=7) CNV. 136

Table 19. CNV types in patients with bilateral CNV..... 137

Table 20. The 32 features used to train the SVM classifier. The thicknesses were taken as averages with the fovea-centered ETDRS grid, where: IA=inner annulus (circle of 3mm diameter, less the central 1mm subfield), OA=outer annulus (circle of 6mm diameter, less the central 1mm subfield and the IA), TA= IA+OA, D=entire 6mm diameter circle. The layer names follow the APOSTEL recommendations(Cruz-Herranz et al., 2016), and are: retinal nerve fiber layer (RNFL), ganglion-cell + inner plexiform layer (GC-IPL), inner nuclear layer (INL), outer plexiform layer (OPL), outer nuclear layer (ONL), photo receptor complex (PR), as well as RPE to Bruch’s and the total retinal thickness (TRT). Foveal thicknesses of the RNFL and GCIPL were excluded. 148

List of Abbreviations

AGE	Advanced Glycation End product
AMD	Age-related Macular Degeneration
AREDS	Age-Related Eye Disease Study Group
BM	Bruch's Membrane
CNN	Convolutional Neural Network
CNV	Choroidal neovascularization
DZ	Dizygotic
ETDRS	Early Treatment Diabetic Retinopathy Study
FA	Fluorescein Angiography
MZ	Monozygotic
GA	Geographic Atrophy
GCIPL	Ganglion Cell and Inner Plexiform Layer
INL	Inner Nuclear Layer
OCT	Optical Coherence Tomography
ONL	Outer Nuclear Layer
PR	Photoreceptor complex
RCT	Randomised Controlled Trials
RNFL	Retinal Nerve Fiber Layer
RPE	Retinal Pigment Epithelium
RPE-BM	Retinal Pigment Epithelium- Bruch's Membrane
SD	Spectral Domain
TRV	Total Retinal Volume
VEGF	Vascular Endothelial Growth Factor

List of Publications and Presentations

Publications arising during the period of the study:

1. Changes in volume of various retinal layers over time in early and intermediate age-related macular degeneration. [Eye \(Lond\)](#). 2019 Mar;33(3):428-434.
2. Changes in macular drusen parameters preceding the development of neovascular age-related macular degeneration. [Eye \(Lond\)](#). 2019 Jun;33(6):910-916.
3. Deep Learning for Prediction of AMD Progression: A Pilot Study. [Invest Ophthalmol Vis Sci](#). 2019 Feb 1;60(2):712-722.
4. Segmented macular layer volumes from spectral domain optical coherence tomography in 184 adult twins: associations with age and heritability. Submitted for publication in Invest Ophthalmol Vis Sci.
5. Predictor of CNV type based on drusen load and retinal layer volumes. Submitted for publication in ophthalmic research.

Conference presentations:

1. Changes in the count, area, volume of drusen in the fellow eye in patients with neovascular AMD. [SOE 2017 \(Barcelona\)](#).
2. Relevance and Validation of Optical Coherence Tomography based on Volumetric Measures in Age-Related Macular Degeneration. [ARVO 2018 \(Hawaii\)](#).
3. Exploration of relative genetic and environmental contributions to variance in macular retinal layer thicknesses as measured by spectral domain optical coherence tomography in a twin study. [EURETINA 2018 \(Vienna\)](#).

1 Chapter 1: Introduction

1.1 Age-related macular degeneration (AMD)

Age-related macular degeneration (AMD) is the leading cause of central vision loss in people over 50 years in the developed world. The prevalence data predict more people will suffer from AMD in the future owing to longevity (Friedman et al., 2004). AMD is asymptomatic in its early course and the appearance of drusen is the clinical hallmark of the disease (Seddon et al., 2006, Abdelsalam et al., 1999). Drusen are whitish-yellow deposits lie beneath the retinal pigment epithelium (RPE) and within Bruch's membrane, which are different in size, shape and configuration (van der Schaft et al., 1992b, Green and Enger, 1993b). There are different types of drusen and some of them are known to be associated with increase the risk for developing advanced AMD such as the large soft confluent one (Ferris et al., 2005, Pauleikhoff et al., 1990a).

AMD has been subdivided into two major types: wet (neovascular or exudative AMD) and dry (non-neovascular or nonexudative AMD). Approximately 80% of vision loss in AMD patients is due to the wet type (Hyman and Neborsky, 2002). While visual loss in wet AMD develops secondary to choroidal neovascularization (CNV), visual loss in dry AMD develops as the result of geographic atrophy affecting the macular area (Bressler et al., 1988a, Green and Enger, 1993b). When one eye is affected by wet AMD, the risk of progression of the fellow eye to wet AMD increases by 10% every year. However, some second eyes progress faster than others (1997, Solomon et al., 2007).

There are several investigational agents that are being explored to delay or prevent progression to symptomatic wet AMD. Early detection and therapeutic intervention of wet AMD have demonstrated to improve visual acuity outcomes. It is vital to identify disease progression at the earliest stage (Wong et al., 2007). Eyes with drusen of 125µm termed intermediate AMD are at risk of conversion to wet AMD (de Sistiernes et al., 2014). However, not every person with soft confluent drusen converts to wet AMD. Similarly not every patient with CNV have soft confluent drusen. Therefore, refining the characteristics of drusen further may help to understand the phenotype that better predict conversion to AMD.

Advances in optical coherence tomography (OCT) technology has allowed for unprecedented in vivo studies of the retina. Spectral domain (SD)-OCT has shown a reliability of 99% in detecting drusen in AMD eyes (Leuschen et al., 2013). Using SD-OCT, it has been shown that 48% of AMD eyes revealed a dynamic increase in drusen volume over time (Yehoshua et al., 2011). Furthermore, drusen area and volume were found to be associated with the development of advanced AMD (both forms: wet and geographic atrophy) (Nathoo et al., 2014).

More recently, analysis of medical images such colour fundus photographs and OCT using algorithms and artificial intelligence has emerged with the ability not only to reliably and automatically rank all relevant features and to recognize associations between markers, but also to provide distinct indicators of the future disease progression (De Fauw et al., 2016). By applying this kind of morphologic imaging biomarkers technology on AMD patients' images, we might be able to better predict the risk of disease progression from early and intermediate stages to advanced stages.

1.2 Risk factors for AMD

It is estimated that there will be more than seventy thousand new cases of AMD per year in the UK (Owen et al., 2012). Elucidating factors that play a role in developing AMD will help in preventing either early developing of the disease and/or progression to late stage AMD. Many studies have searched for factors that could be associated with AMD. A number of factors have been identified and these can be classified into the following groups: 1) sociodemographic factors including age, gender, ethnicity and iris colour; 2) systemic factors such as blood pressure and hypertension, blood lipids and hypercholesterolemia; 3) genetic factors; 4) environmental factors such as nutrition, smoking and sun exposure.

1.2.1 Sociodemographic factors

1.2.1.1 Age

Age is one of the established risk factors associated with AMD. The prevalence and progression of all AMD types increase dramatically with advancing age (Klein et al., 1992, Klein et al., 1997b, Klein et al., 2010, Mitchell et al., 1995). In the Beaver Dam Offspring Study, the prevalence of early AMD was reported to increase from 2.4% in the age group 21-34 years to 9.8% in the age group over 65 years (Klein et al., 2010). In the Blue Mountains Eye Study, the prevalence of late AMD was reported to rise from 0% for those aged 55 years or younger to 18.5% for those aged 85 years or older (Mitchell et al., 1995). Thus, it is clear that people over 65 years of age are the highest risk age group among our population.

1.2.1.2 Gender

There was a lack of consistency in the association between gender and AMD in many different studies but commonly the AMD prevalence is higher in females than males. Pooled data from 3 study populations (the Blue Mountains Eye Study, the Rotterdam study and the Beaver Dam Eye Study) revealed that prevalence of early AMD were higher in females than males with odds ratio of 1.15 (1.10-1.21) (Smith et al., 1997). The same pooled data of the 3 study populations did not find any difference in the prevalence of late AMD between males and females (Smith et al., 2001). Interestingly, the Singapore Malay Eye Study revealed that prevalence of early and late AMD among white participants were higher in females than males but early AMD in Asian Malay people was more prevalent in males than in females, and this was explained as more men were smokers than women (Kawasaki et al., 2008). However, gender was not associated with either early or late AMD in other worldwide studies (Krishnaiah et al., 2005, Goldberg et al., 1988, Schachat et al., 1995).

1.2.1.3 Ethnicity/Race

The prevalence of AMD was reported to be more common in whites than blacks (Sommer et al., 1991, Friedman et al., 1999). The Baltimore Eye Survey revealed that more severe forms of AMD such as large drusen and pigmentary abnormalities, and late AMD were more prevalent in whites aged 70 years or older than in blacks in this age; 2.1% compared with 0% (Friedman et al., 1999). Similarly, AMD accounted for 3% of all blindness among whites aged 80 years or older; it was limited only to whites (Sommer et al., 1991).

The multi-ethnic study of atherosclerosis reported the AMD prevalence in 4 racial/ethnic groups (white, Chinese, Hispanic, and black) (Klein et al., 2006). The

study found the disease prevalence for whites, Chinese, Hispanic, and blacks were 5.4%, 4.6%, 4.2% and 2.4%, respectively. Estimated prevalences of late AMD for whites, Chinese, Hispanic, and blacks were 0.6%, 1.0%, 0.2%, and 0.3%, respectively. The highest frequency of neovascular AMD was in Chinese with odds ratio of 4.30 (1.30-14.27) compared with whites (Klein et al., 2006).

1.2.1.4 Eye colour

The relationship between iris colour and AMD has been controversial. A number of studies reported that those with lightly pigmented irides had a higher risk of developing AMD at an earlier age than those with dark irides (Mitchell et al., 1998, Weiter et al., 1985). Therefore, increased ocular pigmentation tends to decrease the risk of developing AMD. This increased pigmentation may function theoretically as protective to the retina from sunlight exposure. However, other large population studies did not find any association between iris colour and AMD (Klein et al., 1998, Vinding, 1990).

1.2.1.5 Refractive error

An association has been found between refractive error and AMD (Pan et al., 2013). In one study, hyperopia was associated with increased risk of early and late AMD, each diopter increase in spherical equivalent was associated with 16% (OR, 1.16; 95% CI, 1.08-1.25) and 18 % (OR, 1.18; 95% CI, 1.10-1.27) increased risk of any (early + late) and early AMD, respectively (Lin et al., 2016). In contrast, myopia was associated with decreased risk of any and early AMD (Lin et al., 2016). Other studies showed a weak association between hyperopia and early AMD and no association with late AMD (Wang et al., 1998, Li et al., 2014).

1.2.2 Systemic factors

1.2.2.1 Blood pressure and hypertension

There exist conflicting data regarding the effect of blood pressure on AMD. A strong association has been found between high blood pressure and AMD (Bhuachalla et al., 2018, Kahn et al., 1977, Sperduto and Hiller, 1986). Prevalence of AMD progressively increased with increasing duration of systemic hypertension. The risk ratio for any AMD for people diagnosed with hypertension 25 years before the eye examination and concurrently with the eye examination were 1.18 (1.01-1.37) and 1.04 (0.96-1.23), respectively, when compared with those without hypertension (Sperduto and Hiller, 1986). This association, however, was not noted in the Andhra Pradesh Eye Disease Study (Krishnaiah et al., 2005), Blue Mountains Eye Study (Smith et al., 1998), the Eye Disease Case-Control Study (1992), or the Atherosclerosis Risk in Communities Study (Klein et al., 1999). The reasons of these conflicting results are not clear.

1.2.2.2 Blood lipids and hypercholesterolemia

A strong association has been noted between high intake of saturated fat and cholesterol, and AMD (Mares-Perlman et al., 1995, 1992). Persons with high serum total cholesterol had increased odds for neovascular AMD by 400%, when compared with those with low serum total cholesterol and after controlling for other factors (1992). A positive relationship has also been found between high HDL and AMD (Klein et al., 1997a). However, the cardiovascular health study found that the total serum cholesterol had a protective effect against AMD; it has been shown to be inversely associated with early AMD (Klein et al., 2003). Alternatively, other studies

find no association between serum lipids and AMD (Smith et al., 1998, Klein et al., 1999).

No relations were found between the use of lipid-lowering agents and developing of AMD (Klein et al., 2001, McGwin et al., 2006). However, it was noted a modest trend for statin users to have an increased risk of AMD and thus its use might increase the risk of developing AMD (McGwin et al., 2006).

1.2.2.3 Blood glucose and diabetes

Several studies have evaluated the relationship between high blood sugars and/or diabetes and developing of AMD. There were no associations found between blood glucose and AMD (Klein et al., 1999). One study suggested that diabetes was found to be associated with developing GA but not with either early or neovascular AMD (Mitchell and Wang, 1999). GA was significantly associated with diabetes with odds ratio of 4.0 (95% CI, 1.6-10.3).

1.2.3 Genetic factors

Several studies have evaluated the importance of genetic factors in developing AMD. Twin concordance and first-degree relative studies were the first to explore a familial component of the disease (Gottfredsdottir et al., 1999, Klaver et al., 1998a). Investigators investigated the concordance of AMD in 50 twin pairs and 47 spouses and found the disease concordance were 90% and 70% for monozygotic twins and their spouse, respectively ($p=0.0279$) (Gottfredsdottir et al., 1999). Visual impairment and fundus appearance were similar in the nine twin pairs that were concordant. The concordance for early AMD in monozygotic twins was 37% compared with 19% in dizygotic twins, suggesting a role for genes (Hammond et al., 2002). The most heritable components were soft large drusen hard drusen. The

prevalence of AMD in first degree relatives was greater than among those first degree relatives without the disease, suggesting a role for a familial component (Seddon et al., 1997).

A number of genes might be related to AMD. Several studies have suggested a relationship between AMD and the encode genes for metallopeptidase inhibitor (Chen et al., 2010), apolipoprotein E (Zarepari et al., 2004) and Toll-like receptor (Zarepari et al., 2005b). One important gene was identified within the regulation of complement activation locus, encoding complement factor H (CFH), and was associated with developing of AMD (Edwards et al., 2005). CFH (Y402H) variant has a risk for AMD 2-3 times for heterozygote carriers and 3-7 times for homozygote carriers (Zarepari et al., 2005a). It important to note, however, that Y402H variant is not a major factor for AMD in some ethnic groups. Grassi et al. 2006, (Grassi et al., 2006) found wide variations in frequencies of the Y402H allele in some different ethnic groups: Hispanics (0.17+/-0.03), Somalis (0.34+/-0.03), Japanese (0.07+/-0.02), Caucasians (0.34+/-0.03), and African-Americans (0.35+/-0.04). A case-control study reported that the (Y402H) variant is associated with an increased risk of developing GA (grade 4) as well as neovascular AMD (grade 5) (Postel et al., 2006). Thus, the importance of CFH in AMD is in part committed by both the particular ethnic population and the AMD exhibited severity in the population.

Another genes were identified on chromosome 10q26 and found to have a highly significant association with AMD (Jakobsdottir et al., 2005). Furthermore, with linkage mapping and multi-candidate gene screening, multiple genetic loci in almost every chromosome have been found to be associated with AMD. Despite of all these discoveries, the pathophysiology of AMD is not well understood. Current evidence

still suggests that the etiology of AMD is multifactorial, requiring multiple genes as well as environmental factors.

1.2.4 Environmental factors

1.2.4.1 Nutrition

Several studies examined the protective effect of antioxidant vitamin and mineral supplements for preventing the disease or delaying the AMD progression. High-dose of vitamins C (500 IU) and E (400 IU), beta carotene (15 mg), and zinc (20 mg) supplements is associated with decreased risk of progression to advanced AMD as shown in the AREDS trial (2001). There were a reduction in severe visual loss by 19% and a reduction in 5-year progression to late AMD by 25% in high risk individuals. AREDS 2 (phase III, randomized clinical trial) was designed to evaluate the efficacy of adding lutein + zeaxanthin, omega-3 long-chain polyunsaturated fatty acids, or both to the AREDS formulation to reduce the risk of developing advanced AMD (2013). No further reduction in the risk of progression to advanced AMD was found. However, lutein + zeaxanthin could be an appropriate carotenoid substitute in the AREDS formulation because beta carotene was associated with increased risk of lung cancer in former smokers (2013).

Two recent systematic review studies showed that multivitamin antioxidant vitamin and mineral supplementations may slow the progression AMD but will not prevent or delay the onset of AMD (Evans and Lawrenson, 2017b, Evans and Lawrenson, 2017a).

1.2.4.2 Smoking

Smoking is the strongest avoidable risk factor that associated with most types of AMD (Klein et al., 1993, Smith et al., 1996, Christen et al., 1996, Seddon et al.,

1996). These studies described the relative odds were range from 1.1 to nearly 5 for those who are current smokers. The odds ratio for early and late AMD were 1.75 and 3.92, respectively, when compared with non-smokers (Smith et al., 1996). It has also been shown that the mean age for current smokers at the time of AMD diagnosis was lower than in those who never smoked (Smith et al., 2001).

A recent longitudinal population-based study has examined the association of current cigarette smoking and pack-years smoked with the incidence of AMD and found the incidence over 20-year period were 24.4% and 4.5% for early and late AMD, respectively (Myers et al., 2014). The number of pack years and current smoking were associated with an increased risk of transitioning from no AMD to minimal early AMD, from minimal to moderate early AMD and from severe early AMD to late (Myers et al., 2014).

Having ever smoked was associated with an increased the risk of late AMD with odds ratio of 1.83 (Smith et al., 1996). In one study, a minimal reduction in risk of AMD was found in persons who stopped smoking for 15 years (Seddon et al., 1996). Generally speaking, quitting smoking benefit is seen after ten years but do return to that of persons who have never smoked until twenty years after quitting smoking (Khan et al., 2006). Moreover, passive smokers had an odds ratio of AMD of 1.87 (95% CI, 1.03-3.40) (Khan et al., 2006).

1.2.4.3 Light exposure

There was an association found between ultraviolet and/or visible light, and retinal damage in an animal experiment (Ham et al., 1982). Luckily, the human cornea and lens absorb short wavelength light below 295 nm and 400 nm, respectively.

Therefore, almost all radiations less than 400 nm are absorbed by lens and this

might explain why there was no association between ultraviolet or visible light and AMD was found (Taylor et al., 1990). In contrast, the beaver dam eye study revealed a positive association between extended sun exposure and AMD and concluded that lifetime exposure was significantly associated with the risk of early AMD with odds ratio of 2.09 (95% CI, 1.19-3.65) (Cruickshanks et al., 2001). Thus, it has been suggested that individuals can reduce this risk by wearing sunglasses and hats to reduce ultraviolet light exposure to their retinas (Tomany et al., 2004).

1.3 AMD classification

A number of AMD classification schemes have been developed, detecting change in AMD status, particularly conversion to late AMD. The purpose of these schemes is to provide a common nomenclature as well as performing natural history trials, evaluating new therapies, improving communication between eye care providers, and counseling patients regarding prognosis. As a result, AMD prevalence and development over time in widely differing geographical locations can be compared between different studies. Most of these classification schemes share many similar features and their grading systems are relied on the presence and severity of the characteristic features of AMD including drusen, pigmentary abnormalities, CNV and GA.

In 1995, based on morphological abnormalities in the macular area on color fundus images, the International ARM Epidemiological Study Group proposed an international classification (IC) and grading system for Age-related Maculopathy (ARM) and AMD. This study defined ARM as a macular degenerative disorder in patients over 50 years, which is characterized by the presence of drusen and pigmentary abnormalities. Pigmentary abnormalities were defined as areas of

increased pigment (hyperpigmentation) associated with drusen and/or areas of depigmentation (hypopigmentation) of the RPE. This can be explained by the accumulation of drusen that results in RPE hyperplasia but later leads to atrophy. Interestingly, visual acuity was not used as criterion to define the presence or absence of any forms of ARM. In this scheme, ARM was classified into two stages, early and late. Early ARM is characterized by the presence of soft drusen ($\geq 63 \mu\text{m}$) and RPE hypo- or hyperpigmentation ($\leq 175 \mu\text{m}$ in diameter). Late ARM is similar to AMD and includes geographic atrophy and neovascular AMD. Geographic atrophy was defined as any sharply delineated area ($\geq 175 \mu\text{m}$ in diameter) of RPE atrophy with visible choroidal vessels. Neovascular AMD is characterized by the presence of RPE detachment associated with subretinal or sub-RPE neovascular membranes, subretinal hemorrhages, scar or hard exudates that not related to other retinal disease (Bird et al., 1995).

In 2001, another classification system was created by the Age-Related Eye Disease Study Group (AREDS), ignoring using the term ARM. They described a system for grading AMD from fundus photographs. They also evaluated the effect of high-dose vitamin and mineral supplements on development of late AMD. In this system, drusen were classified as small ($< 63 \mu\text{m}$), intermediate ($63\text{-}125 \mu\text{m}$), or large ($> 125 \mu\text{m}$), and AMD was classified into four stages based on the size of drusen as well as the presence of CNV and GA. AREDS category 1 (no AMD) was characterised by no or few small drusen, representing the control group. AREDS category 2 was characterised by a combination of multiple small drusen, few intermediate drusen, or mild RPE abnormalities. AREDS category 3 (intermediate AMD) was characterised by at least one large druse, numerous medium drusen, or GA that does not extend to the centre of the macula. AREDS category 4 qualified as advanced AMD that can be

either wet (CNV) or dry (central GA). Interestingly, intake high doses of antioxidants and zinc (80 mg) showed a beneficial effect in reducing patient's relative risk of progression to late AMD by 25 % in patients with late AMD in the fellow eye (The Age-Related Eye Disease Study Research, 2001).

In 2013, Ferris et al (Ferris et al., 2013) proposed a new classification system that combines the scientific literature with expert opinion, attempting to establish consensus regarding nomenclature and classification systems. Using a modified Delphi process, this system developed a 5-stage classification scale for AMD (Table 1). Eyes with no visible drusen or pigmentary abnormalities were considered to have no signs of AMD. Small drusen was termed as drupelets and considered as normal ageing changes with no clinical significant for developing late AMD. While eyes with medium drusen but without pigmentary abnormalities were considered to have early AMD, eyes with large drusen or with pigmentary abnormalities associated with at least medium drusen were considered to have intermediate AMD. Finally, eyes with CNV or GA were considered to have late AMD. Furthermore, 5-year risk of developing late AMD was estimated to increase approximately 100 fold, ranging from 0.5% to 50% in normal ageing changes and intermediate AMD respectively.

Table 1. AMD Clinical Classification (adapted from (Ferris et al., 2013))

Classification of AMD	Definition (lesions assessed within 2 disc diameters of fovea in either eye)
No apparent aging changes	No drusen and No AMD pigmentary abnormalities*
Normal aging changes	Only drupelets (small drusen ≤ 63 μm) and No AMD pigmentary abnormalities*
Early AMD	Medium drusen >63 μm and ≤ 125 μm and No AMD pigmentary abnormalities*
Intermediate AMD	Large drusen > 125 μm and/or Any AMD pigmentary abnormalities*
Late AMD	Neovascular AMD and/or Any geographic atrophy

AMD = age-related macular degeneration.
*AMD pigmentary abnormalities = any definite hyper- or hypopigmentary abnormalities associated with medium or large drusen but not associated with known disease entities.

While the IC system distinguishes only early AMD from the late stage, both AREDS and the clinical classification provide criteria of an intermediate stage. Distinguishing a normal macula from so-called normal aging process and the latter from early AMD is also provided in the clinical classification system, Table 2 summarises the three classifications' stages. These classifications based on colour fundus photographs that evaluated by graders. However, the agreement between those graders examining some parameters such as drusen count, area and size was moderate in the AREDS study. In addition, it is clear that it is a time-consuming process to manual analysis, identifying and counting drusen on photographs. Thus, this make the applicability of the above mentioned classification systems in the clinical setting is restricted.

Table 2. Summary of different AMD classification systems

	No aging changes	Normal aging changes	Early AMD	Intermediate AMD	Late AMD
International classification	-	-	+	-	+
AREDS classification	+ (used as one stage)		+	+	+
Clinical classification	+	+	+	+	+

1.4 Ageing versus AMD

Distinguishing between age-related and pathological changes occurs in retina is very crucial to understand why some people are susceptible to develop AMD while others did not. A few steps further in the ageing process may result in the pathological form that can be viewed as a disease. With ageing, extracellular debris as hard drusen may form in the periphery, Bruch's membrane thickens and cells are lost. In AMD,

most of these changes are aggravated with other factors, like formation of soft drusen, to develop the disease. In this section, physiological, anatomical and immunological changes seen in AMD as well as in the normal retinal ageing will be discussed to differentiate between them.

1.4.1 Drusen formation

Drusen are typically found with age in old people aged over 55 years and can be classified into different types based on their appearance. Hard drusen, which are considered a part of normal ageing as well as AMD, are small ($\leq 63 \mu\text{m}$) yellow dots with sharp borders. Soft drusen, which are considered to be associated with AMD only and not ageing, are large ($\geq 125 \mu\text{m}$) with either sharp or fuzzy borders. While hard drusen were found in both the macula and periphery, soft drusen were found only in the macula (Rudolf et al., 2008).

There is a difference in composition of hard drusen and soft drusen. Also, peripheral hard drusen and macular hard drusen have different chemical composition (Rudolf et al., 2008). The regional difference in drusen composition may contribute to macular susceptibility for developing AMD. Hard drusen do not increase the risk of developing AMD based on the Copenhagen eyes study, 2.9% of participants developed AMD over 14 years of follow-up (Buch et al., 2005). The study also showed that 26.7% of participants with soft drusen had higher progression rate of AMD.

Reticular pseudodrusen are a variant of soft drusen found subretinally and described as subretinal drusenoid deposits (Spaide and Curcio, 2010). Using OCT, they are apparent internal to the RPE (Zweifel et al., 2010b). Several studies have shown that

reticular pseudodrusen are significantly associated with AMD (Zweifel et al., 2010a, Klein et al., 2008).

1.4.2 Bruch's membrane thickening

Bruch's membrane is a sheet of extracellular matrix located between retina and choroid. It consists of five layers as the following: the RPE basement membrane, the inner collagenous layer, the elastic layer, the outer collagenous layer, and the choriocapillaris endothelium basement membrane. Nutrients diffuse across these five layers into retina to sustain its high metabolic activity. Thus, a stable and regular flow of nutrients and waste materials is required in order to maintain retinal health.

A number of age-related changes can affect the structure and function of Bruch's membrane including lipid accumulation, increased thickness, decreased elasticity and decreased diffusional capacity of different size molecules (Pauleikhoff et al., 1990b, Ugarte et al., 2006). The diffusional capacity decreases in the macula more than in the periphery (Hussain et al., 2010). These changes could be related to reduced matrix degradation and turnover of the membrane.

The matrix metalloproteinase (MMP) system of Bruch's membrane is responsible for matrix degradation has been found to be affected in ageing and AMD eyes (Hussain et al., 2011). A reduction in the activity of MMP2 and MMP9 may be responsible for impaired gelatin degradation of Bruch's membrane, resulting in pathology associated with ageing and AMD.

One of the key enzymes that play a role in regulation of Bruch's membrane turnover is TIMP3 protein, which is a matrix metalloproteinase (MMP) inhibitor (Brew and Nagase, 2010). Over expression of the enzyme might prevent Bruch's membrane turnover and contribute to the membrane thickening. TIMP3 is increasingly

expressed in Bruch's membrane of both ageing and AMD eyes (Spraul et al., 1996). There is an association has been found between TIMP3 variant (rs9625132) and AMD development (Chen et al., 2010). It has been suggested that low levels of active MMP2 and 9 with high levels of TIMP3 contribute to diminished capacity for Bruch's membrane turnover, thickening of Bruch's membrane and disease insult (Kamei and Hollyfield, 1999).

Accumulation of lipid in Bruch's membrane has been observed in ageing retina but there are differences between the macular and peripheral regions in their lipid composition (Gulcan et al., 1993). For example, esterified cholesterol was found to be higher in the macular Bruch's membrane than in the peripheral Bruch's membrane (Curcio et al., 2001). This may explain why AMD affects the macular region and not the peripheral region. Accumulation of an oxidized cholesterol derivative known as 7-ketocholesterol has been identified in Bruch's membrane, contributing to AMD development (Rodriguez and Larrayoz, 2010). Introducing of a 7-ketocholesterol inhibitor in rat model was effective at inhibiting the formation of laser induced CNV (Huang et al., 2012).

1.4.3 Cell loss

1.4.3.1 Neural retina

Rod photoreceptors seem to be more affected by ageing than cone photoreceptors (Curcio et al., 1993, Gao and Hollyfield, 1992). In the macular area, the cones density remains nearly constant, whereas the rods density decreases by 30% between the fourth and ninth decades (Curcio et al., 1993). It has also been found that the peripheral photoreceptors and RPE loss rate are equal (Gao and Hollyfield, 1992). An ageing-associated change of gene expression of rods has been found, rod

photoreceptors tend to change in their functional profiles with age (Parapuram et al., 2010). Rods were found to be absent in AMD disciform scars, whereas cones tend to surround these locations, suggesting that rods are preferentially lost in AMD and cones are able to survive after age-related damage (Shelley et al., 2009a, Curcio et al., 1996). The cone survival depends on rods as described in a recent study that showed rods transplant can limit secondary cone loss secreting cone survival factors (Mohand-Said et al., 2001).

Another characteristic of ageing human retina is changes in dendritic fibers of rod and On-cone bipolar cells. Eliasieh et al., (Eliasieh et al., 2007) found that these fibers length and density are most pronounced in the periphery than the macula and in aged than in young retinas. The authors suggested that despite cell death with age, our systems attempt to maintain visual capability by forming new synapses. In the AMD retina, a large number of photoreceptor dendrites retract into the outer nuclear layer across the entire retina (Sullivan et al., 2007). As a consequence, dendritic outgrowth from postsynaptic bipolar cells is evoked results in synaptic contacts between bipolar cells and photoreceptors across the entire retina. These findings suggested that human retinal neurons have the capacity to form new synapses in both ageing and AMD.

1.4.3.2 RPE

In aged retina, equatorial RPE density was significantly lower than foveal RPE density (Gao and Hollyfield, 1992). Equatorial RPE density decreases at rate of 14 cells/mm²/year from the second to the ninth decade of life, whereas foveal RPE density remains stable over the same period. However, in eyes with AMD, RPE density in the macula decreases over time, resulting in RPE mottling (Green, 1999).

1.4.4 Intracellular debris

1.4.4.1 Oxidative stress

Damage of tissue due to oxidative stress results from imbalance of oxidants and antioxidants. Specific proteins involved in the oxidative pathways were identified only in old rat RPE but not in young rat RPE (Gu et al., 2012). The antioxidant potential of vitreous specimens obtained postmortem from free AMD donors was correlated inversely with age (Berra et al., 2002). Recent studies have assessed oxidative stress markers such as protein carbonyl, 8-hydroxy-29-deoxyguanosine, malondialdehyde and total oxidation status, and concluded that these markers are hugely higher in AMD patient than in age-matched health control (Totan et al., 2009, Venza et al., 2012). These data suggest an aggravated response happens in AMD versus normal ageing.

1.4.4.2 Advanced glycation end products (AGEs)

AGEs are oxidative chemical modifications that accumulate in long-lived proteins with age and contribute to tissue and organ loss of function in ageing and age-related disease (Baynes, 2001). It has been associated with a number of disease such as osteoporosis, osteoarthritis and rheumatoid arthritis (DeGroot et al., 2001, Hein et al., 2003). Accumulation of AGEs within the eye has been detected in ageing vitreous specimens and in AMD tissues (van Deemter et al., 2009, Hammes et al., 1999). It has been shown that accumulation of AGEs in Bruch's membrane could play a crucial role in the RPE age-related dysfunction (Glenn et al., 2012). This may occur via activation of AGE receptors in RPE cells which influence the formation of basal deposits during aging and AMD (Yamada et al., 2006).

1.4.4.3 Lipofuscin

Lipofuscin is an autofluorescent material that accumulates progressively throughout life in RPE and is one of the important markers of retinal ageing (Bonnell et al., 2003). It enters RPE through phagocytosis of photoreceptor outer segment. This phagocytosed material is not completely degraded within lysosomes of the RPE and thus accumulates within RPE over time throughout life (Bonnell et al., 2003, Ardeljan and Chan, 2013). A linear increase of lipofuscin accumulation was found until age 70 in a study of 145 normal subjects aged 15–80 years (Delori et al., 2001). The fluorescence then decreases above age 70 years due to age-related atrophy of RPE cells. Lipofuscin distribution matches and reflects the pattern of age-related loss of photoreceptors but does not predict it (Delori et al., 2001). Lipofuscin produces superoxide ions after exposure to light, particularly blue light, which may compromise retinal cell function and may provide a link to light-induced retinal damage such as AMD (Wassell et al., 1999).

1.4.5 Para-inflammation and Immunity

Para-inflammation is an adaptive response to malfunction or tissue stress, aiming to restore tissue homeostasis and functionality (Medzhitov, 2008, Xu et al., 2009). This response is intermediate between basal homeostatic and inflammatory states. Para-inflammation might play a significant role in initiating and progressing of various chronic inflammatory conditions such as AMD if it is sustained for a period and turned into inflammation. There are some inflammatory responses observed in normal ageing eyes and in eyes with AMD but with greater severity in AMD, suggesting that triggers may exist in both ageing and AMD but with greater magnitude in the latter. This may explain why some people, who live in different

environmental conditions and/or have gene alterations, develop AMD with age, while others do not (Xu et al., 2009).

Several inflammatory responses were observed in AMD including microglial activation, complement activation, and macrophage infiltration (Patel and Chan, 2008, Jha et al., 2007). Recent studies have suggested that retinal microglial activation and choroidal macrophage infiltration involve the pathogenesis of dry and wet AMD respectively (Penfold et al., 2001, Skeie and Mullins, 2009). Complement activation is believed to be also involved in the pathogenesis of both dry and wet AMD (Anderson et al., 2002, Bora et al., 2005). Therefore, it is important to differentiate between the protective age-related inflammatory response and the detrimental inflammation in AMD in order to develop specific immune therapy for AMD patients.

1.4.6 Epigenetics

Epigenetics is a term used to describe a change in gene expression without a change in gene DNA sequence. Modification in gene expression is one of the main mechanisms by which changes in germ layers and tissue may develop with various phenotypes over the development course. This occurs without change in DNA sequence but via genome modifications that affect function or structure (Ardeljan and Chan, 2013). Thus, a new way to examine the non-inheritable risk factors of developing AMD has been offered. Recent study examined monozygotic twins with discordant AMD to monitor risk factors for AMD stage and severity, and found that the twin with the more severe or advanced form of AMD was heavy smoker and/or had lower dietary vitamin D (Seddon et al., 2011). The authors concluded that epigenetic modifications such as environmental and nutritional are involved in

developing of AMD. There is limited data in this field and, therefore, further studies to better understand the role of epigenetic in AMD are required.

1.5 Optical coherence tomography (OCT)

Optical coherence tomography (OCT) is a contactless non-invasive imaging device that enables clinicians to get ocular/retinal sectional scans that resemble to their histological correspondents. Its concept is similar to the B-scan ultrasonography but using light instead of sound, which allows it to measure a smaller structure equal to 5-10 μm compared to 100-150 μm for ultrasound. This makes OCT image resolution nearly 20 times better (Drexler et al., 2003). An OCT B-scan (2-dimensional image) is consistent of several A-scans, with each A-scan representing a one dimensional data. The OCT images are obtained by emitting light and detecting the reflected light echoes using low-coherence interferometry. As our eyes have transparent media that allows light to pass through pupil to reach retina, an in vivo cross-sectional view of the retina can be obtained as a result. This makes OCT as the most important ancillary investigation for diagnosis, evaluation and management of retinal diseases such as AMD and diabetic retinopathy. Recently, OCT has also been introduced in other medical specialties such as cardiology, gastroenterology, and dermatology.

1.5.1 The development of OCT in ophthalmology

The OCT was first introduced in 1991 as an non-invasive imaging device that can produce a two-dimensional image of optical scattering from human internal tissue microstructures (Huang et al., 1991). This was recognised as akin to pulse-echo ultrasound imaging with ability to demonstrate in vitro tomographic imaging in both transparent and turbid media by imaging retina and coronary artery respectively.

In 1996, the first ophthalmic OCT was released by Zeiss. It relied on patented time-domain (TD) technology. In the same year, the first OCT atlas “Imaging of Macular Diseases with Optical Coherence Tomography” was published. This atlas provided essentials for understanding of retinal OCT (Puliafito et al., 1995). However, there was slow clinical adaptation due to limited information about OCT and by 1999 only approximately 180 instruments were only sold (Fujimoto and Swanson, 2016). In 2000, a second generation ophthalmic OCT instrument was developed with ergonomics improvement but only 400 unit were sold. The main issue regarding that was the device took long time to obtain image with acceptable resolution. This was because a reference mirror need to move during the process of measuring light echoes.

In 2002, the first spectral-domain OCT (SD-OCT) was introduced by Wojtkowski et al. (Wojtkowski et al., 2002). This system was initially failed to work probably because of motion artefact due to sensitivity to eye movement. A year later, a powerful sensitivity advantage of SD-OCT was demonstrated which enabled the reference mirror to remain in a fixed position (Choma et al., 2003, de Boer et al., 2003). This led to corresponding increase in axial scanning speed. As a result, a reduction in motion artefact and improvement in signal to noise were achieved. In addition, by improving acquisition speed, there was an increase in the amount of data that can reproducibly and reliably be measured, allowing the entire macula to be scanned. This made 3D imaging and volumetric analysis possible, and allowed for more reliable comparisons of inert-visit measurement. Since 2005, SD technology has brought a resonance in OCT development and research. Consequently, it entered the ophthalmic market and become a standard of care (Fujimoto and Swanson, 2016). Although this technology has progressed significantly during the

last years, there is still potential need to improve speed (swept-source OCT (SS-OCT)), tissue contrast (polarisation sensitive OCT) and flow measurements (OCT Angiography). Figure 1 summarises the OCT development in ophthalmology.

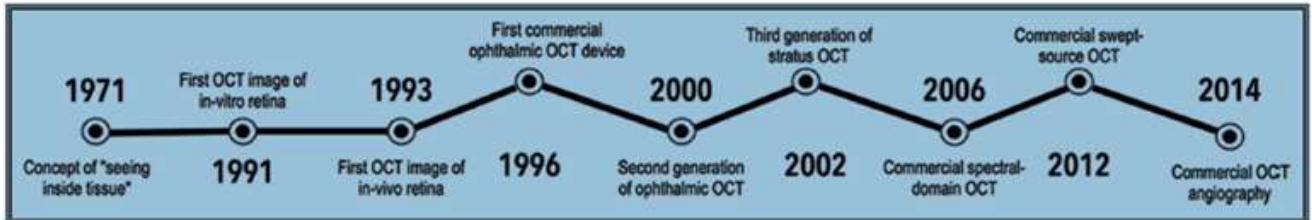


Figure 1. Timeline showing the development of OCT in ophthalmology. (Ref. (Bhende et al., 2018))

1.5.2 Comparison between TD-OCT, SD-OCT and SS-OCT

Of the three OCT technologies that are commercially available, TD-OCT, SD-OCT and SS-OCT. SD-OCT is the current commonly used OCT technology. It is able to scan up to 70.000 A-scans per second with better resolution, visualisation and penetration than TD-OCT. This is because SD-OCT uses a high speed line scan camera and spectrometer, acquiring volumetric data without motion artifacts that acquired in TD due to moving of reference mirror (Potsaid et al., 2008). One disadvantage of using camera-based SD-OCT is a noticeable signal drop-off with scanning depth. SS-OCT does not require a camera and uses a light source with a narrow band (Gabriele et al., 2011). As a result, minimal signal drop-off with depth occurs and this makes SS-OCT superior to SD-OCT. Table 3 shows the difference between the 3 technologies.

Table 3. Table 1. Comparison between the three commercially available OCT technologies. (Adapted from (Gabriele et al., 2011, Bhende et al., 2018))

OCT Type	Light Source	Scanning Speed	Axial Resolution	Primary Advantages	Primary Disadvantages
TD	Broadband width, Diode laser (810 nm)	400 A-scans/second	10 μ m	Intensity information acquired in time domain; no complex conjugate image	Moving reference mirror required limiting acquisition rate
SD	Broadband width, Diode laser (840 nm)	27,000-70,000 A-scans/second	5-7 μ m	No moving reference mirror required; higher sensitivity than TD-OCT; high scanning speed and axial resolution have been attained	Noticeable signal drop-off with depth
SS	Narrow band, swept through broad range, Tunable laser (1050 nm)	100,000-400,000 A-scans/second	5 μ m	No moving reference mirror required; higher sensitivity than TD-OCT; very high scanning speeds can be attained; minimal signal drop-off with depth	Most ophthalmic systems operating at longer wave lengths, with lower axial resolution

1.5.3 OCT image interpretation

Generally, retinal layers appear either bright (hyper-reflective) or dark (hypo-reflective). While the retinal nerve fiber layer (RNFL), ganglion cell layer (GCL) and the plexiform layers appear all hyper-reflective layers, the nuclear layers appear hypo-reflective as shown in figure 2 (Toth et al., 1997).

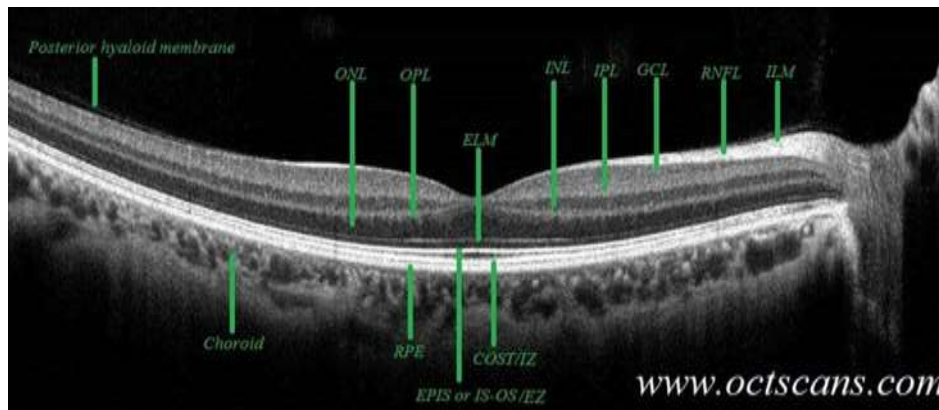


Figure 2. SD-OCT image of a normal right eye. Adapted from Optical Coherence Tomography Scans Website, (<http://www.octscans.com>).

Inner retinal structures in OCT appear to correspond well to their histological counterparts. In contrast, the interpretation of outer retina correlation between OCT and its histological analogues remain controversial. With SD-OCT, four clear bands can be seen. Band 1 has been referred to the external limiting membrane (ELM) (Drexler et al., 2003). Band 2 is felt to represent the boundary between the inner and outer photoreceptor segments (Srinivasan et al., 2006a). This band bends anteriorly in the foveal area which is known as foveal bulge, reflecting cones elongation (Srinivasan et al., 2008). Band 3 has been attributed to as the cone outer segment tip line (COST). Band 4 has been ascribed to the retinal pigment epithelium (RPE) (Puliafito et al., 1995). However, Bands 2 and 3 were not consistent to what was proposed by the IN_OCT Panel in 2014 (Staurenghi et al., 2014). They proposed that bands 2 and 3 represented the photoreceptors ellipsoid zone and cone interdigitation with RPE respectively. In addition, a recent cellular study explored the correlation between the four hyper-reflective bands and their histological correspondences at the fovea (Figure 3) (Cuenca et al., 2018). The first, second, third and fourth hyper-reflective bands corresponded to ELM, ellipsoid zone, cone phagosome zone (located in the top of the RPE) and RPE mitochondria zone (at the RPE basal portion) respectively. These hyper-reflective zone were separated by

three hypo-reflective bands as the following: the most inner hypo-reflective band was the cone myoid zone, the middle band was the cone outer segment and the RPE interdigitation, and the most outer hypo-reflective band was the RPE melanosomes (Figure 3).

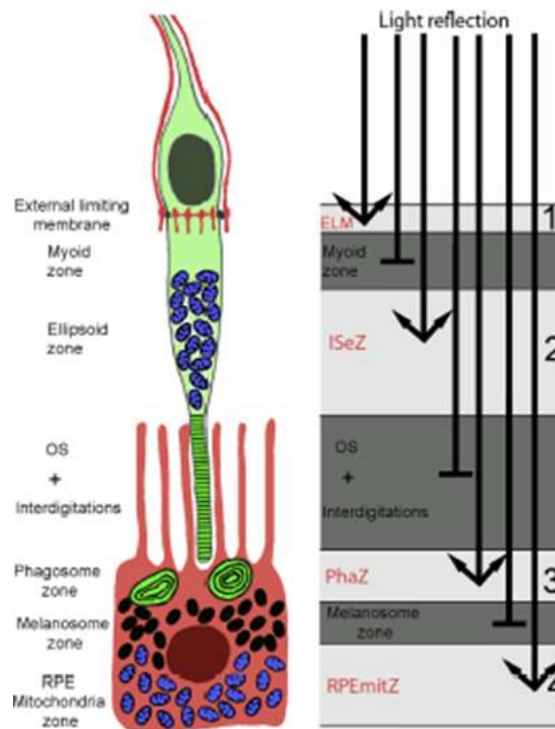


Figure 3. An illustration of hyper-reflective and hypo-reflective bands at the outer retina. (Adapted from (Cuenca et al., 2018))

Abnormal reflectivity on OCT can be seen and divided into hyper-reflective and hypo-reflective lesions. Hyper-reflective lesions might be hard exudates, calcification, blood, scars (e.g. choroidal rupture, healed choroiditis), Choroidal neovascularisation (CNV) and epiretinal membrane. Hypo-reflective lesions can be fluid (retinal oedema, subretinal fluid, sub-RPE fluid) and RPE hypopigmented lesions. Furthermore, some situations such as refractive error and opaque media might be interpreted falsely as hypo-reflective but an overall attenuation of the scan due to diffused hyporeflectivity can be recognised.

1.5.4 Automated image analysis

Manual labelling or visual identification of OCT images becomes no longer possible due to the huge amount of data require to be analysed. There are now different quantitative analytic software that enable to perform several automated retinal measurements. For instance, thickness and volume of central retina in nine subfields can be measured by inbuilt software in almost all commercial OCT machines. This is essential for management of specific retinal diseases like diabetic maculopathy where central macular thickness plays a significant role in decision making to give or stop anti-VEGF injections. Furthermore, automated analysis of multiple AMD biomarkers on OCT using algorithms would be of considerable value (Wintergerst et al., 2017). For example, drusen, one of the earliest AMD signs, can be detected and measured accurately (count, area, and volume) by automated algorithm (Nittala et al., 2012). This has enhanced our ability to assess AMD patients more reliably based on drusen volume (Nittala et al., 2012).

1.5.5 Retinal segmentation

The retina is a multi-layered structure and it is important to segment it to its various layers in order to study the retinal structure in more detail. Recent advancements in OCT imaging technology has enabled to evolve automated segmentation algorithms that are able to segment the retinal structure on OCT. There are currently several research-oriented automated segmentation software such as Orion™ (Voxeleron, Pleasanton, CA), IOWA Reference Algorithm and the built-in software of Spectralis. In this essay, we will focus only on Orion software as we used it in our study.

Orion is a fully automated software for segmentation of retinal layers in volumetric OCT images and produces repeatable retinal thickness and volume values (Figure

4). It is device-independent, processing data from all widely-available commercial OCT devices. The software has been validated in previous studies and comprehensively beta tested worldwide, but is still for research applications only. (Voxeleron website, [1])

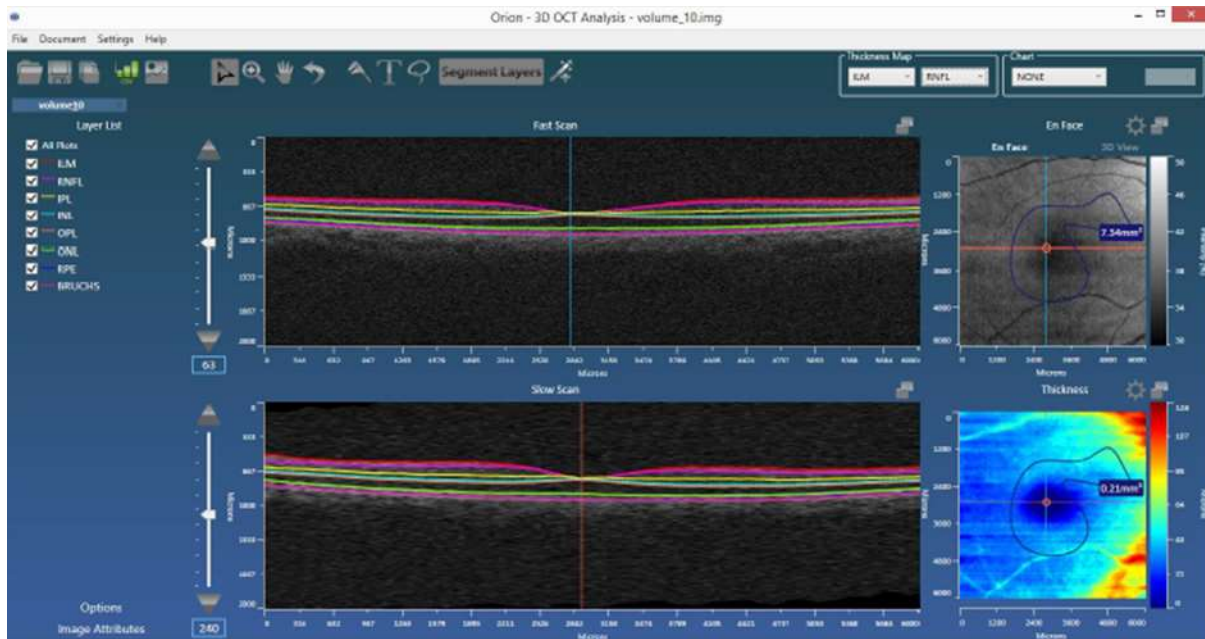


Figure 4. A screenshot of display options of the Orion segmentation software.

Orion automatically segments OCT volumes into seven retinal layers as illustrated in Figure 5 including Macular Retinal Nerve Layer (RNFL), Ganglion Cell Layer and Inner Plexiform Layer (GCIPL), Inner Nuclear Layer (INL), Outer Plexiform layer (OPL), Outer Nuclear Layer (ONL), Photoreceptor complex (PR), Retinal Pigment Epithelium-Bruch's membrane complex (RPE-BM) and total retina, allowing analysis of various metrics such as average thicknesses and volumes of the different layers within the ETDRS zone based on an automatic foveal centration. (Voxeleron website, [1])

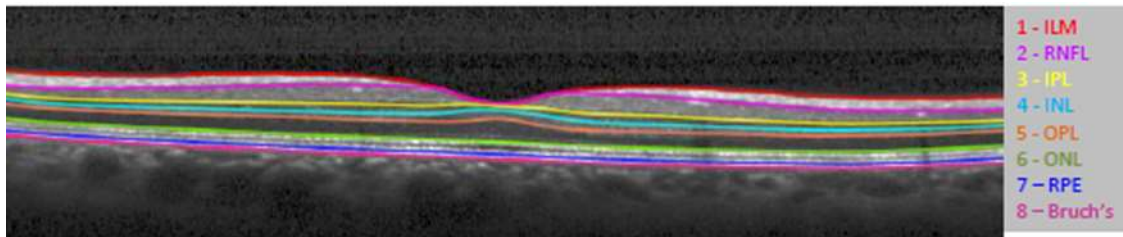


Figure 5. Retinal layer segmentation with detectable layer boundaries in a normal healthy eye as analysed automatically by the Orion software. Layers 1-2 = Retinal Nerve Fiber Layer (RNFL); Layers 2-3 = Ganglion Cell Ganglion Cell and Inner Plexiform Layer (GCIPL); Layers 3-4 = Inner Nuclear Layer (INL); Layers 4-5 = Outer Plexiform Layer (OPL); Layers 5-6 = Outer Nuclear Layer (ONL); Layers 6-7 = Photoreceptor complex (PR); Layers 7-8 = Retinal Pigment Epithelium-Bruch's Membrane complex (RPE-BM); Layers 1-8 = Total Retinal Layers.

1.5.6 Topcon 3D OCT

The 3D OCT (Topcon Corporation, Tokyo, Japan) is a fast SD-OCT with 50,000 A-scans per second, providing high resolution images. The 3D macular scan comprised 128 horizontal scan lines over a 6x6 mm² area and each line comprised 512 A-scans. The device is able to auto focus with auto-fovea centre detection system and auto shot. It offers simultaneous dynamic viewing of 2D, 3D and fundus images as well as allows users to monitor serial OCT images of the same patient simultaneously. The latter is supported by the ability of the user to scan the same location based on the baseline scan. This eliminates subjective alignment error and minimizes follow-up scans variability, resulting in accurate observation of changes over time. (Topcon website, [2])

This device is also powered with macula drusen analysis software that enables to count drusen and measure their area and volume (Figure 6). This built-in software was assessed by Iwama et al., 2012 (Iwama et al., 2012) by comparing manual grading of drusen parameters on colour fundus photography with automated assessment using the 3D OCT. The study found that there was good agreement between the manual and automated way of drusen assessment. This encouraged us

to perform a study to explore the effect of drusen as predictors of AMD conversion to late stage (Lamin et al., 2019a).

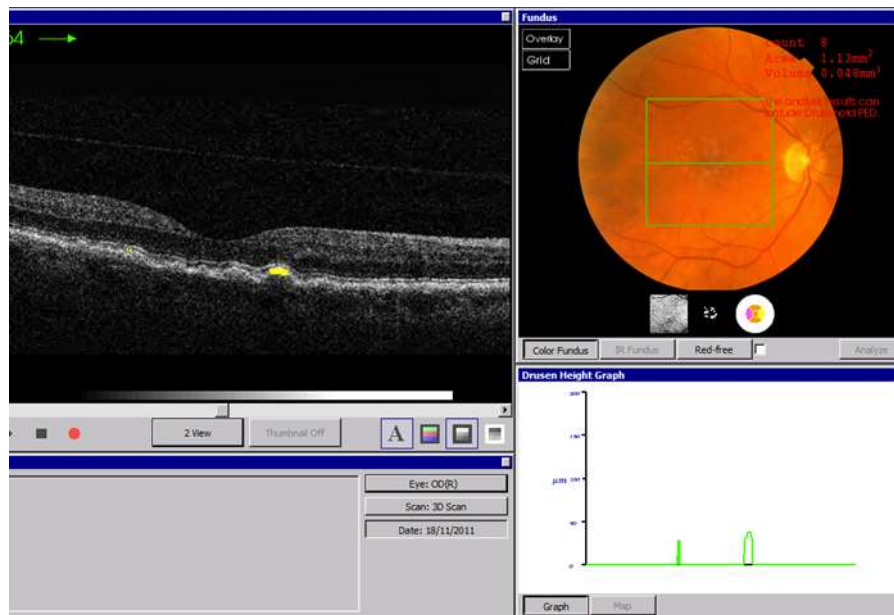


Figure 6. Topcon OCT scan of right eye with AMD showing drusen count, area and volume as illustrated on the top right.

The clinical data of macular normative database incorporated into the Topcon 3D OCT was derived from 173 subjects of several ethnicities origin in the United States. It was included 112 females and 61 males with average of age 42.35 ± 15.59 years (range from 19 to 84 years). The included subjects had best corrected visual acuity of 20/40 or better (Snellen), intraocular pressure ≤ 21 mm Hg, axial length (22-26 mm), and no history of any ocular disease (except cataract) and/or ocular surgery. OCT was performed to those normal subjects, and only scan quality level of 70 or more was accepted and should be free of artefact. After that, images were segmented automatically and verified that no errors existed prior to inclusion in the normative database. The mean macular thickness was then calculated based on the

Early Treatment of Diabetic Retinopathy Study (ETDRS) grid as shown in table 4.
(Topconmedical website, [3]).

Table 4. Macular Mean Thickness and Standard Deviation (SD) by grid ETDRS from the normative database. (Topconmedical website, [3])

	Centre	Inner circle				Outer circle			
		T	S	N	I	T	S	N	I
Mean	233.68	289.64	302.11	304.40	298.36	240.14	256.75	274.62	246.91
SD	19.71	14.86	15.51	15.36	15.42	13.20	13.69	16.60	15.31
CI 95%	77.25	58.24	60.80	60.22	60.43	51.74	53.68	65.06	60.00

1.5.7 OCT in AMD

Drusen, pseudo-drusen and hyper-reflective foci are the early key features of dry AMD. These features with dynamic changes over time have been identified to be risk factors for disease progression. Fundus photography and biomicroscopy have been the traditional gold standard in the evaluation of drusen morphology and development (The Age-Related Eye Disease Study Research, 2001, Ferris et al., 2013). However, these modalities interpretation is subject to significant discrepancy and are not able to outline indistinct drusen (Klein et al., 1991). SD-OCT has strongly replaced them and become the most popular modality in the evaluation of drusen. It is able to visualise drusen shape, area, height, volume, homogeneity and internal reflectivity and other drusen characteristics in details.

1.5.7.1 Early and intermediate AMD

It becomes feasible to automatically distinguish AMD from normal eyes by identifying total retina volumes and abnormal RPE drusen complex thickening and thinning volumes (Farsiu et al., 2014). Drusen are hallmark features of dry AMD. On OCT, soft and hard drusen appear as elevations in the RPE layer with variation in size, shape and reflectivity. The OCT characteristics of drusen have been revealed in

numerous studies (Khanifar et al., 2008, Leuschen et al., 2013, Spaide and Curcio, 2010). They concluded that most of drusen are convex, homogenous with internal reflectivity and without overlying hyper-reflective foci (Khanifar et al., 2008). Hyper-reflective foci overlying drusen are noted in some cases and it is felt to be pigment or RPE migration that associated with the risk of progression to focal atrophy (Ouyang et al., 2013a). In addition to these foci, drusen cores and atypical drusen reflectivity were also associated with RPE atrophy (Leuschen et al., 2013).

Several studies have revealed a dynamic drusen growth pattern with a repeated cycle of increase and decrease in drusen area and volume over time (Yehoshua et al., 2011, Schlanitz et al., 2017). A prospective longitudinal study by Folgar et al. (Folgar et al., 2016) identified that greater baseline drusen volume was associated with significant 2-year progression to wet AMD and an increase in drusen volume by 0.1 mm³ increases the odds of developing CNV by 31%. Abdelfattah et al. (Abdelfattah et al., 2016) suggested that drusen volume measured by OCT can be used as a biomarker for AMD progression to late stage. Lamin et al. (2019a) has shown that drusen volume growth rate across a 6mm macula cube using automated drusen analysis software may be used as a predictor for conversion to CNV especially occult type.

Reticular pseudo drusen or subretinal drusenoid deposits are present in more than 50% in patients with early/intermediate AMD and their prevalence is strongly associated with the presence and severity of AMD (Zarubina et al., 2016). These deposits are located above the RPE as opposed to the true drusen and are best visualized using infrared reflectance and SD-OCT imaging modalities (Saade and Smith, 2014). Like drusen, reticular pseudo drusen can be changed dynamically in shape, volume and stage, and developmentally are drusen independent (Querques

et al., 2012). Regression of reticular drusen were found to be associated with loss of the underlying choroidal thickness and outer retinal atrophy (Spaide, 2013).

Disruption of ellipsoid zone and thinning of photoreceptor layer overlying drusen were observed in eyes with early/intermediate AMD using OCT. It is still unclear if these anatomical changes in the outer retina are happened before or after drusen formation and if results from mechanical compression or change in photoreceptor layer micro-environment from drusen (Schuman et al., 2009). Another abnormal manifestation in retinal layers over drusen that can be detected on OCT is the presence of hyper-reflective haze in the outer nuclear layer over drusen but this can simply be the presence of Henle's layer (Schuman et al., 2009, Lujan et al., 2011).

1.5.7.2 Wet AMD

Wet AMD is referred to the neovascular/exudative type of AMD and is characterised by the formation of CNV. This CNV is associated with retinal pigment detachment and subretinal fluid as a result of its structure immaturity that results in fluid accumulation in different layer levels (Bressler et al., 1988b).

CNV associated with AMD has been classified in several ways based upon the available technology used to detect the presence neovascularisation. Using fluorescein angiography (FA), CNV has been classified as either classic or occult (1991b). Classic CNV is characterised by well-demarcated hyperfluorescence in the early FA phase with progressive dye pooling in the subneurosensory space. Occult or minimally classic (less than 50% classic component) is characterised by mottled hyperfluorescence in the mid FA phase with late leakage of undetermined source. Using ICG angiography, occult CNV can be easily detected by delineating the CNV borders (Lim et al., 1995).

Gass (Gass, 1994) proposed a CNV classification system based on the location and structure of the formed CNV with respect to the RPE layer. CNV proliferated under the RPE was classified as type 1, while CNV proliferated above the RPE was classified as type 2. This classification was not well accepted because of the lack of appropriate imaging modalities. However, a modified Gass' classification was proposed by Freund et al. (Freund et al., 2010) based on OCT. This new classification includes the previous 2 types and added a type 3 neovascularisation, the so-called retinal angiomatous proliferation, which is characterised by intraretinal neovascularisation. OCT is now the modality of choice to identify CNV's earliest signs and disease activity in wet AMD. Combining a variety of imaging modalities such as OCT, FA and ICG might be useful for a comprehensive understanding of the pathophysiology of CNV formation in wet AMD as well as for monitoring disease activity.

1.6 Changes in retinal layers with age, gender, ethnicity and axial length

1.6.1 Introduction

Optical coherence tomography (OCT) yields a cross-sectional representation of the retinal layers with resolution approaching that with histologic section, allowing precise evaluation of the normal macular structure as well as assessment of macular structural pathology. Qualitative assessment of OCT images guides clinical diagnoses, early detection of various retinal disorders and monitoring pathological macular changes. Traditionally, total retinal thickness is the quantitative measure for macular OCT in both clinical and research settings. Recently, development of segmentation layer algorithms have allowed quantification of the thickness or volume

of each retinal layer separately. This is of clinical and scientific interest as layers are often selectively attenuated in different retinal diseases. It is also important to be able to distinguish between physiological and pathological changes by understanding the normal structure of retinal layers, each of which has its specific structure and might be affected by different factors.

Measurements of macular thickness and volume are commonly reported on the basis of the standard Early Treatment of Diabetic Retinopathy macular map (Figure 7), which divides the macula into nine sectors. These include fovea (1mm), inner macula (1-3mm) and outer macula (3-6 mm) which are subdivided into 4 regions including superior, nasal, inferior and temporal. There are 2 different measures of the fovea that have been used by studies; centre point foveal thickness (CPFT) and central foveal thickness (CFT). CPFT is defined as average of six radial scans centered at the foveola. CFT is defined as the central area with a diameter of 1 mm. These measurements were found to be affected by various factors such as age, gender, ethnicity and axial length (AL). This should be taken in consideration when interpreting retinal layer measurements. This section will summarises the impact of age, gender, ethnicity and refractive error on macular layer thicknesses and volumes.

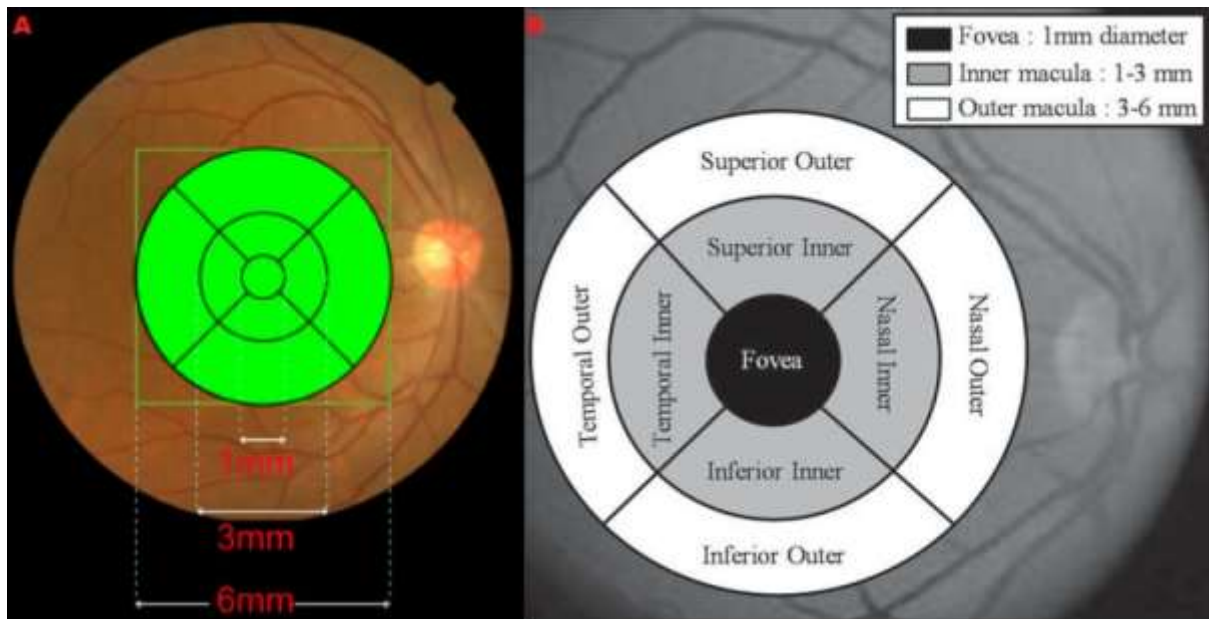


Figure 7. Illustrative images depicting the 9 ETDRS subfields. A, Macular image showing 1 mm, 3 mm and 6 mm circular areas. B, Macular image showing fovea, inner macula and outer macula.

1.6.2 Age impact on macular thicknesses and volumes

Several OCT studies have explored the effect of aging in changing the macular layer measures. It is essential to distinguish aging changes from pathological one. This can help in deep understanding of various macular diseases.

Most of studies that measured CPFT reported an increase with age due to outer retinal layers thickening, as measured using OCT (Duan et al., 2010, Kashani et al., 2010). CPFT values were presented in two age groups (< 50 and \geq 50 years) with greater CPFT values in older age group (149-178 μm) than younger age groups (142-162 μm) (Subhi et al., 2016). The CPFT thickening rate for each decade ranges from 3.6 μm to 5 μm . However, some studies did find any change in CPFT with increasing age (Eriksson and Alm, 2009, Appukuttan et al., 2014).

Recent studies have measured CFT using OCT and found that CFT does not seem to change with age (Appukuttan et al., 2014, Agawa et al., 2011). Other studies reported that the CFT either increase by 2–4 μm per decade (Duan et al., 2010, Kashani et al., 2010) or decrease by 2.7 μm per decade (Eriksson and Alm, 2009). Analysis from the UK Biobank study from the scans of over 32000 participants showed a reduction in CFT with increasing age (Patel et al., 2016).

The total macular thickness and volume were found to have negative correlations with age (Alamouti and Funk, 2003, Eriksson and Alm, 2009, Duan et al., 2010, Kashani et al., 2010, Appukuttan et al., 2014, Nieves-Moreno et al., 2018). Similarly, the UK Biobank study revealed macular thinning with age (Patel et al., 2016). A review study reported that total macular thickness and volume decrease for each decade by 2.1–4.2 μm and 0.10-0.14 mm^3 respectively (Subhi et al., 2016).

A histological study showed that retinal neurons are lost annually by rate of 0.3-0.6 % due to aging process (Repka and Quigley, 1989). In vivo OCT studies observed that inner retinal layer thickness in specific decreases with age and this including retinal nerve fiber layer, ganglion cell layer and inner nuclear layer thicknesses (Ooto et al., 2011, Appukuttan et al., 2014). This might explain why total macular thickness decreases with age and not CFT where inner retinal layers constitutes smaller portion of the total foveal thickness (Figure 8) (Subhi et al., 2016).

A correlation between thicknesses/volumes of specific macular layers and age were performed by different studies with various results. Most studies revealed findings on age-associated changes of inner retinal layers. Reductions in thicknesses of inner retinal layers with increasing age are well-established in studies with a large sample (Subhi et al., 2016). This includes age-associated decrease in thickness of RNFL

(Neuville et al., 2009, Girkin et al., 2011, Ooto et al., 2011, Demirkaya et al., 2013) and GCL/IPL/INL (Ooto et al., 2011, Demirkaya et al., 2013, Nieves-Moreno et al., 2018). However, other studies specifically with small sample did not find age-associated changes in the inner retinal layer thicknesses (Savastano et al., 2014, Wang et al., 2015).

Few studies revealed findings on age-associated changes of outer retinal layers. Increase in OPL thickness and volume has been reported in two studies of normal eyes (Demirkaya et al., 2013, Nieves-Moreno et al., 2018). ONL thinning with age has been reported in a recent study (Nieves-Moreno et al., 2018). Increasing PR layer thickness with age was also recently shown in an OCT study (Pakdel et al., 2018), whereas another study reported PR layer thinning with age (Nieves-Moreno et al., 2018). A positive correlation between foveal RPE thickness and age has also been reported, supporting the finding of increasing CFT with age (Demirkaya et al., 2013). However, the UK Biobank study revealed RPE thinning with age (among those aged over 45) (Ko et al., 2017). It is possible that differences in segmentation methods or population demographics might explain the controversial results.

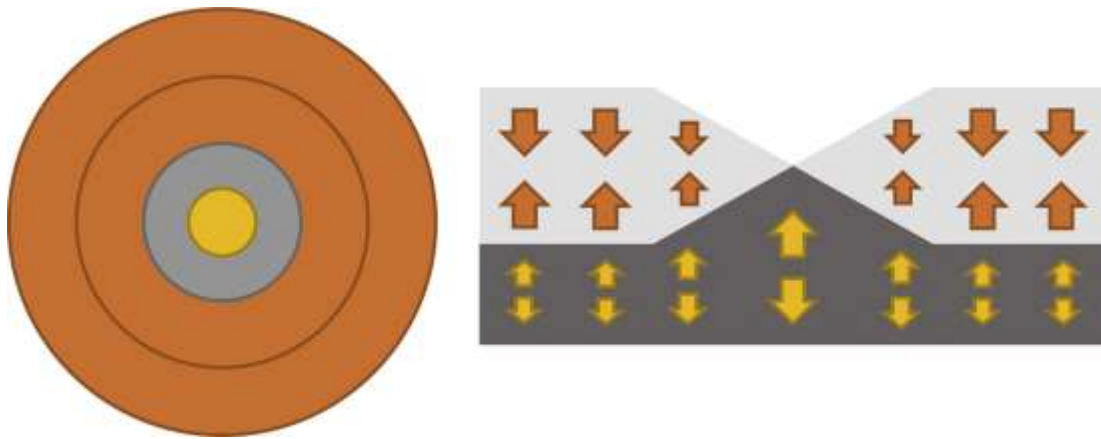


Figure 8. Illustrative images depicting the age-associated changes in macular layer thicknesses. Light yellow colour represents thickness increase and dark orange represents thickness decrease. Ageing results in an overall thickening of the fovea (CFT) and a thinning of the inner and outer macula. (Adapted from ref. ((Subhi et al., 2016)).

1.6.3 Gender impact on macular layer thicknesses and volumes

The impact of gender on foveal and macular thickness has been examined by many studies (Ooto et al., 2011, Appukuttan et al., 2014, Jonas et al., 2016, Nieves-Moreno et al., 2018). Otto et al. (2011) measured the CFT and the total macular thickness of 130 males and 126 females and found both of them significantly greater in males than females. Similarly, Nieves-Moreno et al. (2018) reported that total macular thickness of 179 females and 118 males was considerably greater in males than females.

Song et al. (2010) and Wagner-Schuman et al. (2011) showed that males had 11 μm thicker fovea than females. Jonas et al. (2016) and Nieves-Moreno et al. (2018) showed that males had 8 μm thicker macula than females. RNFL was found to be thicker in females (Ooto et al., 2011, Nieves-Moreno et al., 2018), whereas INL, OPL and OPL were markedly thicker in males (Ooto et al., 2011).

1.6.4 Ethnicity impact on macular layer thicknesses and volumes

A number of studies reported ethnicity-associated changes in CFT and total macular thickness. The CFT for Caucasians, Hispanics and African Americans was measured by Stratus OCT and found to be $200.2 \pm 2.7 \mu\text{m}$, $194.7 \pm 3.9 \mu\text{m}$ and $181.0 \pm 20 \mu\text{m}$ respectively (Kashani et al., 2010). In another study, the CFT for Caucasians and Indians were reported to be, respectively, $272.7 \pm 20 \mu\text{m}$ and $260.1 \pm 18 \mu\text{m}$ as measured by Spectralis OCT (Appukuttan et al., 2014). Recent studies reported that Caucasian people have a significantly thicker CFT and retinal thickness compared to people of Hispanic, African and Asian descent (Girkin et al., 2011, Pilat et al., 2014).

Caucasians were shown to have thicker PR inner and outer segment and ONL in the central field compared to Asians. In contrast, Asians were shown to have thicker RPE (Pilat et al., 2014) and thicker RNFL compared to other ethnicities (Girkin et al., 2011, Appukuttan et al., 2014). One study showed that Africans have the thinnest macular inner retina (Girkin et al., 2011). The variation in thickness observed between Africans/African Americans and Caucasians appears to be driven by differences in foveal pit morphology which is deeper and broader in the Africans (Wagner-Schuman et al., 2011).

1.6.5 Axial length impact on macular layer thicknesses and volumes

Existing literature about axial length-associated change in retinal thickness shows controversial results. No effect of AL on retinal layer thickness has been reported in

a recent study of 146 healthy eyes (Wang et al., 2015). However, decrease in total macular and total macular volume with increasing AL has also been reported (Song et al., 2010). Studies on myopes by Appukuttan et al (2014) and Jonas et al. (2016) showed that myopic eyes had thicker foveas and thinner parafovea.

1.7 Heritability of retina and AMD

1.7.1 Definitions

Heritability describes how much the genetic values attribute to phenotypic variance. In other words, it accounts for differences in someone's traits that can include characteristics like eye colour height, intelligence as well as health problems such as autism and schizophrenia. Statistically, heritability is a ratio/proportion of variances of a phenotype explained by inherited genetic variants. There are 2 different forms of statistics definition for heritability commonly used. Broad sense heritability (H^2) which explains the effect of total genetic values on phenotypic variation. Narrow sense heritability (h^2) which refers to the effect of additive genetic values on phenotypic variation. This can be used as useful tool to determine the degree of phenotype of children from transmitted genes from their parents and to predict risk of disease from parenteral family history. Thus, h^2 is always less than H^2 (total heritability) that can be explained by all genetic factors.

Consequently, from the abovementioned definition of heritability, there is a dependence on the population to study the effect of genetics and environmental factors. This means that these factors are population specific. As a result, Genetic and environmental variances can vary across populations. Theoretically, the heritability of one trait in one population cannot be predicted in another population. However, in practice, similar traits' heritabilities of different populations of the same

species are commonly similar, or even in different species. Heritability of the same trait can also vary between sexes as well as early and late life (Visscher et al., 2008).

1.7.2 Estimations

Several data sources are frequently used to estimate heritability. Traditionally and commonly, heritability has been estimated from twins' studies, taking advantage that monozygotic (MZ) twin pairs have almost no differences in their DNA. In addition to that, MZ pairs have the same shared environment and any phenotypic traits differences would be attributed to unique environmental factors. In contrast, dizygotic twins (DZ) share approximately 50% of their DNA like other sibling pairs. Moreover, both MZ and DZ twin pairs are assumed to have the same shared environmental factors. Thus, if a trait appears to be more similar in MZ twins than DZ twins, genetics are likely to play an important role in determining that trait. As a result, comparing a trait in MZ twins against DZ twins are used by researchers to calculate an estimate of its heritability. Therefore, formal calculation of heritability by twin modelling permits estimation of the proportion of the variance in a trait that is attributable to genetic factors.

The value of heritability estimate ranges from zero to one. The smaller the heritability, the more characteristic is likely to be due to environmental factors. There are various characteristics that have heritability of zero like language spoken and religion because they are not influenced by genetics. In contrast, the higher the heritability, the more the characteristic is likely to come from genetics with very low environmental contributions. Several disorders such as phenylketonuria have high heritability because they are caused by single gene mutation. Most of multifactorial

diseases are influenced by a combination of genetic and environmental and therefore have a heritability somewhere in the middle.

Heritability does not provide information about what proportion of a trait is influenced by genetics and what proportion is influenced by environmental factors. For example, heritability of 0.8 means 80% of a trait variability in a population is influenced by genetic factors among people but does not mean that the trait is 80% caused by genetics. Importantly, heritability can help to understand the influences of genetic and environmental factors on complex traits.

1.7.3 Heritability studies of retina

Recent twin studies have demonstrated significant heritability for macular thickness, macular pigment optical density and spatial patterns, retinal vascular patterns and peripapillary RNFL.

1.7.3.1 Macular thickness

The ability to measure macular thickness accurately has recently become possible, using OCT. Macular thickness is being used in monitoring retinal disorders such as diabetic macular edema during treatment. Clearly it is essential to determine to what extent genetic factors influence a person's macular topography. By studying the role of genetic factors on healthy macula, a deep understanding of how disease influences its thickness can be achieved. Studies in twins offer quantification of relative contributions of genetic and environmental factors to variance in retinal structures such as macular thickness.

Recent twins study has examined the genetic contribution to variance in macular thickness, as assessed by OCT. Chamberlain et al (Chamberlain et al., 2006) explored the heritability of macular thickness using classical twin study. They

examined 109 twin pairs (58 MZ and 51 DZ), aged 50 to 85 years. Retinal thickness correlation was markedly higher in MZ than in DZ in all macular regions. The intrapair correlation for MZ and DZ twins was, respectively, 0.88 and 0.44 for the foveal region, 0.79 and 0.47 for the inner macular region, and 0.8 and 0.50 for the outer macular region. The heritability of the macular thickness for the fovea, inner macula and outer macula was estimated as 85%, 81%, and 81%, respectively. These findings suggest that genetic factors might affect the macular thickness in older healthy subjects.

1.7.3.2 Peripapillary RNFL

Premature loss of RNFL is characteristic of open angle glaucoma that occurs at accelerated rate in contrast to RNFL aging loss that occurs over a longer period of time late in life. A number of genes involved in the disease have been identified. However, these identified genes account for a small proportion of total number of glaucoma patients. Many studies suggest the importance of family history as a major risk factor but there are few data to assess the hereditary effect on glaucoma.

Recent twins study has examined the genetic influence in determining the amount of peripapillary RNFL in healthy adults, using OCT. Hougaard et al (Hougaard et al., 2003) explored the heritability of peripapillary RNFL thickness, using classical twin study. They examined 50 twin pairs (25 MZ and 25 DZ), aged 20 to 45 years. The within-pair difference in peripapillary RNFL thickness was 4.6% in MZ as compared to 7.3% in DZ pairs. The RNFL thickness measurement was found to decrease 3.8 μm per decade. The heritability of the peripapillary thickness was estimated as 66% but this value increased to 83% when corrected for the effect of age. These findings suggest that genetic factors might affect peripapillary RNFL thickness in healthy adults.

1.7.3.3 Retinal vascular patterns

Human retinal vasculature pattern varies significantly in people (Taarnhoj et al., 2008). The importance of these variations is not completely understood for health and disease. However, correlations were found between retinal vascular fractals and ocular and systemic diseases such as diabetic retinopathy, Alzheimer and stroke. Moreover, it is found that retinal vascular fractals can predict long term microvascular complications in type 1 diabetes mellitus (Broe et al., 2014).

Genetic and environmental factors influence on vessels' pattern have been examined using retinal blood vessels because they are the only part of human vessels that can be visualised directly in vivo. Vergmann et al (Vergmann et al., 2017) explored the heritability of retinal vascular fractals using classical twin study. They examined 99 twin pairs (50 MZ and 49 DZ), aged 20 to 46 years, using the box-counting method. The intrapair correlation was markedly higher in MZ than in DZ pairs. The intrapair correlation for MZ and DZ twins was 0.505 and 0.108, respectively. The heritability was estimated as 54%. These findings suggest that genetic factors might demonstrate the branching pattern of the retinal vessels in healthy adult twins.

1.7.3.4 Macular pigment optical density

Macular pigment (MP) is referred exclusively to two polar carotenoids (lutein and zeaxanthin). The concentration of MP is highest within retinal layers of inner and outer plexiform layers, and is concentrated maximally at the foveal area and decreases towards periphery (Handelman et al., 1988). Several studies have evaluated the MP pattern, using the fundus autofluorescence technique (Berendschot and van Norren, 2006, Dietzel et al., 2011, Zeimer et al., 2012).

Although MP appears to decline monotonically in density in most people, it shows a second distribution peak at 0.5° to 1.0° eccentricity in some people. It has been proposed that the second peak ring might follow the inner plexiform layer (Berendschot and van Norren, 2006).

It has been suggested that MP has a role in protecting the retina from oxidative damage by its ability to absorb blue light. This property of MP and its location and distribution may play a role in reducing the risk of AMD as shown in recent studies (Nolan et al., 2007, Loane et al., 2008, Kernt et al., 2012). One study showed that eyes with AMD appeared to have lower prevalence of the ring like structures than healthy eyes (Dietzel et al., 2011). Another study found atypical MP profile to be associated with older age and cigarette smoking, which are risk factor for AMD (Kirby et al., 2010). Other factors that can affect the MP pattern were also determined such as diet, gender and percentage body fat (Curran-Celentano et al., 2001, Nolan et al., 2004). Therefore, investigating the role of genes in determining the MP levels becomes essential. A classic twin study is ideal for this purpose.

Tariq et al (Tariq et al., 2014) explored the macular pigment optical density heritability using classical twin study. They examined 314 twins (88 MZ and 69 DZ pairs), aged 16 to 50 years, using fundus auto -fluorescence. The correlation of the ring like patterns of macular pigment was markedly higher in MZ than in DZ. The intrapair correlation for MZ and DZ twins was, respectively, 0.75 and 0.22, reflected in heritability estimates of 85%. The heritability was estimated as 84% of the total variance. Liew et al (Liew et al., 2005) also investigated the macular pigment optical density and found that the intrapair correlation for MZ and DZ is 0.83 and 0.50 respectively. These findings suggest that genetic factors might affect the macular pigment optical density.

1.7.4 Heritability of AMD

A number of environmental factors were identified to be associated with AMD. The multifactorial nature of the disease makes the possibility to find genetic contributions difficult. Heritability has helped to sort out this issue. Twins studies have shown remarkable degrees of concordance of AMD in MZ pairs versus DZ pairs. Klein et al (Klein et al., 1994) examined 9 MZ pairs and found that the fundus appearance and the visual impairment incidence were similar in 8 of the 9 pairs. Meyers et al (Meyers et al., 1995) demonstrated higher concordance of AMD in MZ (25 of 25) than in DZ (5 of 12) twin pairs, suggesting the importance of genetic factors. Similar findings were demonstrated by other studies, confirming that genetic factors play a significant role in the etiology of AMD (Hammond et al., 2002, Grizzard et al., 2003).

Seddon et al (Seddon et al., 2005) examined 840 twins (210 MZ, 181 DZ twin pairs and 58 singletons). Of those 840, 241, 162 and 106 were diagnosed with early, intermediate and advanced AMD, respectively. They found that heritability estimates were 0.46, 0.67 and 0.71 for overall AMD, intermediate and advanced AMD respectively. Clearly, it can be said that the more severe form of the disease the higher heritability may have.

The risk for first degree relative has been studied by Klaver et al (Klaver et al., 1998a). They compared first degree relatives of 87 patients with advanced AMD with first degree relatives of 135 control individuals without AMD. The lifetime risk estimate for first degree relatives of advanced AMD and controls was 50% (95% CI = 26-73%) and 12% (95% CI = 2-16%), respectively. The risk was considerably higher for first degree relatives who are affected by the diseases. Similar findings were found by Seddon et al., who reported that the prevalence of AMD was 26.9% and

11.6% for first degree relatives of patients with neovascular AMD and controls respectively. Together, these studies confirmed a significant genetic influence in the etiology of AMD.

1.8 Drusen quantification

1.8.1 Introduction

Age-related macular degeneration (AMD) is one of the main causes of central vision impairment and legal blindness among the elderly worldwide (Evans et al., 2004, Friedman et al., 2004, Pascolini and Mariotti, 2012). Drusen are the clinical hallmark of early AMD. They can be observed ophthalmoscopically as yellowish white deposits and histopathologically as focal accumulations of extracellular material localised between the RPE and the inner collagenous layer of Bruch's membrane (Sarks et al., 1994, van der Schaft et al., 1992a). Drusen were classified as small (< 63 μm), intermediate (63 – 125 μm) or large (> 125 μm) as well as soft or hard (The Age-Related Eye Disease Study Research, 2001).

Drusen are dynamic objects that could enlarge or regress in size through repeated cycles of expansion and shrinkage (Yehoshua et al., 2011). A recent natural history study of drusen has shown that the average drusen volume was found to increase over time and are more likely to progress to GA or CNV (Yehoshua et al., 2011). Similarly, drusen can regress and this can also lead to GA or CNV. It is also possible for drusen to regress and disappear without any residual sequelae (Bressler et al., 1995, Klein et al., 2007). This becomes a desirable outcome in clinical trials that trying to prevent or slow further progression to late AMD (Parodi et al., 2009, Jobling et al., 2015, Garcia Filho et al., 2014).

Drusen analysis in AMD is regarded as the main subject of interest when it comes to disease diagnosis, classification and progression. Number, area and size of drusen have been evaluated by numerous longitudinal studies to assess their correlation with risk of progression to late AMD (Bressler et al., 1990b, Wang et al., 2003, Klein et al., 2002). Several reports confirmed that confluent large drusen are risk factor for development of GA or CNV (Ferris et al., 2005, Klein et al., 2007). These parameters are now used for AMD staging and for predicating the likelihood of progression to advanced AMD.

1.8.2 Drusen quantification using colour fundus photography

Traditionally, fundus photography is the gold standard technique in the evaluation of patients with drusen. Drusen count, area and volume are measured manually by examining colour fundus photographs using a set of standardised circles. Drusen quantification are required to classify AMD as well as to assess the risk of progression to advanced AMD. Therefore, colour fundus photography becomes a fundamental tool in different AMD classification systems and large epidemiologic studies such as the Age-Related Eye Disease Study Group, the International Classification system and the Wisconsin classification system (The Age-Related Eye Disease Study Research, 2001, Bird et al., 1995, Klein et al., 1991).

Currently, a new clinical AMD classification system that combines the scientific literature with expert opinion has been introduced, attempting to establish consensus regarding nomenclature and classification systems as well as to make it easier in practical use (Ferris et al., 2013). This system developed a 5-stage classification scale for AMD. Eyes with no visible drusen or pigmentary abnormalities were

considered to have no signs of AMD. Small drusen was termed as drupelets and considered as normal ageing changes with no clinical significant for developing late AMD. While eyes with medium drusen but without pigmentary abnormalities were considered to have early AMD, eyes with large drusen or with pigmentary abnormalities associated with at least medium drusen were considered to have intermediate AMD. Finally, eyes with CNV or GA were considered to have late AMD.

Despite these classification systems that are based on colour fundus photograph were validated and proven to be useful, there are several drawbacks associated with manual grading of drusen, such as, interpersonal variability even with experienced graders and its time and effort consuming (Klein et al., 1991, Shin et al., 1999). Furthermore, the difficulty in outlining indistinct drusen and the lack of providing direct information regarding drusen anatomy and their effect on surrounding retinal tissue are crucial limitations for achieving objective clinical assessment.

Consequently, an automated detection and measurement of drusen from fundal photographs has been introduced as an attempt to make the grading of photographs easier and cheaper for clinicians and researchers (Bartlett and Eperjesi, 2007, Friberg et al., 2007, Smith et al., 2005). Although there is a great advancement in this field, these automated techniques have not gained acceptance owing to their failure to distinguish between drusen and other pale lesions as well as variable results compared with the manual method (Morgan et al., 1994). As a result, they have not been widely used in research or clinical settings.

1.8.3 Drusen quantification using OCT

The introduction of OCT in ophthalmic field have revolutionised our understanding of different retinal pathologies. OCT provides *in vivo* cross sectional images of different

retinal structures that is analogous to the histological structure. Recently, developed spectral domain OCT (SD-OCT) technology allows detection of fine abnormal retinal pathology (Srinivasan et al., 2006b, Wojtkowski et al., 2005). SD-OCT can provide drusen visualisation as well as it can detect any changes in adjacent retinal anatomy. These information have been used to detail pathological features and longitudinal changes around drusen location like the development of drusen-associated atrophy (Wu et al., 2014, Ouyang et al., 2013b).

Various automated segmentation algorithms to detect and quantify drusen on SD-OCT images have been developed (Gregori et al., 2011, Yi et al., 2009, Farsiu et al., 2008, Schlanitz et al., 2011, Iwama et al., 2012, Chen et al., 2013). Most of these algorithms segmented drusen based on the distance between an abnormal elevated RPE and a virtual normal RPE floor or calculated Bruch's membrane. Very few of these algorithms have been validated for accurate measurement of drusen area, height and volume (Schlanitz et al., 2011, Gregori et al., 2011, Schlanitz et al., 2010, Chiu et al., 2012). Several recent studies showed that changes in drusen area and volume over time can be assessed automatically using SD-OCT (Abdelfattah et al., 2016, Folgar et al., 2016, de Sisternes et al., 2014, Yehoshua et al., 2011, Nathoo et al., 2014). Thus, this strategy could change clinical practice significantly as a useful alternative method to drusen measurement by human graders using colour fundus photographs.

Currently, there are three SD-OCT devices provided with automated segmentation algorithms including Cirrus (Carl Zeiss Meditec Inc., Dublin, CA), 3D OCT (Topcon, Tokyo, Japan) and Spectralis (Heidelberg Engineering, GmbH, Heidelberg, Germany). Schlanitz et al. (Schlanitz et al., 2010) compared the performance of the automated segmentation algorithms in the three SD-OCT devices by analysing a

total of 1356 drusen. They concluded that Cirrus showed significantly fewer errors in detecting drusen than 3D OCT, while Spectralis did not detect drusen accurately owing to its failure of offering a true RPE segmentation. However, Iwama et al. (Iwama et al., 2012) has also evaluated the algorithm in 3D OCT and demonstrated that their algorithm allowed automated drusen area and volume assessment with minimal segmentation failures and good agreement with the assessment by certified graders on colour fundus photography.

1.8.4 Comparing drusen quantification by OCT with colour fundus photography

The representation of drusen is different between colour fundus photography and OCT. In colour fundus images, drusen are spotted as a yellow clusters within the retina, while in SD-OCT algorithm defines drusen as a degree of deformity in the retinal pigment epithelial layer (RPE) (Diniz et al., 2014, Jain et al., 2010).

Consequently, small drusen are not detected by OCT as they do not elevate RPE layer considerably. As a result, drusen count and area are underestimated by SD-OCT compared to fundus photography (Gregori et al., 2014, Yehoshua et al., 2013, Diniz et al., 2014). However, drusen volume are measured reliably by SD-OCT (Gregori et al., 2011). It is possible for drusen volume to decrease by 88% without any apparent change in colour fundus photographs and still be accurately measured by SD-OCT algorithm, which render this technique superior to colour fundus photography (Yehoshua et al., 2011). In addition, SD-OCT algorithm can measure true drusen not pseudodrusen (reticular drusen or subretinal drusenoid deposits), which lie above the RPE layer (Sivaprasad et al., 2016).

1.8.5 Recent clinical studies based on OCT drusen quantification

The ability of SD-OCT to measure drusen count, area and volume encouraged researchers to study the effect of these parameters on disease progression to advanced AMD (CNV or GA). Several reports have been published in this regard with variant results. Yehoshua et al. (Yehoshua et al., 2011) evaluated prospectively the change in drusen area and volume of 143 eyes over 2 years using SD-OCT. The changes in drusen volume were more prominent over a longer follow up periods (12 and 24 months) than at 6 months time. In this study 48% of eyes showed an increase in drusen volume while 40% remained stable and 12 % decreased at 12 months.

de Sisternes et al. (de Sisternes et al., 2014) using SD-OCT studied quantitative characteristics of drusen (count, area, volume and other features of drusen) to predict the likelihood of progression from early and intermediate AMD to CNV. Their retrospective study represented the results of 186 eyes of 128 AMD patients followed over a period of 5 years. They demonstrated that drusen volume, area, height and reflectivity are key features that can predict disease progression and drusen volume is the most sensitive predictor for progression within 30 months.

Nathoo et al. (Nathoo et al., 2014) collected retrospective data of 83 AMD patients to analyse the association of drusen load with the development of late AMD. The authors found an association between drusen volume and drusen area, and the development of CNV or GA over a period of 2 years using SD-OCT. Abdelfattah et al. (Abdelfattah et al., 2016) followed retrospectively 89 patients with wet AMD in one eye and for a total follow up period of two years. This study showed that a drusen

volume of 0.03 mm³ and more, in the fellow eye, is associated with four-fold increase in the development of late stage AMD. Furthermore, the baseline drusen volume was significantly higher in eyes developed late stage AMD. Folgar et al. (Folgar et al., 2016) reported similar findings and interestingly in their study for each 0.1 mm³ increase in baseline volume there was an increase of 31% in risk of developing CNV. On the other hand, Silva et al. (Silva et al., 2011) showed that there was no association between drusen measurements and disease progression to CNV. In their study drusen area and number were evaluated as predictive risk factors of developing CNV in the fellow eyes of patients with wet AMD using multimodal imaging including SD-OCT.

A recent study of 31 eyes evaluated drusen volume changes and their association with vascular changes and capillary retinal perfusion in intermediate AMD over a year follow-up (Reiter et al., 2019). The authors demonstrated that the increase in drusen volume was not associated with vascular changes or capillary retinal perfusion. A physiological-approached study of 15 AMD patients measured oxygen concentration at the outer retina, and then compared correlations between retinal thinning and drusen height and between retinal thinning and retinal hypoxia and found that the latter had a stronger correlation, indicating the potential value of this kind of study and its ability to detect earlier changes than OCT do (McHugh et al., 2019).

1.9 Overall hypothesis of this thesis

There are no markers that inform the time of conversion from early/intermediate AMD to wet AMD. For this reason, there is an unmet need to identify biomarkers that can fully predict the progression to wet AMD in order to allow early intervention before permanent damage. This study is designed to determine whether changes in imaging characteristics can more precisely explain conversion and be used to predict progression to wet AMD. I studied cohorts of normal eyes with aging, eyes with early/intermediate AMD and fellow eyes of patients with unilateral wet AMD to predict the rate of conversion to wet AMD.

1.10 Aims and objectives of this thesis

This study was designed to fulfil the following objectives:

1. To identify changes in retinal layer volumes in AMD eyes, which might be used as biomarkers for disease conversion.
2. To evaluate whether heritability was responsible for ageing changes of the retinal layer volumes.
3. To evaluate whether any of drusen parameters (count, area, volume) would predict AMD progression to CNV.
4. To identify biomarkers that can predict CNV type (occult or classic).
5. To evaluate whether artificial intelligence such as deep learning methods using OCT imaging data can predict the likelihood of progression from early/intermediate AMD to wet AMD

2 Chapter 2: Methodology

2.1 General methods

This is a retrospective observational cohort study of patients attending a tertiary referral medical retina clinic in Moorfields Eye Hospital between April 2010 and December 2018. Clinical and demographic data were collected from the medical records of the patients. Available OCT scans and FFA images were also collected and correlated with the patients' clinical data.

2.1.1 Study population

Patients with unilateral neovascular AMD and early or intermediate AMD in the fellow eye with 2 years follow-up were selected for the study. The eligible patients' fellow eyes were divided into progressors and non-progressors. The progressors were defined as fellow eyes with new onset macular fluid on "Year 2" scans confirmed by fluorescein angiography to show the presence of CNV. The non-progressors were the fellow eyes that had not converted on "Year 2" scans. In chapter 6, the progressors were classified based on the type of CNV into classic and occult.

A control group was also included in the study from normal healthy fellow eyes of patients with branch retinal vein occlusion.

2.1.2 Data collection

A baseline demographic data including age, sex, and laterality was recorded for all participants. Drusen measurements such as count, area and volume as well as retinal layer volumes such as retinal nerve fiber layer, ganglion cell-inner plexiform layer, inner nuclear layer, outer nuclear layer, photoreceptors, retinal pigment epithelium-Bruch's membrane complex and total retinal volume were collected at

baseline, year 1 and year 2. These collected data were tabulated into an Excel spreadsheet before transferring them into SPSS for statistical analysis.

2.1.3 Inclusion criteria

The inclusion criteria for the AMD eyes included early or intermediate AMD in the study eye and neovascular AMD in the fellow eye. Inclusion criteria also required the availability of three annual SDOCT scans captured at 12-15 months intervals. At least three scans over two years was required prior to conversion.

2.1.4 Exclusion criteria

Exclusion criteria were development of CNV within two years of the follow-up. Eyes with geographic atrophy, polypoidal choroidal vasculopathy, vitelliform lesions or other macular pathology such as diabetic retinopathy were excluded from the study. As we know that 20% of all AMD patients have polyps, for this reason we excluded these patients based on clinical suspicion and/or ICG availability. In addition, study eyes with poor quality OCT scan images (signal strength < 30), high refractive error (≥ 6 dioptres), glaucoma, previous retinal surgery or any other posterior segment disease were also excluded from the study.

2.1.5 Ethical approval

The Ethical Review Board of Moorfields Eye Hospital approved the data collection from the hospital medical records (ROAD 17/004). In chapter 4, the study had also local research ethics committee approval from the TwinsUK registry based at St Thomas' Hospital and participants gave informed consent. These studies were conducted in accordance with the tenets of the Declaration of Helsinki.

2.2 Retinal imaging, drusen measurements and retinal layer segmentation

Macular OCT images were acquired from one/both eye/s using a 6x6 mm macular cube scan (3D OCT, Topcon Corporation). All eyes had three SD-OCT scan images at baseline, year one and year two. The 3D OCT had a 6 μm axial image resolution and imaging speed of 18,000 axial scans per second. On the 3D OCT, the 3D macular scan used was 128 line raster with 512 A-scans each, within 6x6 mm². This kind of imaging gives a detailed structure of the retina similar to its histological structure. However, the choroidal layers could not be measured using this method.

The drusen characteristics in the fellow eye of each patient were determined using the drusen quantification software version 2.00 that is available on the Topcon 3D OCT device. Drusen measurements including drusen count, area and volume within the 6-mm cube centred on the fovea were collected retrospectively at baseline, year 1 and year 2. The algorithm on 3D OCT, which was validated in a previous study (Iwama et al., 2012), defines drusen based on calculating the difference between the elevated RPE caused by drusen and a virtual line representing the presumed Bruch's membrane. This study also showed that small drusen were poorly detected. Topcon 3D-OCT-2000 has a smallest drusen detection limit of 340 μm (Schlanitz et al., 2011).

Macular layer volumes were derived for circles of 3 and 6 mm diameter around the foveal centre, using automated layer segmentation software (Orion, Voxeleron LLC). The following layer volumes were derived: retinal nerve fiber layer (RNFL), ganglion cell-inner plexiform layer (GCIPL), inner nuclear layer (INL), outer nuclear layer (ONL), photoreceptors (PR), retinal pigment epithelium-Bruch's membrane complex

(RPE-BM) and total retinal volume (TRV). The layer boundaries are shown for a typical participant's OCT scan in Figure 9.

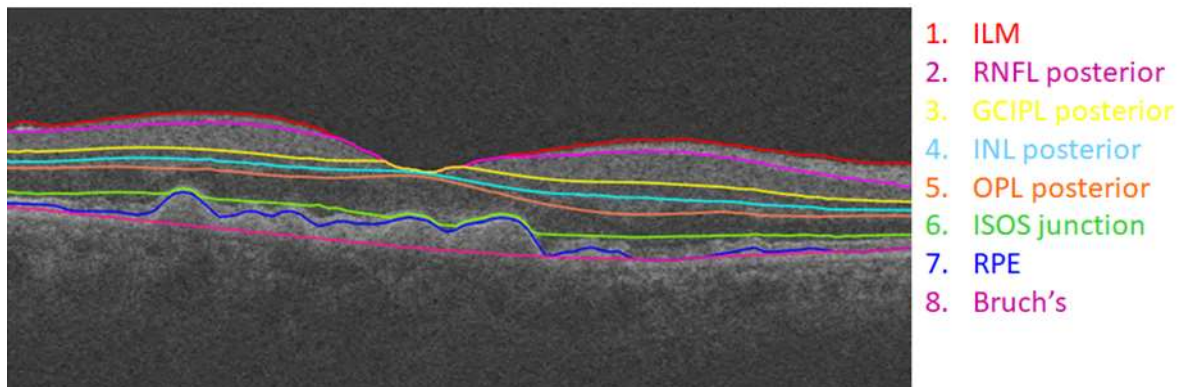


Figure 9. Retinal layer segmentation with detectable layer boundaries in a normal eye as analysed automatically by the Orion software. Layers 1-2 = Retinal Nerve Fiber Layer (RNFL); Layers 2-3 = Ganglion Cell Ganglion Cell and Inner Plexiform Layer (GCIPL); Layers 3-4 = Inner Nuclear Layer (INL); Layers 4-5 = Outer Plexiform Layer (OPL); Layers 5-6 = Outer Nuclear Layer (ONL); Layers 6-7 = Photoreceptor complex (PR); Layers 7-8 = Retinal Pigment Epithelium-Bruch's Membrane complex (RPE-BM); Layers 1-8 = Total Retinal Layers

2.3 Statistical Analysis

A test for normality (Shapiro-Wilks) was performed for each parameter. Where the distribution found to be normal, Student's *t*-test was used; otherwise, nonparametric *t*-tests (Mann-Whitney U and Wilcoxon signed-rank) were used.

The baseline measurements were analysed as predictors of progression to CNV using logistic regression analysis. Change in drusen measurements (count, area and volume) and/or retinal layer volumes from baseline to year 1 (first year) and from year 1 to year 2 (second year) were compared between the AMD eyes and the control group with the Mann-Whitney U test. A sub-analysis within each group was performed comparing drusen measurements and/or retinal layer volumes between the first year and the second year using Wilcoxon signed-rank test.

All statistical analyses were performed using SPSS software (IBM SPSS Statistics for Windows, Version 24.0). *P* values of < 0.05 were considered statistically significant.

3 Chapter 3: Changes in volume of various retinal layers over time in early and intermediate AMD

3.1 Introduction

Age –related macular degeneration (AMD) is one of the major causes of irreversible vision loss and blindness among people over 50 years of age in the western world (van Leeuwen et al., 2003, Friedman et al., 2004, Resnikoff et al., 2004). It is a progressive degenerative disease of the macula and is generally considered as a disease of the outer retina. AMD can be classified clinically into early, intermediate and advanced stage to characterize disease severity (Ferris et al., 2013). There are two advanced forms of AMD: neovascular (exudative or wet) AMD (nAMD) and geographic atrophy (GA).

Although nAMD is less common than GA, nAMD is responsible for 90% of all advanced cases of severe visual loss and legal blindness due to the development of choroidal neovascularisation (CNV) (Ferris et al., 1984). CNV is abnormal choroidal blood vessels that grow through Bruch membrane into the subretinal space, leading to the accumulation of subretinal fluid and pigment epithelium detachment (Green and Enger, 1993a, Campochiaro et al., 1999). CNV can develop into a discform scar as it matures. Therefore, there is an unmet need to identify biomarkers that can fully predict the progression to nAMD in order to initiate early treatment to reduce vision loss.

Different retinal layers have been described histologically as being affected by AMD. Photo-receptor cells loss (predominately rods) was found to occur in the earlier stage of AMD (Curcio et al., 1996, Jackson et al., 2002, Medeiros and Curcio, 2001), while an atrophy of the ganglion cell layer (GCL) occurs in the late stage of the disease (Medeiros and Curcio, 2001).

The advancement in OCT's image resolution have allowed us to compare in vivo retinal layers to the histological structure and improve segmentation to assess individual retinal layers. Several studies performed manual segmentation of retina and demonstrated that there are changes in the photoreceptor layer thickness, which is affected by drusen dynamics (Schuman et al., 2009, Hartmann et al., 2012, Sadigh et al., 2013, Sadigh et al., 2015).

Recently, automated segmentation software programmes that enable analysis layers of the retina qualitatively and quantitatively have been introduced (Tan et al., 2016, Terry et al., 2016). Using these softwares, recent studies of AMD eyes have demonstrated that there are changes not only in the outer retinal layers as previously established but also in the inner retina such as the ganglion cell complex (GCC) thickness, which includes GCL and inner plexiform layer (IPL) (Savastano et al., 2014, Lee and Yu, 2015, Yenice et al., 2015, Zucchiatti et al., 2015, Muftuoglu et al., 2017).

3.2 Aims

In this study, we aimed to look at change in retinal layer volumetric measures on OCT in eyes with early/intermediate AMD compared to a control population over time to understand the longitudinal changes in these layers. It is also compared between the eyes that progressed to wet AMD and others that did not.

3.3 Methods

In addition to the methods have been discussed in chapter 2, the following analysis was also used in this study.

Comparisons of mean of all retinal layer volumes between AMD eyes and control eyes were performed at baseline and year 2. Volume changes from baseline to year-2 were also compared in each group and between the 2 groups.

A sub-analysis was performed in the AMD eyes comparing retinal layer volumes between AMD eyes that progressed (progressors) to wet AMD and others that did not progress (non-progressors). Mean volumes of retinal layers were compared between the 2 groups at baseline and year 2. Longitudinal changes of retinal layer volumes over the 2-year follow-up were also compared within each group and between the groups. The baseline retinal layer volumes were also analysed as predictors of progression to wet AMD using logistic regression analysis that generated the odds ratio (OR) with 95% confidence intervals (CIs).

3.4 Results

3.4.1 Demographics of Participants

102 eyes of 102 individuals were included in the study. 71 participants (42 females [59.2%] and 28 males [39.4%]) were included in the AMD group and 31 participants (19 females [61.3%] and 12 males [38.7%]) were included in the control group. Mean (SD) ages were 74 (8.5) years and 64.1 (6.4) years for AMD and controls respectively.

Of the 71 AMD participants, 31 patients progressed to wet AMD at 24 months \pm 2 months, while 40 did not progress (Figure 10). The progressors consisted of 23

females and 8 males. The non-progressors consisted of 20 females and 20 males. Mean ages were similar between the two subgroups. Table 5 summarises the participant demographics.

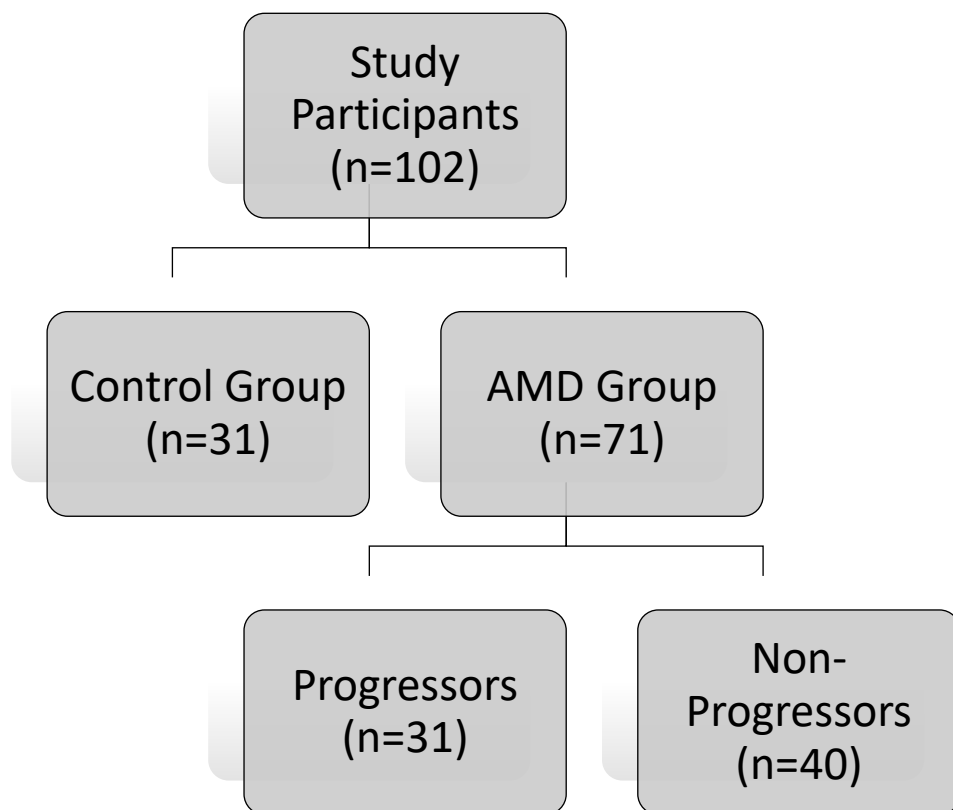


Figure 10. Flow chart of the study participants of Chapter 3

Table 5. Demographics of the Study Participants

Variable	Control	AMD	AMD Non-Progressors	AMD Progressors
Number of Eyes	31	71	40	31
Age				
Mean (SD)	64.1 (6.4)	74 (8.5)	72 (8.7)	76 (7.5)
Median	65	76	72.5	77
Minimum- Maximum	54 – 79	57 - 91	57-89	62-91
Sex				
Female, n (%)	19 (61.3%)	43 (60.6%)	20 (50%)	23 (74.2%)
Male, n (%)	12 (38.7 %)	28 (39.4%)	20 (50%)	8 (25.8%)
Laterality				
Right, n (%)	21 (67.7%)	48 (67.6%)	26 (65%)	22 (71%)
Left, n (%)	10 (32.3%)	23 (32.4%)	14 (35%)	9 (29%)
Follow-Up Exam / Conversion (months)	-	-		
Mean (SD)			23.75 (1.33)	23.32 (2.06)
Median			24	24
Minimum – Maximum			20 - 26	17 - 27

3.4.2 AMD versus Control

3.4.2.1 Mean Retinal Layer Volumes at Baseline and Year 2

Table 6 shows mean volumes of individual retinal layers in the central macular area (6 mm diameter) measured at two time points, baseline and year 2. There were statistically significant differences between the 2 groups in mean volumes of GCIPL, INL, PR and RPE-BM at both baseline and year 2. The GCIPL and INL had less volumes in AMD eyes than controls at baseline (both $P < 0.05$) and year 2 (both $P < 0.05$). Conversely, PR and RPE-BM volumes were greater in AMD eyes than controls at baseline (both $P < 0.05$) and year 2 (both $P < 0.05$). Otherwise, no significant differences were found between the 2 groups in volumes of other retinal layers.

Table 6. Mean Retinal Layer Volumes at Baseline and Year 2 in Age-Related Macular Degeneration Eyes (n = 71) and Control Eyes (n = 31)

Retinal Layer and Time Point		AMD Group (n = 71) Mean (SD)	Control Group (n = 31) Mean (SD)	P Value
TRV	Baseline	8.22 (.44)	8.29 (.35)	0.469
	Year 2	8.16 (.45)	8.23 (.42)	0.563
RNFL	Baseline	1.12 (.13)	1.09 (.08)	0.506
	Year 2	1.09 (.13)	1.08 (.07)	0.438
GCIPL	Baseline	1.84 (.19)	1.97 (.14)	0.001
	Year 2	1.85 (.18)	1.95 (.16)	0.011
INL	Baseline	1.00 (.07)	1.03 (.06)	0.026
	Year 2	.990 (.07)	1.03 (.06)	0.014
OPL	Baseline	.666 (.12)	.672 (.06)	0.544
	Year 2	.705 (.11)	.675 (.07)	0.133
ONL	Baseline	2.29 (.22)	2.24 (.17)	0.438
	Year 2	2.21 (.21)	2.23 (.16)	0.426
PR	Baseline	1.28 (.09)	1.25 (.06)	0.006
	Year 2	1.30 (.08)	1.25 (.06)	0.008
RPE-BM	Baseline	.148 (.08)	.102 (.11)	0.000
	Year 2	.169 (.11)	.102 (.09)	0.000

Statistically significant values with $P < 0.05$ are in bold.

TRV = Total Retinal Volume; RNFL = Retinal Nerve fiber Layer; GCIPL = Ganglion Cell and Inner Plexiform Layer; INL = Inner Nuclear Layer; OPL = Outer Plexiform Layer; ONL = Outer Nuclear Layer; PR = Photoreceptors; RPE-BM = Retinal Pigment Epithelium-Bruch's Membrane complex

3.4.2.2 Longitudinal Volume Change from Baseline to Year 2

Longitudinal comparisons from baseline to year 2 in AMD and control eyes are shown in table 7. Mean total retinal volumes (TRV) decreased significantly from baseline to year 2 in both AMD and control eyes by 0.0561 ($P = 0.018$) and 0.0579 ($P = 0.011$) respectively. From baseline to year 2 in AMD eyes, mean volumes of RNFL and ONL decreased by 0.0232 mm³ ($P = 0.033$) and 0.0851 mm³ ($P = 0.001$) respectively. In contrast, there were significant increase in mean volumes of OPL and RPE-BM in AMD eyes by 0.0391 mm³ ($P = 0.000$) and 0.0209 mm³ ($P = 0.000$) respectively.

From baseline to year 2, there were significant differences between AMD eyes and controls in longitudinal volume change of OPL ($P = 0.02$), ONL ($P = 0.008$) and RPE-BM ($P = 0.02$). Otherwise, no significant difference was found between the 2 groups in the longitudinal volume change from baseline to year 2 of other retinal layers.

Differentiation between AMD and control groups by volume measurements and longitudinal volume change are shown in Figure 11. It can be noted that, despite some overlap existed between AMD and controls, the GCIPL, INL, and ONL volumes of the AMD eyes were reduced substantially compared to control eyes.

Table 7. Longitudinal Change in Retinal Layer Volumes in Age-Related Macular Degeneration Eyes (n = 71) and Control Eyes (n = 31).

Retinal Layer and Group		Volume Change (Baseline – year 2) Mean (SD)	<i>P</i> Value*	<i>P</i> Value [‡]
TRV	AMD	.0561 (.195)	0.018	0.956
	Control	.0579 (.118)	0.011	
RNFL	AMD	.0232 (.09)	0.033	0.904
	Control	.0184 (.05)	0.052	
GCIPL	AMD	-.0077 (.114)	0.324	0.757
	Control	.0171 (.074)	0.075	
INL	AMD	.0131 (.056)	0.053	0.361
	Control	.0035 (.045)	0.672	
OPL	AMD	-.0391 (.094)	0.000	0.02
	Control	-.0028 (.058)	0.792	
ONL	AMD	.0851 (.148)	0.001	0.008
	Control	.0206 (.06)	0.799	
PR	AMD	-.0184 (.072)	0.130	0.175
	Control	.0011 (.067)	0.926	
RPE-BM	AMD	-.0209 (.052)	0.000	0.02
	Control	.0007 (.023)	0.754	

Statistically significant values with *P* < 0.05 are in bold.

TRV = Total Retinal Volume; RNFL = Retinal Nerve Fiber Layer; GCIPL = Ganglion Cell and Inner Plexiform Layer; INL = Inner Nuclear Layer; OPL = Outer Plexiform Layer; ONL = Outer Nuclear Layer; PR = Photoreceptors; RPE-BM = Retinal Pigment Epithelium-Bruch’s Membrane complex

*Wilcoxon signed-rank test and Paired *t*-test for paired volume measurements, baseline versus year 2.

[‡] Mann-Whitney U test and Independent *t*-test, AMD group versus control group.

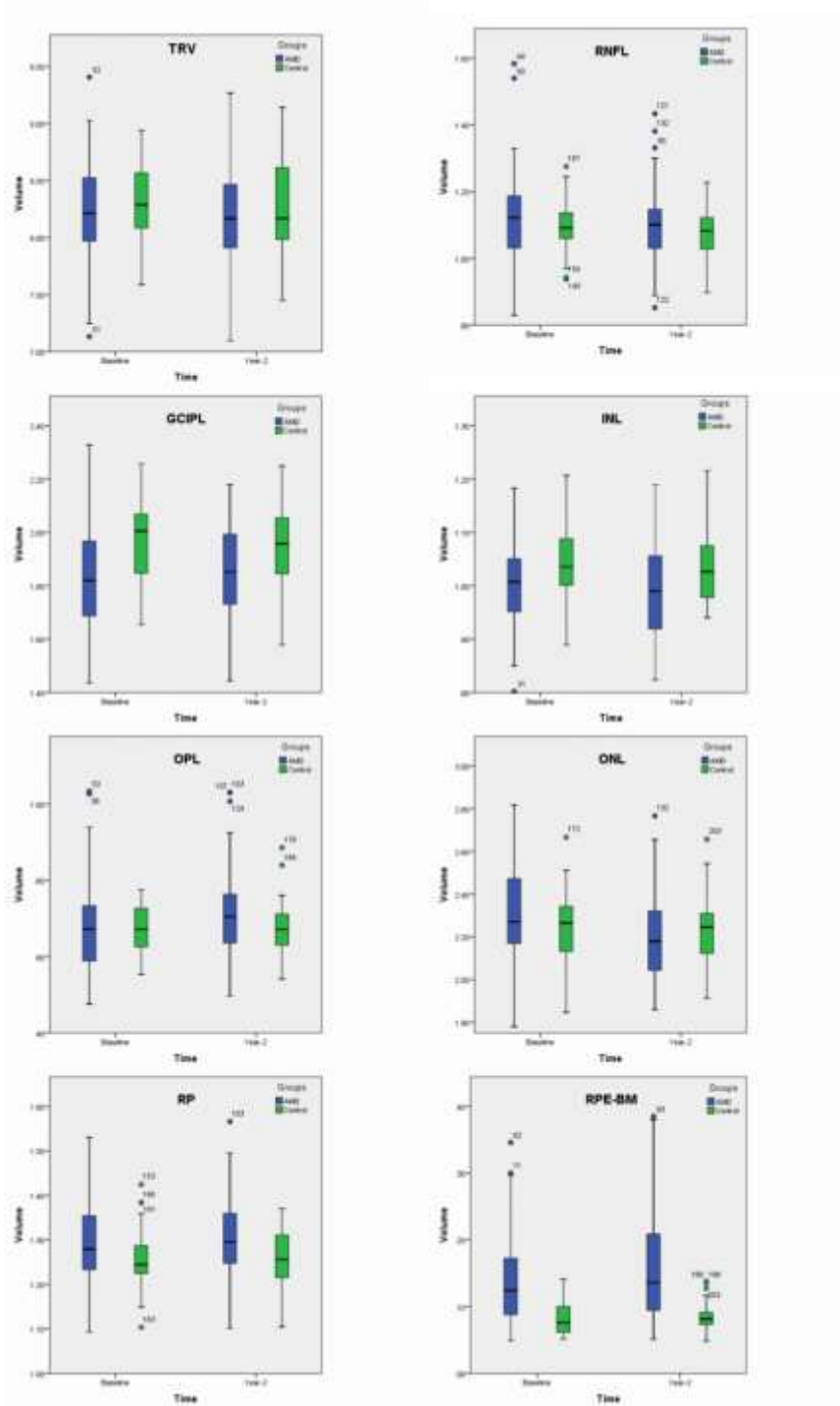


Figure 11. Box plots showing longitudinal volume change of AMD and control eyes in total retinal volume (TRV), Retinal Nerve Fiber Layer (RNFL), Ganglion Cell and Inner Plexiform Layer (GCIPL), Inner Nuclear Layer (INL), Outer Plexiform Layer (OPL), Outer Nuclear Layer (ONL), Photoreceptors (PR), and Retinal Pigment Epithelium-Bruch's Membrane complex (RPE-BM). AMD = age-related macular degeneration.

3.4.3 Progressors versus Non-Progressors

3.4.3.1 Mean Retinal Layer Volumes at Baseline and Year 2

Table 8 shows mean volumes of retinal layers of progressors and non-progressors at two time points, baseline and year 2. There were statistically significant difference between the progressors and non-progressors in mean volumes of GCIPL ($p= 0.001$) and OPL ($p= 0.035$) at baseline, and RPE-BM (0.017) at year 2. GCIPL and OPL volumes were smaller in progressors than non-progressors at baseline. Conversely, RPE-BM volume was greater in the progressing group than non-progressing one at year 2. Otherwise, no significant difference was found between the 2 groups in volumes of other retinal layers.

3.4.3.2 Longitudinal Volume Change from Baseline to Year 2

Longitudinal comparisons from baseline to year 2 in progressing and non-progressing eyes are shown in table 9. Despite decreasing of mean TRV from baseline to year 2 in both groups, the reduction was a statistically significant ($P = 0.038$) only in the non-progressing eyes by rate of 0.0614 mm^3 .

Regarding the inner retinal layers, there was a significant decrease in mean volume of GCIPL by 0.0214 mm^3 (0.017) in non-progressing eyes only. This reduction in the GCIPL volume was statistically significant between the 2 groups, suggesting early layer loss. In addition, there was a significant reduction in the INL volume in progressors only by $.9768 \text{ mm}^3$ ($P = 0.042$).

Regarding the outer retinal layers, there were significant expansion in the volume of OPL and RPE-BM and reduction in the volume of ONL in both groups over the 2-year follow-up. There was also an increase in PR volume from baseline to year 2 in non-progressors by 0.0240 mm^3 ($P = 0.034$).

Table 8. Mean Retinal Layer Volumes at Baseline and Year 2 in Non-Progressers (n = 40) and Progressers (n = 31).

Retinal Layer and Time Point		Non-Progressors Group (n = 40) Mean (SD)	Progressors Group (n = 31) Mean (SD)	P Value
TRV	Baseline	8.27 (.35)	8.15 (.53)	0.286
	Year 2	8.21 (.38)	8.10 (.54)	0.352
RNFL	Baseline	1.11 (.10)	1.13 (.16)	0.586
	Year 2	1.09 (.10)	1.09 (.17)	0.451
GCIPL	Baseline	1.91 (.17)	1.76 (.18)	0.001
	Year 2	1.88 (.17)	1.80 (.19)	0.051
INL	Baseline	1.00 (.07)	.997 (.08)	0.571
	Year 2	1.00 (.06)	.976 (.08)	0.214
OPL	Baseline	.690 (.10)	.634 (.14)	0.035
	Year 2	.725 (.10)	.678 (.12)	0.097
ONL	Baseline	2.26 (.15)	2.33 (.28)	0.220
	Year 2	2.19 (.17)	2.24 (.25)	0.355
PR	Baseline	1.28 (.08)	1.29 (.09)	0.685
	Year 2	1.30 (.08)	1.30 (.09)	0.869
RPE-BM	Baseline	.141 (.09)	.158 (.07)	0.074
	Year 2	.159 (.13)	.183 (.08)	0.017

Statistically significant values with $P < 0.05$ are in bold.

TRV = Total Retinal Volume; RNFL = Retinal Nerve fiber Layer; GCIPL = Ganglion Cell and Inner Plexiform Layer; INL = Inner Nuclear Layer; OPL = Outer Plexiform Layer; ONL = Outer Nuclear Layer; PR = Photoreceptors; RPE-BM = Retinal Pigment Epithelium-Bruch's Membrane complex

Table 9. Longitudinal Change in Retinal Layer Volumes in Non-Progressors (n = 40) and Progressors (n = 31)

Retinal Layer and Group		Volume Change (Baseline – year 2) Mean (SD)	<i>P</i> Value*	<i>P</i> Value [‡]
TRV	Non-Progressors	.0614 (.180)	0.038	0.805
	Progressors	.0494 (.216)	0.214	
RNFL	Non-Progressors	.0158 (.072)	0.083	0.711
	Progressors	.0328 (.109)	0.081	
GCIPL	Non-Progressors	.0214 (.089)	0.017	0.028
	Progressors	-.0454 (.132)	0.337	
INL	Non-Progressors	.0071 (.068)	0.437	0.354
	Progressors	.0208 (.089)	0.042	
OPL	Non-Progressors	-.0352 (.082)	0.010	0.643
	Progressors	-.0441 (.110)	0.033	
ONL	Non-Progressors	.0761 (.099)	0.000	0.935
	Progressors	.0968 (.195)	0.01	
PR	Non-Progressors	-.0240 (.068)	0.034	0.360
	Progressors	-.0113 (.077)	0.427	
RPE-BM	Non-Progressors	-.0178 (.056)	0.05	0.297
	Progressors	-.0248 (.047)	0.007	

Statistically significant values with $P < 0.05$ are in bold.

TRV = Total Retinal Volume; RNFL = Retinal Nerve Fiber Layer; GCIPL = Ganglion Cell and Inner Plexiform Layer; INL = Inner Nuclear Layer; OPL = Outer Plexiform Layer; ONL = Outer Nuclear Layer; PR = Photoreceptors; RPE-BM = Retinal Pigment Epithelium-Bruch's Membrane complex

*Wilcoxon signed-rank test and Paired *t*-test for paired volume measurements in each group, baseline versus year 2.

[‡] Mann-Whitney U test and Independent *t*-test, Progressors group versus non-progressors group.

3.4.3.3 Prediction of progression to wet AMD based on baseline retinal layer volumes

Baseline volumes of RNFL, GCIPL, INL, OPL, PR and RPE-BM were assessed as predictors of progression to wet AMD (Table 10). Logistic regression analysis of these measurements revealed that baseline volume of GCIPL was the only statistically significant among all other layers. For every one-unit decrease in GCIPL volume, we expect a 0.005 increase in the log-odds of progression to wet AMD.

Table 10. Assessing predictors for AMD progression using logistic regression analysis

Baseline Retinal Volumes	B	SE	Odds Ratio	95% CI	P value
RNFL	3.614	2.655	37.131	.204 - 6755.431	.173
GCIPL	-5.224	2.576	.005	.000 - .839	.043
INL	1.534	5.603	4.636	.000 - 272676	.784
OPL	-4.897	6.833	.007	.000 - 4894.59	.474
ONL	-.646	2.574	.524	.003 - 81.270	.802
PR	7.192	5.760	1328.353	.017 - 106176904.040	.212
RPE-BM	2.632	3.464	13.904	.016 - 12342.559	.447

3.5 Discussion

The present study showed that some retinal layer volumes are significantly different between AMD and control eyes. The volume of inner retinal layers (GCIPL and INL) were lesser in AMD eyes than in controls, while the volume of outer retinal layers (PR and RPE-BM) were greater in AMD eyes as compared to controls. In addition, some retinal layers underwent volume change in AMD eyes over the 2-year follow-up. There was a reduction in ONL volume in AMD eyes over the follow-up period. In contrast, OPL and RPE-BM increased in volume from baseline to year 2 in AMD

eyes. Therefore, measurements of inner and outer retinal layer volumes differentiated AMD eyes from control ones.

Sub-analysis of the AMD eyes from baseline to year 2 showed that change in the inner retinal volumes (GCIPL and INL) might differentiate the progressors from the non-progressors, whereas the outer retinal volumes did not. The volume of GCIPL at baseline was thinner in the progressors and this volume did not change significantly over the 2-year follow-up. However, the INL volume decreased significantly in the progressors from baseline to year 2. Taken together, these findings suggest that GCIPL is affected firstly during the early stage of the disease, followed by INL that continues to decrease significantly prior to conversion.

The current finding of GCIPL and INL thinning in early/intermediate AMD is consistent with previous studies using OCT (Savastano et al., 2014, Lee and Yu, 2015, Yenice et al., 2015, Zucchiatti et al., 2015, Borrelli et al., 2017, Camacho et al., 2017, Muftuoglu et al., 2017). Different theories were proposed to explain the underlying mechanism of GCIPL and INL thinning. One theory is that this may occur as a result of retinal microvascular abnormality that leads to reduction in inner retina perfusion and ischemia (Toto et al., 2016, Toto et al., 2017, Feigl et al., 2007, Villegas-Perez et al., 1998). Toto and colleagues (2016, 2017) investigated alteration in superficial and deep retinal plexuses in patients affected by early/intermediate AMD using optical coherence tomography angiography (OCTA). The authors found that both retinal plexuses are changed and these changes start immediately at the early disease stages, resulting in damage of the inner and the outer retina. Evidence of a number of changes in the inner retinal vasculature has also been reported in an animal model (Villegas-Perez et al., 1998). Feigl et al., (2007) reviewed previous psychophysical and electrophysiological studies in early AMD and proposed that

most of the function impairment starts at the level of postreceptor cell layers, especially those located in the INL and IPL. These inner retinal cell layers are primarily affected by chronic ischemia as reported previously (Yu and Cringle, 2001, Cringle et al., 2002). Postreceptor cell layers are located in the watershed zone between central retinal artery and choroid, and therefore are more vulnerable to ischemia than the photoreceptors that are located closer to the choroid. This might explain why the photoreceptors are more resistant to ischemic distress than the postreceptor cells. However, the exact reason for retinal vascular changes and retinal cell layers ischemia in AMD remain unclear.

Another theory is that synaptic malformation due to photoreceptors loss could lead to reducing transneuronal input to inner retina, triggering the inner retina degeneration process (Strettoi et al., 2002). Evidence of disorganised synaptic architecture of the OPL and IPL in a retinal degenerative mice has been reported (Blanks et al., 1974). This type of anterograde degeneration (Wallerian degeneration) can extend to the brain tissue as shown in recent studies, which have found a reduction in the visual white matter volume in AMD (Yoshimine et al., 2018, Hernowo et al., 2014). A similar findings has also been reported in glaucoma (Hernowo et al., 2011). In contrast, thinning of inner retinal layers can be resulted from neurological diseases (Petzold et al., 2017, Gulmez Sevim et al., 2019); thinning of the RNFL and GCIPL has been shown to be associated with dementia, Parkinson disease and multiple sclerosis (Ko et al., 2018, Khawaja et al., 2016). This might be explained by the mechanism of retrograde transneuronal degeneration from the brain tissue to the inner retina.

The expansion in OPL layer volume in AMD eyes during the 2-year follow-up should be interpreted with caution as this layer is difficult to be imaged using OCT because a change in the angle of incidence of the OCT beam on the OPL can show it as

thicker if Henle's fibres are revealed. Being a thin, plexiform layer, its variance is therefore high. So if this change is indeed real, it could occur mechanically as the retina attempts to preserve structural integrity through the role of the Muller cells. It is also consistent with a light microscopic study that demonstrated that there is a displacement of nuclei from the ONL into the OPL secondary to shrinkage of their attached fibres (Gartner and Henkind, 1981). OPL thickening with age has also been reported in a study of 297 healthy eyes (Nieves-Moreno et al., 2018). Thus, the OPL volume increase might represent remodelling or might also be a consequence of mechanical factors, including expansion as neighbouring cellular layers might reduce in volume.

Despite no statistically difference in ONL volume between AMD eyes and controls, the reduction in ONL volume from baseline to year 2 in AMD eyes was statistically significant and this may indicate later degeneration of the photoreceptor nuclei. This finding is consistent with histopathology result that demonstrated ONL thinning in ageing models (Machida et al., 2000, Gartner and Henkind, 1981, Shelley et al., 2009b). These findings have also been confirmed by recent studies using OCT that showed ONL thinning in eyes with intermediate AMD (Sadigh et al., 2013, Schuman et al., 2009, Brandl et al., 2019). This does not translate to visual loss in eyes with intermediate AMD suggesting that the volume of photoreceptors does have a certain level of redundancy and so existing nuclei may be sufficient to maintain synaptic connections and maintain visual function.

Another interesting finding was the expansion of PR volume in AMD eyes which could be due to swelling of the cone distal axon as shown in a histological study (Shelley et al., 2009b). As the RPE ages, function, including phagocytosis of photoreceptor outer segments, may decline, which might explain this increase in PR

layer volume with age and in AMD (Bonilha, 2008). Increase in PR volume has been shown in a study of 68 normal eyes (Pakdel et al., 2018), agreeing with the results of the present study. Another explanation similar to that of the OPL expansion is that PR expansion might be due to displacement of nuclei from the ONL to the layer of ellipsoid zones of the rods and cones (Gartner and Henkind, 1981). Behbehani et al.(2017) also observed this in patients with multiple sclerosis and concluded that this was not “compensatory” thickening to the GCIPL thinning. However, a recent OCT study has reported a lesser PR thickness in eyes with early AMD stages compared to age-matched healthy eyes (Brandl et al., 2019). Reduction in PR outer segment thickness has also been shown in a longitudinal OCT study of 85 dry AMD eyes (Nittala et al., 2019). Using different methodology including OCT device, segmentation software and participant’s demographics might explain the disagreement with present study.

Finally, the current study showed that RPE-BM volume was greater in AMD eyes than controls and there was a significant increase in its volume from baseline to year 2. This finding is consistent with a recent study using Spectrals OCT (Brandl et al., 2019). These findings can be explained in term of drusen formation, extracellular deposits that accumulate between RPE and BM. A previous study found that RPE-BM thickening was associated with progression to advanced AMD (Ferrara et al., 2017).

This, to our knowledge, is the first study to explore longitudinally the change in retinal layer volumes in AMD eyes using OCT. Moreover, our study evaluated both the inner and outer retina that has not been done in most of the previous studies.

Limitations of the present study are no adjustments were made for age, sex, ethnicity and axial length or refraction. These factors affect retinal layer thickness and volume as shown in previous studies (Subhi et al., 2016), therefore, including them in a future study is required. .

In summary, our data showed abnormal retinal layer volumes and total volume changes in eyes with early and intermediate AMD. The inner and outer retinal layer volume measurements differentiated AMD eyes from control eyes. The mean GCIPL and INL volumes were less in eyes with AMD as compared to control eyes, while the mean PR and RPE-BM volumes were higher. Moreover, OPL and RPE-BM volumes were found to increase, whereas the volume of ONL was found to decrease during the 2-year follow-up in AMD eyes. In progressors, there was a progressive reduction in the volume of INL and ONL, and a significant expansion in the volume of RPE-BM, but the GCIPL volume remained unchanged. The thinning of GCIPL volume at baseline may be used as a biomarker for disease conversion.

By interpreting the whole data, we can conclude that reduction in GCIPL volume is followed by the reduction in INL volume as the disease progresses. These findings suggest that GCIPL and INL atrophies may precede ONL atrophy in AMD eyes, and migration of the latter nuclei to adjacent layers (OPL and RP) might be the cause of their expansions. This study shows that although significant efforts are made to study the outer retina in AMD, there are inner retinal changes that occur in these eyes and little attention has been paid to them as the changes are subtle and not visible with the naked eyes on routine retinal imaging.

4 Chapter 4: Retinal layer volumes: age associations and heritability (Twin Study)

4.1 Introduction

Spectral domain optical coherence tomography (OCT) yields a cross-sectional representation of the retinal layers allowing precise assessment of retinal structural pathology. Qualitative assessment of OCT images guides clinical diagnoses. For macular OCT, the quantitative measure traditionally used, in both clinical and research settings, is total retinal thickness, often divided into circular subfields around the foveal centre. More recently, segmentation algorithms have allowed quantification of the thickness or volume of each layer separately, from the thickness of the retinal nerve fibre layer (RNFL) down to the thickness of the retinal pigment epithelium (RPE). This is of clinical and scientific interest as layers are often selectively attenuated in different retinal diseases. In addition, thinning of retinal layers can be associated with neurological diseases (Petzold et al., 2017, Gulmez Sevim et al., 2019); thinning of the RNFL has been shown to be associated with cognitive impairment, with evidence that such measurements could have predictive value (Ko et al., 2018). Similarly thinning of the RPE-Bruch's membrane (RPE-BM) with age have also been observed in the Biobank cohort aged 40-69 years (Ko et al., 2017).

Twin studies allow investigation of relative genetic and environmental contributions to phenotypic traits. By making measurements in monozygotic (MZ) and dizygotic (DZ) twin pairs, intra-pair correlation can be compared: a significantly higher

correlation in MZ twins indicates that genetic factors are important. Formal calculation of heritability by twin modelling permits estimation of the proportion of the variance in a trait that is attributable to genetic factors. Previous twin studies have demonstrated significant heritability for macular thickness (Chamberlain et al., 2006), macular pigment optical density (Liew et al., 2005, Hogg et al., 2012) and spatial patterns (a ring-like distribution of macular pigment that can be seen by fundus autofluorescence) (Hogg et al., 2012, Tariq et al., 2014), retinal vascular patterns (Vergmann et al., 2017) and peripapillary RNFL (Hougaard et al., 2003).

4.2 Aims

In the present study, we analysed segmented layer volumes from macular OCT scans in a twin cohort using an automated segmentation algorithm to investigate heritability of each layer separately. We also explored associations with age and right-left eye correlations in the same cohort.

4.3 Methods

Parts of the methods have been discussed in chapter 2. Additional methodologies are as follows:

4.3.1 Participants

Participants were recruited from the TwinsUK registry based at St Thomas' Hospital. This is a cohort of largely healthy adult twins, who have volunteered for research studies (Moayyeri et al., 2013). The participants in the present study were taking part in a larger electroretinography study (Bhatti et al., 2017). Figure 12 demonstrates the study participants of the present study.

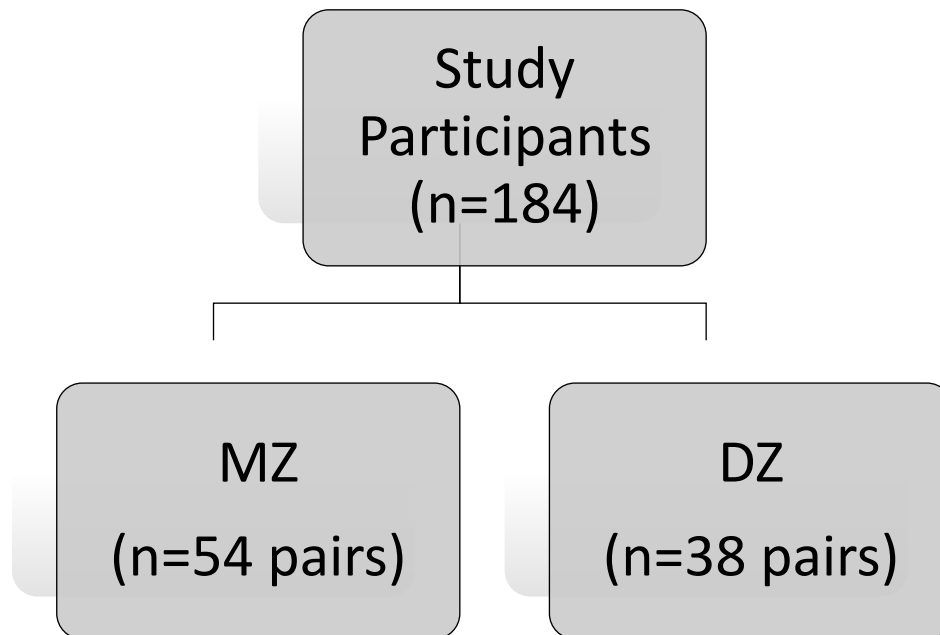


Figure 12. Flow chart of the study participants of Chapter 4.

4.3.2 Calculating correlations

Coefficients of intra-pair correlation were calculated for MZ and DZ twins. Pearson coefficients were used, with Spearman coefficients also calculated for any parameters found to differ significantly from a normal distribution (Kolmogorov-Smirnov test). Correlations with age were also calculated, as well as coefficients of inter-eye correlation for each parameter.

4.3.3 Calculating heritability

Age-adjusted heritability was estimated formally for each of the layer volumes (averaged between eyes for each participant), using maximum likelihood structural equation twin modelling as described previously (Mahroo et al., 2014), using the OpenMx package (<http://openmx.psyc.virginia.edu>) in the R statistical computing

environment (<http://www.r-project.org>). The variance of a trait is estimated by some combination of the contributions from 3 factors: the additive genetic component (A); the shared environment (C), or the non-additive genetic component (D); the unique environment (E). Univariate ACE or ADE models were executed with standardized path coefficients and expected variance and covariance matrices. Goodness of fit of the full and reduced ACE and ADE models were compared with the observed data. The most parsimonious model to explain the observed variance was selected using the Akaike information criterion; this was identified as the AE model for most of the phenotypes. Heritability was calculated as the proportion of total variance of the trait (V) resulting from the additive genetic effect (A) in the best-fitting model.

4.4 Results

Macular OCT images from 184 participants (54 MZ pairs; 38 DZ pairs) were included for analysis. In 4 participants, the image from one eye only was used due to a poor quality scan in the fellow eye. Mean (SD) age was 62.0 (11.1) years. For MZ pairs, mean (SD) age was 60.1 (11.6) years and ranged from 32 to 84 years. For DZ pairs, mean (SD) age was 64.8 (10.0) years, ranging from 36 to 86 years. MZ pairs were slightly younger ($p=0.044$), and so age-adjusted heritability estimates were generated. The majority of twins were females (all of the DZ pairs, and 93% of the MZ pairs), reflecting the demographics of the TwinsUK cohort.

4.4.1 Mean values and correlations with age

Table 11 shows means and standard deviations for the various layer volumes for the whole cohort. None of the parameters were found to differ significantly from a normal distribution with the exception of RPE-BM volume. Correlations with age are also given in Table 11. Here, parameters from both twins were averaged for each pair, so

that each pair contributed only once. Significant negative correlations with age were observed for TRV (for 3 mm and 6 mm circles), RNFL (6 mm circle), GCIPL (3 and 6 mm), and INL (3 mm).

Significant positive correlations with age were observed for PR (for 3 and 6 mm circles), RPE (3 and 6 mm), and OPL (6 mm circle). The age correlations were moderately strong (magnitude >0.4) for GCIPL (for 3 and 6 mm) and for PR (6 mm circle). These parameters are plotted against age in Figure 13. Using a simple linear fit, GCIPL volume declined by 0.022 mm^3 (3 mm circle) and 0.067 mm^3 (6 mm circle) per decade. PR volume (6 mm circle) increased by 0.033 mm^3 per decade.

4.4.2 Inter-eye correlations

The final column of Table 11 gives the inter-eye correlation coefficient for each parameter. All inter-eye correlations were highly significant ($p < 1 \times 10^{-8}$). Correlations were highest (>0.8) for TRV and GCIPL (both for the 6 mm circle); all segmented layer volumes showed a higher correlation for the 6 mm circle compared with the 3 mm circle.

Table 11. Segmented layer volumes, correlations with age, and correlations between eyes. Mean (SD) values are given for the whole cohort (n=184). Correlations with age are given (with parameters from both twins averaged within each twin pair). Inter-eye correlations are given for the cohort.

Circle diameter (mm)	Parameter	Mean (SD) value (mm ³)	Correlation with age		Inter-eye correlation coefficient
			Correlation coefficient	p value	
3	TRV	2.178 (0.098)	-0.270*	0.009	0.768*
	RNFL	0.209 (0.019)	-0.077	0.464	0.565*
	GCIPL	0.548 (0.053)	-0.499*	4.21x10⁻⁷	0.748*
	INL	0.289 (0.026)	-0.353*	5.52x10⁻⁴	0.633*
	OPL	0.195 (0.029)	0.194	0.064	0.417*
	ONL	0.625 (0.048)	-0.126	0.231	0.634*
	PR	0.314 (0.032)	0.364*	3.56x10⁻⁴	0.433*
	RPE-BM	0.041 (0.070)	0.245* (0.231*)	0.018 (0.025)	0.469* (0.681*)
6	TRV	8.331 (0.371)	-0.335*	0.001	0.863*
	RNFL	1.158 (0.127)	-0.535*	4.01x10⁻⁸	0.754*
	GCIPL	1.967 (0.168)	-0.483*	1.07x10⁻⁶	0.835*
	INL	1.001 (0.084)	-0.157	0.134	0.748*
	OPL	0.688 (0.077)	0.245*	0.018	0.428*
	ONL	2.252 (0.130)	-0.163	0.119	0.774*
	PR	1.266 (0.099)	0.424*	2.50x10⁻⁵	0.508*
	RPE-BM	0.144 (0.176)	0.260* (0.263*)	0.012 (0.011)	0.537* (0.673*)
<p>All inter-eye correlations were highly significant ($p < 1 \times 10^{-8}$).</p> <p>All are Pearson correlation coefficients, but for RPE-BM parameters, Spearman coefficients are also given in parentheses as these parameters deviated from a normal distribution.</p> <p>*Asterisk denotes significance ($p < 0.05$).</p>					

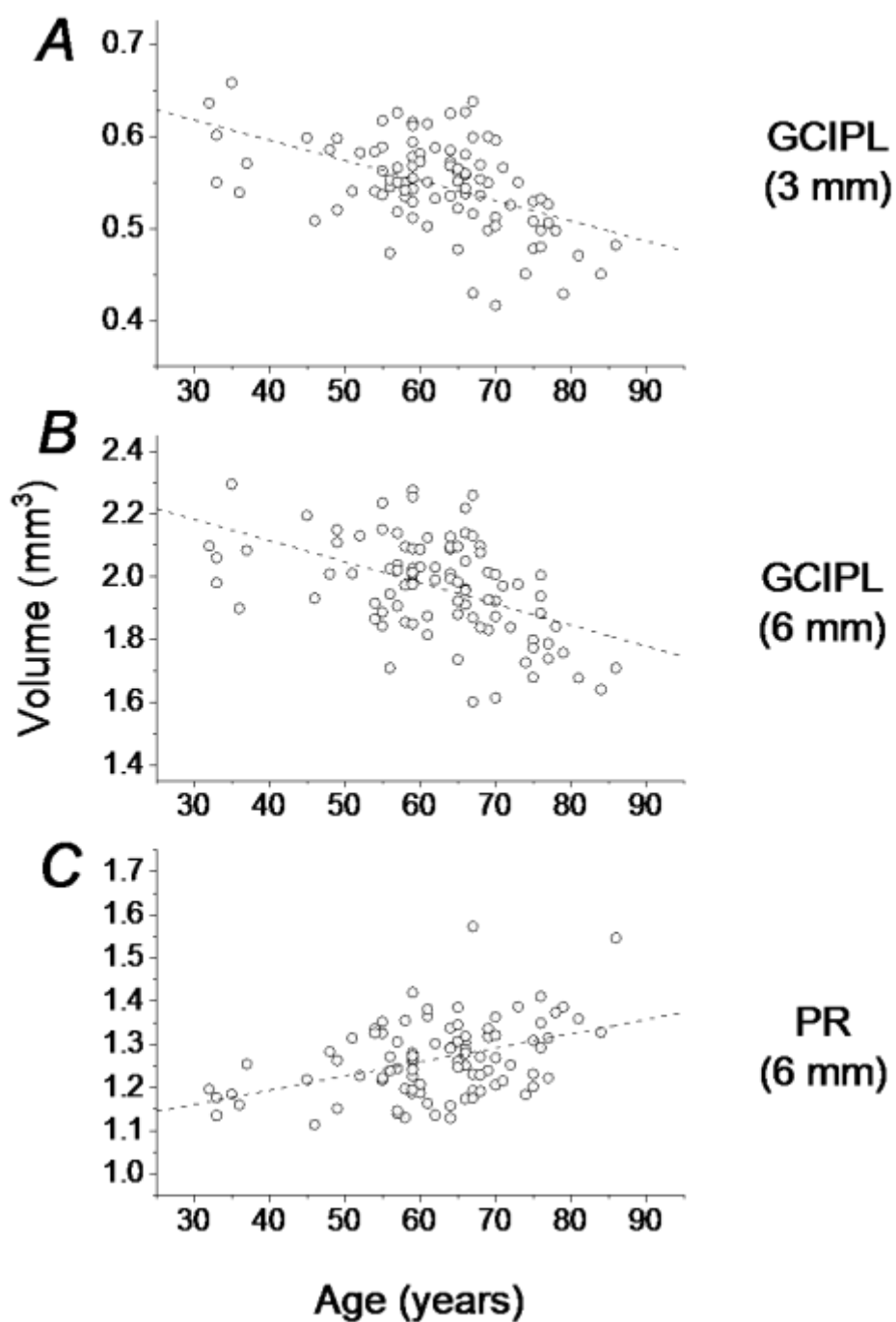


Figure 13. Selected layer volumes plotted as function of age. Points average both twins from each pair. Dashed lines show linear fits. A, GCIPL volume in 3 mm diameter central circle. Linear fit declines by 0.022 mm³ per decade. B, GCIPL volume in 6 mm diameter circle. Linear fit declines by 0.067 mm³ per decade. C, PR volume in 6 mm diameter circle. Linear fit increases by 0.033 mm³ per decade.

4.4.3 Correlations in MZ and DZ twins and estimates of heritability

Table 12 gives coefficients of intra-pair correlation for MZ and DZ twins. The majority were statistically significant, and all were stronger in MZ than DZ twins, consistent with significant heritability. Age-adjusted heritability estimates are also given in Table 12. The majority of parameters appeared to fit best with the AE model. Total retinal volume showed high heritability for both the 3 mm and 6 mm circles (point estimates of 83.0 and 87.5% respectively). Of the segmented layer volumes, heritability appeared highest for GCIPL (point estimates of 83.7 and 85.8% for the 3 and 6 mm circles respectively) and lowest for RPE-BM volumes (confidence intervals overlapping zero). Figure 14 plots TRV and GCIPL volumes (for the 6 mm circles) for twin pairs, illustrating the tighter correlation observed in MZ pairs for these parameters. Figure 15 plots MZ and DZ correlation coefficients for all parameters.

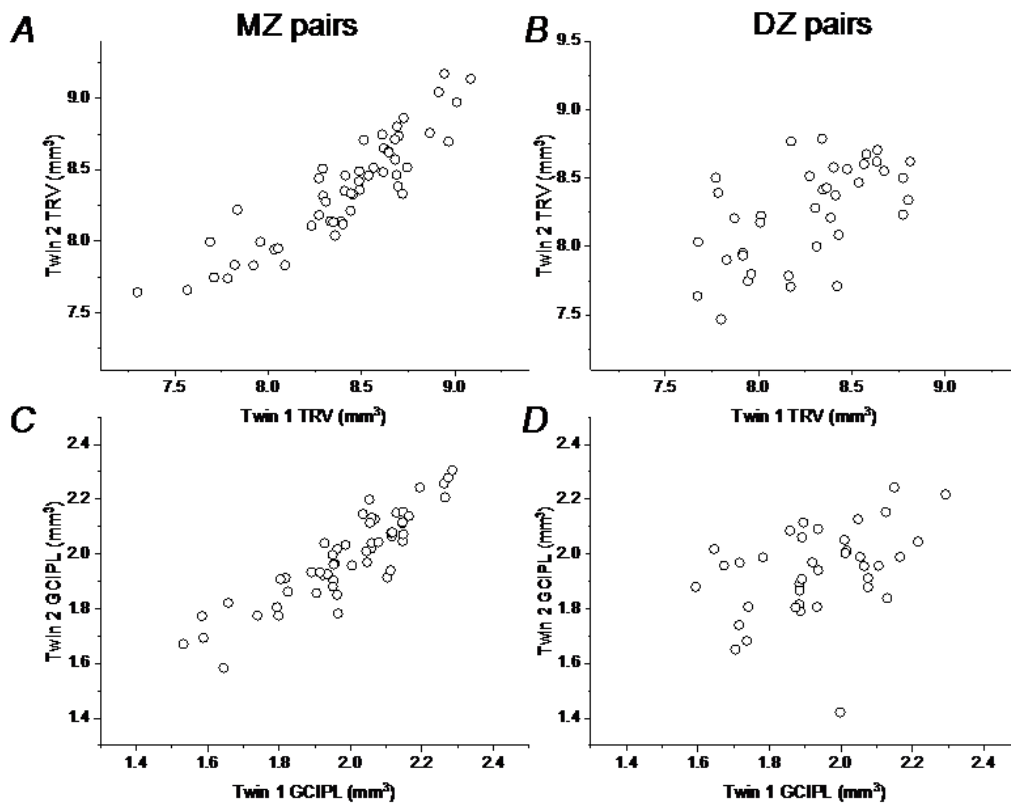


Figure 14. Selected layer volumes plotted for twin pairs (twin 2 is plotted against twin 1). Left-hand panels are for monozygotic pairs; right-hand panels show dizygotic pairs. A and B, points plot total retinal volume for the 6 mm diameter circle. C and D, Ganglion cell-inner plexiform layer volume for the 6 mm diameter circle.

Table 12. MZ and DZ coefficients of intra-pair correlation for segmented layer volumes, and age-adjusted estimates of heritability.

Circle diameter (mm)	Parameter	Coefficients of intra-pair correlations				Heritability (%) Point estimate (95% CI)
		MZ pairs		DZ pairs		
		Coefficient	<i>p</i> value	Coefficient	<i>p</i> value	
3	TRV	0.848*	6.16x10⁻¹⁶	0.466*	0.003	83.0 (73.9-88.7)
	RNFL	0.440*	8.61x10⁻⁴	0.234	0.158	42.9 (20.5-60.6)
	GCIPL	0.875*	4.84x10⁻¹⁸	0.357*	0.027	83.7 (74.0-89.6)
	INL	0.707*	2.31x10⁻⁹	0.668*	4.53x10⁻⁶	70.0 (56.2-80.0)
	OPL	0.508*	8.80x10⁻⁵	0.325*	0.047	50.2 (28.9-66.2)
	ONL	0.522*	5.20x10⁻⁵	0.508*	0.001	55.6 (37.2-69.3)
	PR	0.525*	4.65x10⁻⁵	0.474*	0.003	42.9 (22.9-59.1)
	RPE-BM	0.206 (0.664*)	0.136 (4.36x10 ⁻⁸)	0.104 (0.344*)	0.533 (0.034)	15.4 [†] (<0.1-49.0)
6	TRV	0.899*	2.85x10⁻²⁰	0.576*	1.53x10⁻⁴	87.5 (80.7-91.8)
	RNFL	0.806*	2.04x10⁻¹³	0.481*	0.002	71.3 (57.4-80.8)
	GCIPL	0.890*	2.20x10⁻¹⁹	0.401*	0.013	85.8 (77.4-91.0)
	INL	0.708*	2.18x10⁻⁹	0.574*	1.66x10⁻⁴	71.4[†] (58.2-80.5)
	OPL	0.434*	0.001	0.238*	0.150	38.3 (15.5-56.9)
	ONL	0.686*	1.02x10⁻⁸	0.568*	2.02x10⁻⁴	69.0[†] (54.7-78.9)
	PR	0.649*	1.08x10⁻⁷	0.397*	0.014	55.4 (35.4-70.1)
	RPE-BM	0.213 (0.651*)	0.122 (1.01x10 ⁻⁷)	0.165 (0.307)	0.323 (0.061)	16.3 (<0.1-37.0)

All are Pearson correlation coefficients; for RPE-BM parameters, Spearman coefficients are also given in parentheses as these parameters deviated from a normal distribution. *Asterisk denotes significance (*p* < 0.05).
Heritability estimates are from the AE model which provided the best fit for most parameters.
†Denotes the following parameters, which showed a marginally better fit with other models: for INL at 6 mm, ACE model generated a heritability estimate of 12.3% (<0.1-58.0%); for ONL at 6 mm, ACE model generated estimate of 22.6% (<0.1-73.6%); for RPE at 3 mm, E appeared the best fitting model.

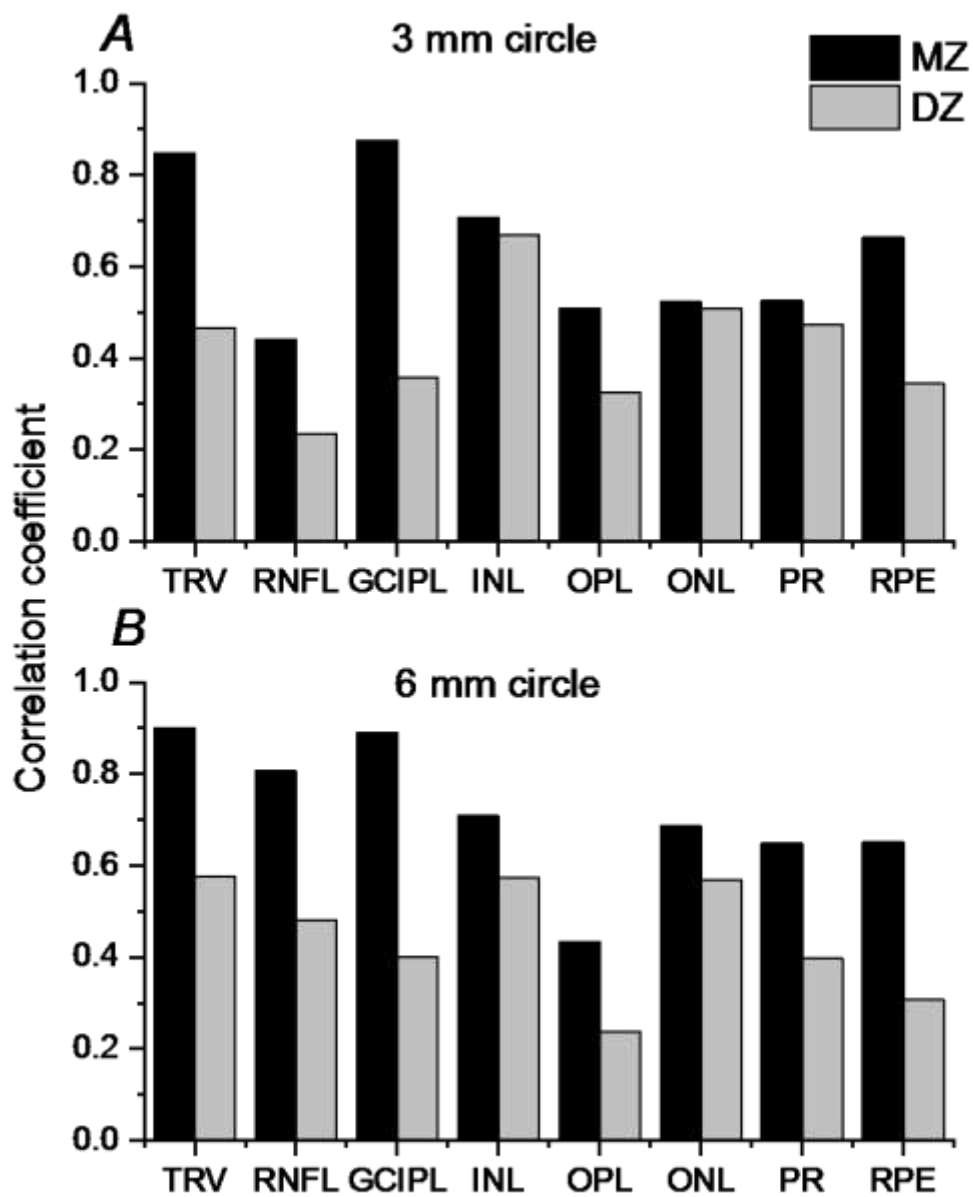


Figure 15. Coefficients for intra-pair correlation for monozygotic and dizygotic pairs for segmented layer volumes. For RPE, Spearman coefficients are plotted as these volumes deviated from a normal distribution; Pearson coefficients are plotted for all other layers.

4.5 Discussion

This study analysed segmented retinal layer volumes from spectral domain macular OCT scans obtained from 184 twin participants. Means (and standard deviations) were derived for each layer for circular regions of 3 and 6 mm in diameter around the foveal centre. Total retinal volume, and volumes of inner retinal layers (RNFL, GCIPL, INL) decreased with age; increasing volume with age was observed for PR, RPE-BM and OPL. Inter-eye correlations were all significant, and were highest for TRV and GCIPL volume. Intra-pair correlation was greater in all cases for MZ pairs than DZ pairs, and heritability estimates were highest (point estimates >80%) for TRV and GCIPL volume, and lowest for RPE-BM.

Reduction in retinal thickness (and RNFL thinning) with increasing age is well-established (Alamouti and Funk, 2003, Ooto et al., 2011, Subhi et al., 2016, Nieves-Moreno et al., 2018). Recently, analysis from the UK Biobank study, confirmed a reduction in macular thickness with increasing age (in fields other than the central 1 mm subfield) from the scans of over 32000 participants (Patel et al., 2016). The finding in the present study of increasing volume with age in some outer retinal layers (OPL, PR and RPE-BM) is consistent with the findings of our previous study (Chapter 3).

Increase in PR outer segment volume has been shown in a study of 68 normal eyes (Pakdel et al., 2018), agreeing with the results of the present study. OPL thickening with age has also been reported in a study of 297 healthy eyes (Nieves-Moreno et al., 2018). Interestingly, the same study reported PR layer thinning with age. It is possible that methodological differences explain the disagreement with the present study – that study used the Heidelberg Spectralis OCT device; thickness

measurements vary between devices (Pierro et al., 2010), and segmentation may also differ (Terry et al., 2016). Increasing OPL layer thickness with age, as found in the present study, was also recently reported in an OCT study of macaque eyes (Renner L, et al. IOVS 2019;60:ARVO E-Abstract 202) and OPL remodelling in aged vervet monkeys has been reported from a histological study (Garneau J, et al. IOVS 2019;60:ARVO E-Abstract 3102). The OPL volume increase might represent remodelling or might also be a consequence of mechanical factors, including expansion as neighbouring cellular layers might reduce in volume with age.

A positive correlation between foveal RPE thickness and age has also been reported by other authors (Demirkaya et al., 2013). However, the UK Biobank study revealed RPE thinning with age (among those aged over 45) (Ko et al., 2017), and it is possible that differences in segmentation methods or population demographics might explain why increase in volume with age was apparent in the present study. As the RPE ages, function, including phagocytosis of photoreceptor outer segments, may decline, which might explain an increase in photoreceptor layer volume with age (Bonilha, 2008).

Our study demonstrated significant heritability of the majority of segmented layer volumes, with point estimates suggesting that 87.5% and 85.8% of the variance in TRV and in GCIPL volume respectively could be explained by genetic factors (for the 6 mm diameter central area). Outer retinal layer volumes (especially RPE-BM) appeared to show lower heritability. This could represent a greater influence of, or vulnerability to, environmental factors. It could also relate to greater accuracy in quantification of the inner layers. If outer layer segmentation is less reliable, and more prone to measurement error, then this will manifest as a unique environmental factor, and act to reduce the estimated heritability. Inter-eye correlation (which can,

with limitations, act as a surrogate for repeatability given that both eyes of a healthy individual are highly correlated) was lower for the outer retinal layers, consistent with this notion.

Limitations of the present study include its cross-sectional nature, which make conclusions regarding effects of age somewhat tentative; a longitudinal study would be needed to accurately assess change with age. The conclusions are dependent on the accuracy of the segmentation algorithm, and it is possible that different methods might yield differing findings. No adjustments were made for axial length or refraction. The TwinsUK cohort is largely female and of European descent, thus limiting generalisability to other demographics. Finally, a larger sample size would add power and help narrow the confidence intervals of the heritability estimates.

5 Chapter 5: Changes in number, area and volume of drusen in fellow eye of patients with neovascular AMD

5.1 Introduction

Drusen are extracellular focal deposits that accumulate between the basal lamina of the retinal pigment epithelium (RPE) and the inner collagenous layer of the Bruch's membrane. They appear as yellowish white deposits on biomicroscopy and colour fundus photographs and have a predilection for the macula (Sarks et al., 1994, van der Schaft et al., 1992a).

Drusen vary in size. They are the hallmark of age related macular degeneration (AMD). The classification of AMD is based on the size of drusen (Ferris et al., 2013). Small drusen or drupelets defined as $\leq 63 \mu\text{m}$ in size have low risk of progression to advanced AMD. Early AMD is characterised by the presence of medium sized drusen ($>63\mu\text{m}$ to $\leq 125\mu\text{m}$). The presence of large drusen defined as size of $>125\mu\text{m}$ or more categorises the eye to having intermediate AMD. These eyes with intermediate AMD are at risk of progression to advanced AMD developing either choroidal neovascularisation (CNV) or geographic atrophy or both. They may also be associated with retinal epithelial pigmentary changes. The risk of development of CNV in the second eye in patients with unilateral advanced AMD is variable and can range from 20-50% over 5-10 years (1993, Klein et al., 1997b, Klein et al., 2002, Mitchell et al., 2002, Wang et al., 2007). Therefore, identifying new risk factors that can predict this conversion CNV more accurately is useful for counselling patients.

Although size and area of large drusen are established risk factors, more detailed drusen analysis has become an area of interest with the availability of more advanced imaging technology. Fundus colour photography is the gold standard used in the evaluation of patients with drusen in clinical practice and research (The Age-Related Eye Disease Study Research, 2001). However, there are several drawbacks associated with fundus photography, such as, interpersonal variability and it is time and effort consuming (Klein et al., 1991, Shin et al., 1999). Furthermore, the difficulty in outlining indistinct drusen, variability of fundus pigmentation, the effect of media opacity on photographic quality are crucial limitations for achieving objective clinical assessment of drusen. The fundus photographs also do not show the three-dimensional topography of drusen.

The introduction of OCT in ophthalmic field have revolutionised our understanding of different retinal pathologies. OCT provides *in vivo* cross sectional images of different retinal structures that is analogues to the histological structure. Recently developed SD-OCT technology is able to provide real-time, high-resolution images of the macular area in two and three dimensions (Srinivasan et al., 2006b, Wojtkowski et al., 2005). Emerging of automated drusen segmentation algorithms has allowed to delineate drusen and longitudinally track changes in drusen count, area and volume in AMD eyes (Schlanitz et al., 2010, Iwama et al., 2012, Gregori et al., 2011).

The drusen segmentation algorithm defines drusen as a degree of deformity in the RPE (Schlanitz et al., 2010, Diniz et al., 2014, Jain et al., 2010). Consequently, small drusen are not detected by OCT as they do not elevate RPE layer considerably. As a result, drusen count and area are underestimated by OCT compared to fundus photography (Gregori et al., 2014, Yehoshua et al., 2013, Diniz et al., 2014).

However, the volume of drusen are measured reliably by SD-OCT, which render this

technique superior to colour fundus photography (Gregori et al., 2011). In addition, SD-OCT has the ability to differentiate between drusen and pseudodrusen (reticular drusen or subretinal drusenoid deposits), which lie above the RPE layer (Sivaprasad et al., 2016). Therefore, both modalities are considered as complementary to each other.

Most of the previous studies have been conducted using the Cirrus OCT (Zeiss, USA) algorithm. The Topcon SD-OCT also has an in-built automated drusen analysis algorithm but has very limited publications on its use. Moreover, the detection limit of drusen is different with Cirrus OCT compared to Topcon OCT. One study has evaluated the Topcon algorithm and demonstrated that this algorithm has the ability to make an automated assessment of drusen area and volume with minimal segmentation failures. The study also showed that there was a good agreement with an assessment was performed by certified graders on colour fundus photography (Iwama et al., 2012). As Topcon OCT is widely used in daily practice, it is important to evaluate whether the Topcon drusen analysis algorithm provides the same outcomes as other similar algorithms over time.

5.2 Aims

In this study, we quantified the drusen load in terms of numbers, area and volume using the automated Topcon drusen analysis algorithm in fellow eyes of patients with unilateral neovascular AMD. Our objectives were to evaluate the change in these drusen parameters over time and to evaluate whether any of these parameters could predict conversion to CNV.

5.3 Methods

The methods have been discussed in the methods section in chapter 2. As the data was not normally distributed and to adjust for baseline drusen parameters, we transformed the drusen area and volume to square root and cubic root as previously reported (Yehoshua et al., 2011, Gregori et al., 2011, Abdelfattah et al., 2016, Garcia Filho et al., 2014). We also assessed the variables that influenced the change in drusen parameters over the 2 years and the gradient of change over 1 and 2 years.

5.4 Results

5.4.1 Patients

After reviewing the medical records of 1671 patients who treated with anti-VEGF therapy at Moorfields Eye Hospital between August 2008 and September 2016, 248 patients were identified whom met the inclusion criteria. We excluded all patients who did not have an OCT scan done at 12 ± 2 months and 24 ± 2 months from baseline. We also excluded patients with at least one of the following; SD-OCT scans with an instrument image quality metric <30 , scans with poor foveal centration and presence of artefacts. Among the 248 patients involved in the study, 161 (65%) were females and 87 (35%) were males with a mean age of 73.5 years (SD, 8.6). 199 had intermediate AMD and 49 had early AMD. At 2 years ± 2 months, 69 eyes (28 %) developed CNV while 179 eyes (72 %) did not develop late stage AMD. Study development is detailed in figure 16.

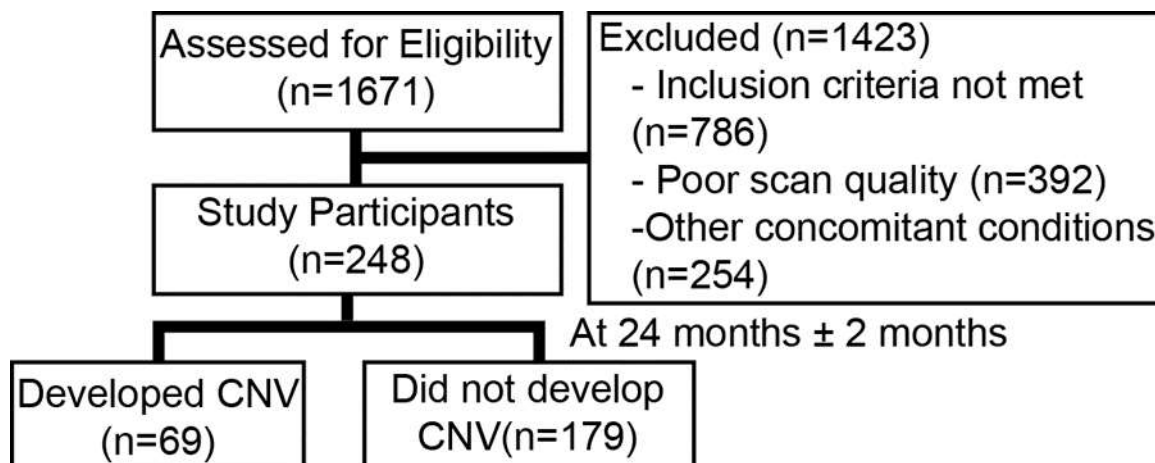


Figure 16. Flow chart for study participant selection. Retrospective analysis of 1671 patients yielded 248 patients who were included in this trial.

5.4.2 Baseline drusen count, area and volume

measurements

At baseline, the mean (SD) drusen count, drusen area and drusen volume were 6.58 (7.1), 1.42 mm² (1.85) and 0.06 mm³ (0.09) respectively (square root drusen area and cube root drusen volume were, 0.9231mm (0.76) and 0.288 mm (0.2) respectively). Baseline drusen count, square root area and cube root volume measurements were compared between the two groups (69 CNV-developed eyes vs 179 non CNV-developed one) using the Mann-Whitney U test. These three baseline drusen parameters (count, area, and volume) were greater in CNV-developed eyes than non CNV-developed as shown in table 13.

Table 13. Comparing baseline drusen count, area and volume between eyes that developed CNV and eyes that did not develop.

Drusen Measurements	Non CNV-developed eyes (n= 179)	CNV-developed eyes (n= 69)	<i>P value</i>
Mean Drusen Count (SD)	5.42 (6.67)	9.57 (7.41)	< 0.001
Mean Drusen Square Root Area (SD)	0.8101 mm (0.79)	1.2162 mm (0.58)	< 0.001
Mean Drusen Cube Root Volume (SD)	0.2499 mm (0.21)	0.3870 mm (0.14)	< 0.001

5.4.3 Prediction of progression to CNV based on baseline drusen measurements

Baseline count, area and volume measurements as well as age and sex were assessed as predictors of progression to CNV (Table 14). Logistic regression analysis of these drusen measurements revealed that, baseline volume was a significant predictor for developing CNV at 2 years of follow-up. Each 0.1 mm increase in the cubed root of baseline drusen volume increases the odds of progressing to CNV by 40% (95% CI 1.2-1.4; $P < 0.001$).

Table 14. Assessing predictors for CNV progression using logistic regression analysis

	Odds Ratio	95% CI	P value
Age	1.067	1 - 1.1	< 0.001
Sex	2.02	1 - 3.7	0.027
Drusen Count	1.078	1 - 1.1	< 0.001
Square Root Drusen Area, 0.1 mm increase	1.069	1-1.1	< 0.001
Cube Root Drusen Volume, 0.1 mm increase	1.4	1.2-1.6	< 0.001

5.4.4 Change in drusen measurements over two time points (year 1 and year 2)

We also compared the change rate of drusen counts, areas and volumes measurements between the 2 groups (progressed eyes and non-progressed) during the 1st year and 2nd year using Mann-Whitney-U test (Table 15). The change rate between the 2 groups in the 2nd year was statistically significant, particularly drusen volume ($P = 0.019$) and area ($P = 0.027$). However, the rate of change between the 2 groups in the 1st year was not statistically significant. Change in drusen morphology is shown in Figure 17.

Table 15. Comparing the change in drusen count, area and volume between the two groups in the first and second year

Time	Drusen parameters	Group 1 (n = 179)	Group 2 (n = 69)	P value
Year 1	Count Change	1.15	1.33	0.484
	Square Root Area Change	0.12 (0.27)	0.11 (0.24)	0.902
	Cube Root Volume Change	0.02 (0.08)	0.02 (0.07)	0.834
Year 2	Count Change	0.69	1.64	0.052
	Square Root Area Change	0.12 (0.27)	0.19 (0.27)	0.027
	Cube Root Volume Change	0.03 (0.09)	0.05 (0.07)	0.019

Figure 18 shows the gradient at which the overall drusen volume changed in the two groups and the data shows that the total drusen volume increases steeply in the year preceding the development of CNV.

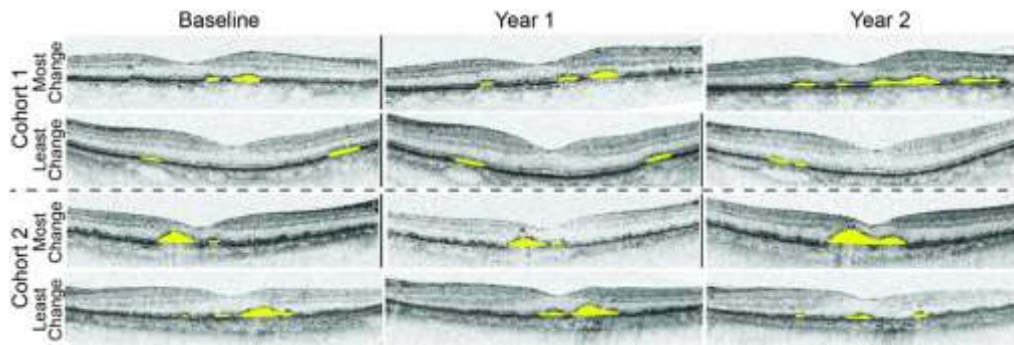


Figure 17. Change in drusen volume from baseline to 2 years. Shown here are the foveal scans for the subjects with the greatest and least change from baseline to year 2 for each cohort. The yellow is what the Topcon OCT designated as drusen volume for the scan. Note that least change could also be a decrease in volume (top set).

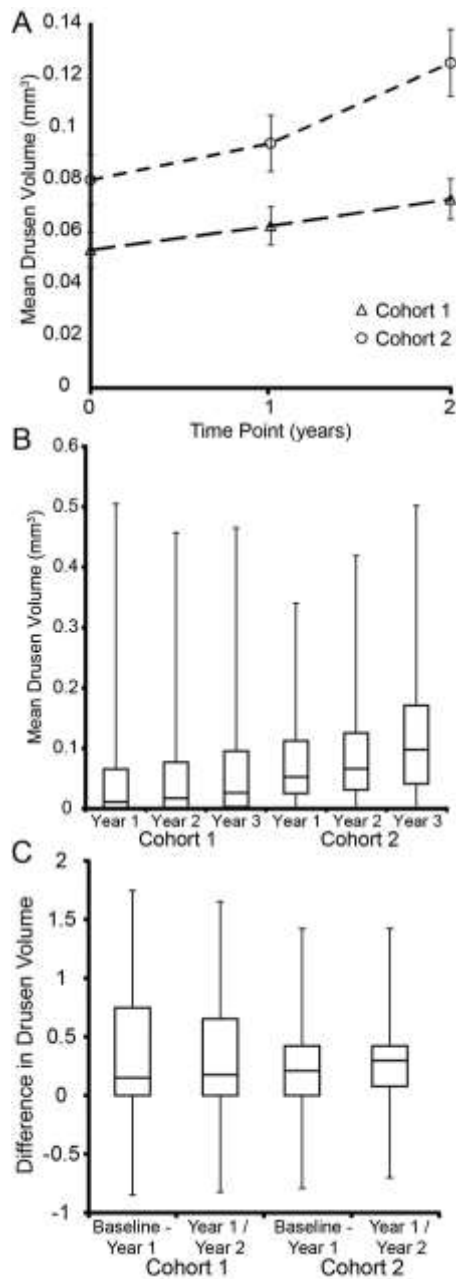


Figure 18. Mean volume and change from baseline to year 2 in those with and without CNV. (A) Shows the mean drusen volume, error bars or SEM. (B) shows the distributions of drusen volumes. While on average that with CNV had more drusen volume this was not absolute with the ranges overlapping nearly entirely. (C) On average those who went on to develop CNV had a greater increase in drusen volume, however again there was considerable overlap with those who did not.

5.5 Discussion

This study confirms that increasing total drusen volume on SD-OCT is a predictor of conversion to CNV in the fellow eyes of patients with unilateral neovascular AMD. Our study shows that there is an accelerated increase in total drusen volume the year preceding the onset of CNV. The mean rate of increase in cube root drusen volume is 0.05 mm in the year preceding the development of CNV, compared with the first year follow-up of the same group as well as the non CNV-developed group that had a mean growth rate of cubic root drusen volume to be 0.02-0.03 mm per year. The cube root transformation of drusen volume and the square root transformation of drusen area were performed to eliminate the dependence of the drusen growth rate on the baseline drusen size (Yehoshua et al., 2011, Gregori et al., 2011, Abdelfattah et al., 2016, Garcia Filho et al., 2014).

The study also shows that the patients with increased drusen growth rate may form an enriched cohort for clinical trials, evaluating preventive measures for the development of CNV as the event rate for this cohort will be higher than recruiting any patient with unilateral CNV when the reported probability of occurrence of CNV in the fellow eye is only around 10– 12% per year. It will also shorten the duration of the clinical trial. A previous study on drusen volume showed that recruiting patients with a baseline volume of $> 0.03 \text{ mm}^3$ or 0.31 mm cube root volume in the central 3 mm diameter would result in 50% an increase in baseline volume and would enrich a prevention trial cohort and shorten the trial duration (Schaal et al., 2016). Adding a parameter of drusen growth rate of 0.05 mm cube root volume across 6 mm diameter of the macula centred at the fovea will further reduce the sample size.

Previous studies such as the Age-Related Eye Disease Study and Beaver Dam Eye Study used colour photographs to estimate drusen area. They showed that larger drusen areas were associated with a higher risk for progression to advanced AMD. Despite drusen area and volumes are highly correlated, OCT drusen volume are not corresponding to drusen area from colour fundus photographs. Moreover, it has been demonstrated that drusen volumes might be more repeatable metrics when compared to drusen area. Measurements of drusen area are inherently unstable due to poorly demarcated edges of drusen. As a result, a large change in drusen area can be gotten from a small difference in the diameter or border of the drusen. In contrast, drusen volume can be affected minimally by a small difference in their diameter or border owing to the topographic profile of drusen, the thickness of a druse at its edge is small relative to the center. One challenge of using drusen volume to risk stratify patients at a point in time is that drusen can fluctuate over time as they appear and disappear as shown previously. Yehoshua et al. (2011) evaluated prospectively the change in drusen area and volume of 143 eyes over 2 years using OCT and found a significant change in drusen volume. In their study 48% of eyes showed an increase in drusen volume while 40% remained stable and 12 % decreased at 12 months.

Our findings are consistent with recent studies that showed OCT drusen volume may serve as earlier and more sensitive predictor for the development of advanced AMD (Abdelfattah et al., 2016, Folgar et al., 2016). Abdelfattah et al. (2016) followed retrospectively 89 patients with wet AMD in one eye and for a total follow up period of two years. This study showed that a drusen volume of 0.03 mm^3 and more, in the fellow eye, is associated with four-fold increase in the development of late stage AMD. Furthermore, the baseline drusen volume was significantly higher in eyes

developed late stage AMD. Folgar et al. (2016) reported similar findings and interestingly in their study for each 0.1 mm^3 increase in baseline volume there was an increase of 31% in risk of developing CNV. Similarly, de Sisternes et al. (2014) using SD-OCT studied quantitative characteristics of drusen (count, area, volume and other features of drusen) to predict the likelihood of progression from early and intermediate AMD to CNV. Their retrospective study represented the results of 186 eyes of 128 AMD patients followed over a period of 5 years. They demonstrated that drusen volume, area, height and reflectivity are key features that can predict disease progression and drusen volume is the most sensitive predictor for progression within 30 months. Moreover, Nathoo et al. (2014) collected retrospective data of 83 AMD patients to analyse the association of drusen load with the development of late AMD. The authors found an association between drusen volume and drusen area, and the development of CNV or GA over a period of 2 years using SD-OCT.

To our knowledge, our study is the first in being used 3D OCT-2000 algorithm to study drusen quantification longitudinally and the largest study (sample size) of drusen volume for AMD patients who developed CNV (N=69). Our findings might be applied to clinical practice in order to counsel patients more accurately about the time to second eye involvement.

Limitations of this study are the use of commercially available software that does not allow user correction of segmentation. While theoretically a limitation, this limitation is surpassed by the essential nature of the work. It is essential understanding for clinical care as SD-OCT segmentation and drusen identification correction is not currently cost/time effective in clinical practice. Therefore, understanding of change based on 'raw' outputs is needed. Additionally, the inherent differences between devices, makes comparisons between devices not possible and therefore requires

each device to be independently verified. These differences result in two categories of differences.

First, we did not subdivide drusen measurements into smaller macular subfield within the total macular field of 6 mm cube as the algorithm did not permit this analysis.

Updated versions of this software are anticipated to provide this analysis. However, the study shows that the results obtained on drusen volume in 6 mm cube parallels that obtained in 3 mm central macula and can be used as a predictor of CNV.

Secondly, we did not adjust for other known risk factors of disease progression such as smoking, raised BMI and genetic factors. We also excluded a large proportion of patients for whom scans were not available at the strict time-points planned for this study. The rationale for establishing a standardised 2-year follow-up interval was based on 2-year study endpoints, which showed that a greater baseline drusen volume was predicative of an increased 2-year progression to CNV (Folgar et al., 2016).

In summary, this study has shown that prognostic 2-year risk of converting to CNV was obtained from baseline OCT drusen volume measurements. Furthermore, drusen volume growth rate across a 6 mm macula cube using the automatic Topcon drusen analysis software may be also used as a predictor for conversion to CNV. Serial OCTs over a shorter time interval may provide better information than the two time points that we have chosen.

6 Chapter 6: Predictor of CNV type based on drusen load and retinal layer volumes

6.1 Introduction

Age-related macular degeneration (AMD) is a leading cause of severe vision loss in people over the age of 50 years in developed countries (Klaver et al., 1998b, Buch et al., 2005). There are 2 main forms of the disease: the dry form (including early and intermediate AMD and geographic atrophy) and the wet form. Wet AMD develops when new choroidal blood vessels grow and break through the Bruch's membrane. This phenomenon is defined as choroidal neovascularization (CNV). CNV occurs in approximately 10-15% of all AMD cases, and these eyes are at high risk for severe visual loss, because it often results in elevation of the retinal pigment epithelium (RPE) with adjacent sub-retinal and intra-retinal fluid and hemorrhage (Rosenfeld et al., 2006). CNV can be classified based on fluorescence angiography into occult, classic or mixed lesion types (1991a). Classic lesions are often aggressive with early and severe loss of vision, while occult lesions are often stable with less visual loss (Bressler et al., 1990a).

It is important to distinguish between occult and classic CNV lesions, because the natural course of the disease and its prognosis and benefit from certain treatments vary between different types of CNV (1996, Stevens et al., 1997). This was specifically realised when PDT or laser treatment were the first lines of treatment. PDT has been established only for those lesions that are predominantly classic CNV (1999), while laser photocoagulation has been used mainly for those lesions that have some evidence of classic CNV (1991a). Furthermore, the importance of

classifying CNV lesions as classic and occult has also been reported recently in the anti-VEGF era in MARINA and ANCHOR trials that assessed ranibizumab as intravitreal treatment of CNV secondary to AMD. MARINA trial was for occult CNVs (Chang et al., 2007), whereas ANCHOR trial was for predominantly classic lesions (Brown et al., 2006). Currently, the clinical relevance of CNV classification in wet AMD eyes is uncertain. This is because anti-VEGF agents were found to be effective in treating CNV regardless of its type (Invernizzi et al., 2019). However, classic CNV is associated with poor prognosis, risk of atrophy and fibrosis after anti-VEGF therapy compared to occult CNV (CATT).

This was confirmed in a recent analysis of randomized controlled trials of wet AMD eyes treated with anti-VEGF agents which has reported its results using CNV types in order to show the difference in trials' outcomes (Daniel et al., 2018). New trials to test novel therapies also specify the CNV type among their inclusion criteria (Danis et al., 2014, Jaffe et al., 2017). Thus, CNV classification will allow for more effective trials as prognosis and treatment may vary based on CNV type.

The risk of developing occult CNV in the second eye of patients with unilateral occult CNV has been found to be high (Chang et al., 1995). Various studies on patients with unilateral CNV secondary to AMD have identified important risk factors for development of CNV in the fellow eye (Roy and Kaiser-Kupfer, 1990, 1993, Pieramici and Bressler, 1998, Sandberg et al., 1998). The characteristics of drusen of the fellow eye are reported to be correlated with the type of CNV in the affected eye (Marsiglia et al., 2015, Pauleikhoff et al., 1990a, Abugreen et al., 2003). For example, occult CNV are more likely to be associated with intermediate drusen than pure classic CNV that may occur in eyes with no or small drusen (Abugreen et al., 2003). However, very few studies investigated the correlation between clinical

characteristics such as drusen load preceding the development of CNV in the same eye. We reported that the mean change in macular drusen load in eyes that converted to wet AMD increase a year before conversion to wet AMD especially in eyes with occult CNV (Lamin et al., 2019a).

6.2 Aims

In this study, we aim to investigate a cohort of patients who were undergoing treatment for unilateral CNV and who developed CNV in the fellow eye at the end of the two-year study period. In the fellow eye, automated drusen and retinal layer quantification measurements were obtained from spectral domain OCT scans prior to the conversion onset. The aim of this study was to investigate whether any correlation existed between these parameters and the subsequent CNV type in the same eye (i.e. fellow eyes). We also investigated correlation in CNV type between the two eyes in these patients as it is known that drusen phenotypes are similar between eyes. So we hypothesised that certain drusen or retinal layer quantification parameters may indeed better explain the symmetry of type of bilateral CNV.

6.3 Methods

Parts of the methods have been discussed in chapter 2 and an additional discussion will be added here. Consecutive FA and OCT images of patients with unilateral wet AMD were reviewed from the database of Moorfields Eye Hospital. For inclusion in this study, patients were required to have CNV in one eye as evidenced by FA, and had developed a CNV lesion in the fellow eye with at least 2 years of follow-up before developing the lesion. We excluded all patients with polypoidal choroidal vasculopathy based on ICG availability or clinical suspicion, subfoveal fibrosis or ungradable CNV due to haemorrhage or poor imaging quality. Eyes with CNV

secondary to other causes rather than AMD or without available FA images were also excluded.

The classification of CNV lesions was graded independently by two ophthalmologists (A.L. and A.E.) for each patient on the basis of early, mid and late frames of FA. The CNV type was classified based on FA as occult, classic or RAP. Mixed lesions were classified as classic CNV because the number of participants were small and classic CNV holds bad prognosis. Any discrepancies between the two ophthalmologists were resolved by a third expert consultant (S.S.). Details of this part has been discussed in chapter 2.

Agreement of CNV type between the 2 eyes in cases where the fellow eye developed CNV was quantified with the Kappa (k) statistic.

6.4 Results

6.4.1 Demographic features of participants

A total of 209 patients with unilateral wet AMD and had their FA available were identified (Figure 19). Seventy patients met the inclusion criteria. Of these 70 patients, 19 were excluded due to absence of FA in the fellow eye. In those 51 patients' fellow eyes, 29 eyes were classified with occult CNV, 20 eyes with a classic CNV and 2 eyes with a RAP type. As RAP lesions were rare, we only compared the differences in the quantifications of drusen load and retinal layer volume between the classic and occult types.

For drusen load quantifications, the whole cohort of 29 occult CNVs and 20 classic CNVs were included in the study. For occult lesion participants, the mean (SD) age of 22 females (75%) and 7 males (25%) was 75.7 (7.5) years, ranging from 60 to 88

years. For classic lesion participants, the mean (SD) age of 14 females (70%) and 6 males (30%) was 75.8 (6.5) years and ranged from 65 to 85 years.

For retinal layer segmentation analysis, only 17 participants were included (10 occult and 7 classic). Other participants were excluded because their macular OCT images of the 2 year protocol were not available. For occult lesion participants, the mean (SD) age of 7 females (70%) and 3 males (30%) was 82.4 (7.6) years, ranging from 71 to 93 years. For classic lesion participants, the mean (SD) age of 4 females (57%) and 3 males (43%) was 80.2 (7.5) years and ranged from 71 to 91 years.

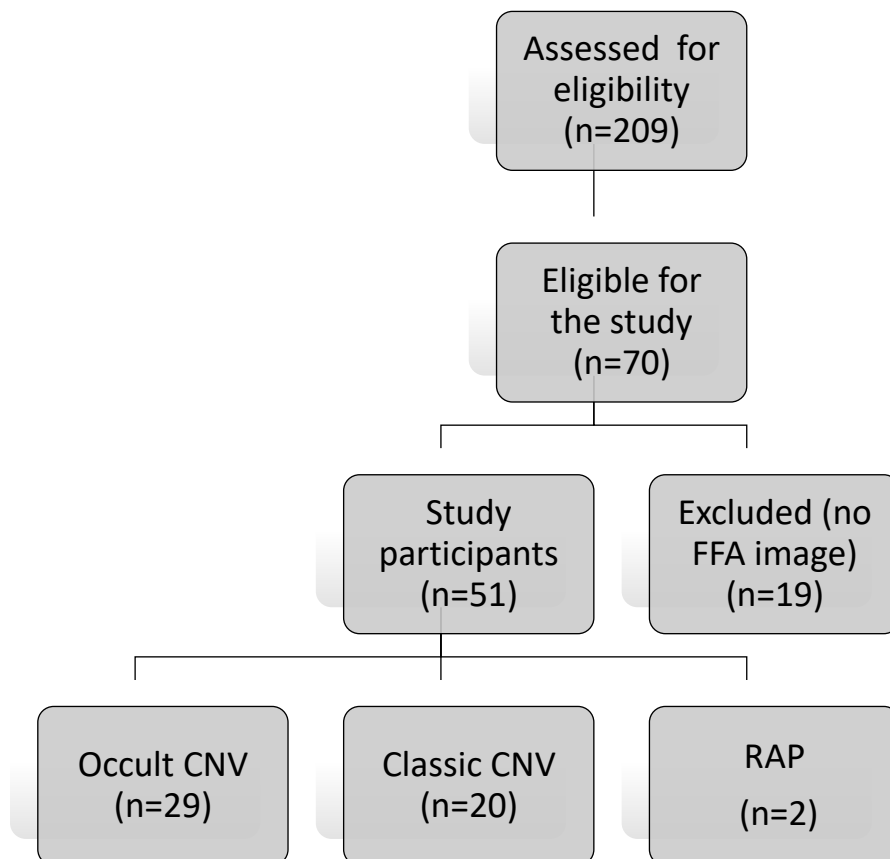


Figure 19. Flow chart of the present study of Chapter 6.

6.4.2 Drusen load in occult and classic CNV

Table 16 shows means and standard deviations of drusen load including count, area and volume at baseline, year 1 and year 2 and longitudinal change in drusen area and volume from baseline to year 1 and from year 1 to year 2. While drusen parameters (count, area, volume) were alike in both CNV groups, the rates of change of drusen area and drusen volume were higher in the occult group in the year preceding the development of CNV.

Table 16. Drusen parameters in AMD eyes prior to convert to either occult (N=29) or classic (N=20) CNV.

Drusen parameter	Time point	Occult (N=29)	Classic (N=20)	P value
		Mean (SD)	Mean (SD)	
Drusen Count	Baseline	9.93 (8)	8.50 (5.7)	0.729
	Year 1	11.48 (7.8)	9.85 (6)	0.561
	Year 2	11.69 (8.8)	11.65 (7)	0.791
Drusen Area (mm²)	Baseline	1.49 (1.2)	1.77 (1.38)	0.483
	Year 1	1.84 (1.48)	2.21 (1.7)	0.528
	Year 2	2.63 (1.8)	2.46 (1.8)	0.707
Drusen Volume (mm³)	Baseline	.070 (.07)	.078 (.06)	0.464
	Year 1	.085 (.089)	.104 (.084)	0.309
	Year 2	.131 (.114)	.118 (.1)	0.640
Change in drusen Area (mm²)	Baseline-Year 1	.354 (.61)	.44 (.89)	0.855
	Year 1-Year2	.788 (.8)	.252 (.7)	0.046
Change in drusen Volume (mm³)	Baseline-Year 1	.014 (.02)	.026 (.04)	0.784
	Year 1-Year2	.046 (.04)	.013 (.03)	0.022

6.4.3 Retinal layer volumes in occult and classic CNV

Table 17 shows means and standard deviations for the various layer volumes for 17 participants preceding the development of CNV. There were statistically significant

differences between the 2 CNV types in mean volume of ONL (3 mm). The ONL volume was thinner in eyes preceding classic CNVs than occult CNVs at baseline and year 1, indicating early decrease in photoreceptor volume in eyes that progress to classic CNV type. Otherwise, no significant differences were found between the 2 CNV lesions in volumes of other retinal layers.

Table 17. Mean retinal layer volumes at 3 mm and 6 mm in AMD eyes prior to convert to either occult (N=10) or classic (N=7) CNV.

Retinal Layer	Time point	Mean Retinal layer Volumes at 3 mm			Mean Retinal layer Volumes at 6 mm		
		Occult (n=10)	Classic (n=7)	P value	Occult (n=10)	Classic (n=7)	P value
TRV	Baseline	2.19 (.19)	2.07 (.12)	.118	8.32 (.65)	7.92 (.48)	.283
	Year 1	2.17 (.18)	2.03 (.12)	.118	8.24 (.62)	7.85 (.54)	.283
	Year 2	2.17 (.18)	2.03 (.12)	.172	8.27 (.62)	7.88 (.54)	.283
RNFL	Baseline	.215 (.03)	.200 (.02)	.205	1.19 (.17)	1.11 (.23)	.283
	Year 1	.206 (.04)	.196 (.02)	.770	1.16 (.19)	1.06 (.22)	.495
	Year 2	.217 (.02)	.196 (.03)	.283	1.15 (.14)	1.05 (.31)	.495
GCIPL	Baseline	.508 (.07)	.511 (.04)	.845	1.75 (.24)	1.76 (.13)	.558
	Year 1	.508 (.08)	.498 (.04)	1	1.73 (.18)	1.73 (.13)	.922
	Year 2	.526 (.07)	.500 (.07)	.558	1.82 (.20)	1.74 (.17)	.283
INL	Baseline	.301 (.03)	.278 (.02)	.143	1 (.08)	.90 (.06)	.435
	Year 1	.301 (.03)	.269 (.02)	.143	1 (.08)	.96 (.09)	.696
	Year 2	.288 (.03)	.270 (.02)	.380	.99 (.09)	.96 (.07)	.696
OPL	Baseline	.161 (.04)	.183 (.04)	.380	.592 (.13)	.623 (.11)	.626
	Year 1	.156 (.03)	.190 (.06)	.435	.577 (.10)	.627 (.11)	.380
	Year 2	.186 (.04)	.182 (.04)	.922	.648 (.12)	.624 (.11)	.696
ONL	Baseline	.689 (.06)	.589 (.06)	.011	2.47 (.24)	2.21 (.23)	.064
	Year 1	.686 (.08)	.576 (.07)	.015	2.48 (.27)	2.24 (.24)	.079
	Year 2	.626 (.08)	.584 (.08)	.495	2.34 (.28)	2.27 (.28)	.558
PR	Baseline	.318 (.02)	.306 (.02)	.495	1.29 (.11)	1.23 (.10)	.435
	Year 1	.316 (.02)	.304 (.02)	.380	1.28 (.09)	1.21 (.09)	.172
	Year 2	.325 (.03)	.302 (.02)	.172	1.30 (.09)	1.22 (.09)	.172
RPE-BM	Baseline	.047 (.02)	.048 (.06)	.329	.137 (.03)	.157 (.07)	.696
	Year 1	.048 (.02)	.054 (.06)	.495	.135 (.04)	.171 (.08)	.283
	Year 2	.067 (.04)	.068 (.05)	.845	.152 (.05)	.200 (.07)	.172

Table 18 shows longitudinal change of retinal layer volumes at 3 mm and 6 mm from baseline to year 1 and from year 1 to year 2 in occult and classic CNV lesions. From baseline to year 1, no differences were found between the 2 CNV types or even within each CNV group. From year 1 to year 2, most of retinal layer volume changes were observed in the outer retina, particularly in the occult group. There were significant differences between the 2 CNV groups in longitudinal volume of ONL (3 mm and 6 mm) and OPL (3 mm). There was a progressive reduction in the volume of ONL, and an expansion in the volume of OPL in eyes that developed occult CNV. In the occult CNV group, INL (3 mm) and ONL volumes (3 mm and 6 mm) decreased significantly from year 1 to year 2. In contrast, there were significant increase in mean volumes of OPL (3 mm and 6 mm) and RPE-BM (3 mm) from year 1 to year 2. In the classic CNV group, only RPE-BM volume (6 mm) increased significantly from year 1 to year 2.

Table 18. Longitudinal Change in Retinal Layer volumes at 3 mm and 6 mm in AMD eyes prior to convert to either occult (N=10) or classic (N=7) CNV.

Circle diameter (mm)	Retinal layer volume	CNV subtype	Year 1 volume change			Year 2 volume change		
			Mean (mm ³)	P Value*	P Value ‡	Mean (mm ³)	P Value*	P Value ‡
3	TRV	Occult	-.0189	.059	.380	-.0048	.721	.626
		Classic	-.0357	.128		.003	.735	
	RNFL	Occult	-.0089	.203	1	.011	.285	.770
		Classic	-.0042	.612		.0008	1	
	GCIPL	Occult	-.0004	.878	.696	.017	.333	.329
		Classic	-.0134	.499		.002	.612	
	INL	Occult	.0007	.646	.118	-.0131	.037	.143
		Classic	-.0091	.176		.001	.866	
	OPL	Occult	-.0052	.333	.770	.029	.007	.015
		Classic	.006	.866		-.0077	1	
	ONL	Occult	-.0029	.959	.435	-.0599	.005	.002
		Classic	-.0130	.176		.008	.499	
	PR	Occult	-.0021	.721	.770	.009	.646	.435
		Classic	-.0020	.735		-.0023	.499	
RPE-BM	Occult	.0007	.241	1	.018	.007	.495	
	Classic	.005	.063		.014	.063		
6	TRV	Occult	-.0845	.093	.845	.0269	.721	.922
		Classic	-.0667	.237		.0299	.735	
	RNFL	Occult	-.0337	.445	.770	-.0024	.575	.845
		Classic	-.0466	.237		-.0099	.735	
	GCIPL	Occult	-.0283	.333	.922	.0907	.114	.205
		Classic	-.0311	.237		.0067	.735	
	INL	Occult	-.0041	.646	.696	-.0136	.241	.435
		Classic	-.0073	1		.0000	.735	
	OPL	Occult	-.0147	.139	.558	.0714	.028	.118
		Classic	.0048	.866		-.0033	.866	
	ONL	Occult	.0071	.646	.495	-.1417	.013	.025
		Classic	.0311	.310		.0298	.499	
	PR	Occult	-.0109	.333	.626	.0225	.878	1
		Classic	-.0175	.176		.0066	1	
RPE-BM	Occult	-.0010	.575	.283	.0166	.074	.558	
	Classic	.0143	.091		.0287	.043		

*Wilcoxon signed-rank test for paired volume measurements, Year 1 (baseline versus year 1) and Year 2 (year 1 versus year 2).
‡Mann Whitney U test, Occult versus Classic.

6.4.4 Correlation in CNV type between the two eyes

Table 19 summarises CNV types in patients with bilateral CNV. Of the 51 patients with bilateral CNV, 48 (94%) had similar CNV types in both eyes: 27 patients had occult CNV in both eyes, 19 patients had classic lesions in both eyes and 2 patients had RAP lesions in both eyes. The kappa statistic was 0.89 (95% CI 0.76-1.0) indicating a strong level of agreement between the two eyes.

Table 19. CNV types in patients with bilateral CNV

		CNV type in fellow eye			Total
		Occult	Classic	RAP	
CNV type in 1 st eye	Occult	27	1	0	28
	Classic	2	19	0	21
	RAP	0	0	2	2
Total		29	20	2	51

6.5 Discussion

In this study we compared the 2-year change in drusen load and retinal layer volumes between eyes that developed occult and classic CNV lesion at the end of 2 year follow-up period. When comparing drusen load between the 2 CNV types, there were significant increases in drusen area and volume in the preceding 12 months prior to develop occult CNV, whereas no significant differences were found in means of drusen count, area and volume at baseline, year 1 or year 2 between the 2 CNV groups. When comparing retinal layer volumes between the 2 CNV types, thinning of baseline ONL was found in the classic CNV groups, and significant differences in change volumes of ONL and OPL were found between the 2 CNV groups in year 2

only (no differences between the 2 CNVs were found in year 1). In occult CNVs, the volumes of ONL and INL were found to be reduced, whereas OPL and RPE-BM volumes were found to be expanded from year 1 to year 2. It is likely that occult CNV pushes up the inner retinal layers as it grows below the RPE, resulting in thinning in the inner retina. In classic CNVs, only RPE-BM volume increased from year 1 to year 2. This possible be explained by the fact that the lesion has broken through the RPE so the inner retina is less affected anatomically. We also investigated, in the same cohort, agreement between CNV type in second eyes developing CNV and the first eye CNV. Agreement was high (kappa statistic 0.89).

Drusen load findings of our study support findings reported previously in the literature. It has been reported that the clinical features in the fellow eye correlate with the type of CNV in the affected eye in AMD patients with unilateral CNV using colour fundus photography (Abugreen et al., 2003, Sivaprasad et al., 2006).

Abugreen et al. (2003) found that the fellow eyes of occult CNV have significantly more severe AMD features compared to the eyes with classic CNV. Similarly, Sivaprasad et al. (2006) showed that this kind of association between the CNV type in the affected eye and the severity of the disease in the fellow eye can be only applied on Caucasians in compared to the Chinese patients who did not show a similar disease pattern.

It is important to notice that the present study investigated longitudinally the correlation between prior drusen load quantifications using SD-OCT and subsequent CNV type in the same eye. Our data showed that a greater increase in OCT drusen area and volume can be seen in the year before developing occult CNV in compared to other eyes that developed classic CNV. As these drusen quantifications were measured by SD-OCT, the scans only detected soft drusen and no other type of

drusen such as RPD could be quantified. Thus, our findings of no significant differences between the 2 CNV groups in means of OCT drusen count, area and volume at baseline, year 1 or year 2 are consistent with the recent work of Marsiglia et al. (2015), who showed that soft drusen on colour photographs in one eye are not associated with CNV type in the other eye.

Our study demonstrated significant baseline thinning of ONL in eyes that developed classic CNV. The Thinning of ONL in AMD eyes has been reported in recent studies using OCT that showed ONL thinning in eyes with intermediate AMD (Schuman et al., 2009, Sadigh et al., 2013, Brandl et al., 2019). We also reported in a recent study that ONL layer is either not affected at early AMD stages or the amount of damage is not significant to be detected at earlier stages of the disease (Lamin et al., 2019b). Our finding suggests that ONL degenerates earlier in eyes that will develop classic CNV type than occult one but does not visibly worsen over time. Additional finding in this study supports this hypothesis which is a significant reduction in ONL volume in the eyes that developed occult CNV. Other notable observation in this study was that OPL increased in volume in the occult type. OPL thickening with age and in AMD has been reported recently (Nieves-Moreno et al., 2018, Lamin et al., 2019b). This increase in OPL volume may represent a compensatory expansion as a consequence to ONL thinning.

Finally, the observed symmetry in CNV types between the 2 eyes was high and this may give us an idea of the likelihood symmetry between the 2 eyes when trying to predicate the CNV type that most likely to be developed in a fellow eye of a patient with unilateral wet AMD. The symmetry of CNV type between eyes of AMD patients has been reported previously in a study of 115 patients and showed that patients with unilateral occult CNV have a high risk of developing occult CNV in the fellow

eye (Chang et al., 1995). However, a recent study reported a poor agreement (kappa statistic 0.16) in the symmetry of CNV between the 2 eyes in patients with bilateral wet AMD (Mann et al., 2011). It is possible that methodological differences explain the disagreement with the present study.

To our knowledge, this is the first study to longitudinally investigate a difference in retinal layer volumes and drusen load between occult and classic CNVs in order to identify imaging biomarkers. These biomarkers may aid in predicating the CNV type before developing in AMD eyes. This will allow for more individualised patients care and more effective trials because prognosis and treatment may vary based on CNV type.

Limitations include- retrospective study; possible ascertainment bias as only included patients with active CNV undergoing treatment. No adjustments were made for axial length or refraction. Further longitudinal studies involve other factors such as subretinal drusenoid deposits, pigmentary changes and choroidal thickness may enable the development of a risk score based on weight evidence of each imaging marker.

In summary, the association between simple automated quantification of drusen and retinal layer volumes using the method described, and subsequent CNV type would suggest that multiple pathogenetic mechanisms explain whether develop occult or classic CNV. This hypothesis might be tested by further studies on larger cohorts of patients. The observations of the present study provide imaging biomarkers that may help in predicating the type of CNV. Also, the strong agreement between CNV types in patients with bilateral CNV is consistent with distinct pathogenetic mechanisms or patient-specific modifiers, with some patients more at risk of one type than another,

which may support separating these subgroups in future trials of novel therapies or treatment regimens.

7 Chapter 7: Deep learning for prediction of AMD progression

7.1 Introduction

Advanced age-related macular degeneration (AMD) is a leading cause of vision loss for people over 50 and accounts for 8.7% of all blindness worldwide (Wong et al., 2014). AMD proceeds in distinct stages from early, to intermediate, to advanced. In advanced, wet (neovascular) AMD, blood vessel growth (choroidal neovascularization - CNV) can lead to irreversible damage to the photoreceptors and rapid vision loss. Currently, patients can progress to wet AMD without symptoms or any measurable change. Thus, it is of the utmost importance to try and determine which patients are at the highest risk for conversion to wet AMD to allow intervention before permanent damage.

Neovascularization is typically diagnosed based on signs of exudation, seen either by fundus examination and confirmed using fluorescein angiography (Spaide, 2004) or by visualizing fluid pockets seen cross-sectionally using depth resolved optical coherence tomography (OCT) images (Rosenfeld, 2016). In the absence of exudation, indocyanine green angiography (ICGA) imaging may be useful in identifying patients at risk of leakage (Schneider et al., 1997, Hanutsaha et al., 1998). This ability to see subclinical neovascularization in the macula has been underutilized in part due to the lack of therapeutics, but also given its cost and discomfort (de Oliveira Dias et al., 2018).

More recently, however, OCT angiography (OCTA), and in particular swept-source (SS) OCTA, is beginning to address these issues with a more patient-friendly ability

to image subclinical neovascularization (Choi et al., 2015). Like the more established structural OCT, the approach is non-contact and requires no injections and is very fast. OCTA images blood flow by taking multiple images in the same location and using a decorrelation algorithm to detect the motion of the blood cells as signal (Zarubina et al., 2016). By these means OCTA is able to resolve, for example, flow in the capillary beds. Being able to see the choriocapillaris and delineate areas of perfusion / non-perfusion opens a new window onto vascular health in the retina, including the much-needed ability to see and assess subclinical neovascular complexes.

The prognostic value of vascular abnormalities in predicting exudative AMD is an area of active investigation. While the early studies using fluorescent dye imaging (Hanutsaha et al., 1998, Schneider et al., 1997) have shown that subclinical irregularities (plaques, spots) are valuable biomarkers, new noninvasive techniques seek to build on this. The more recent findings correlating SS OCTA with ICGA imaging for example attempt to bridge this early work to the newer technologies (Roisman et al., 2016, Chung et al., 2018, Hirano et al., 2018). It is still an open area of research, however, and tremendous interest exists in utilizing more established imaging techniques such as structural OCT and fundus photography alongside more advanced algorithms to create clinical biomarkers stratifying a patient's level of risk of conversion to wet AMD. The motivation is pragmatic given that structural OCT imaging is the standard of care in the management of ocular diseases, is more affordable than OCTA, and has higher utilization and legacy data. It thus remains the most compelling modality to study for indications of subclinical CNV.

Another area of active research de Sisternes et al., (2014), for example, used traditional, feature-based modeling techniques applied to a number of hand-crafted

features, or parameters, for prediction of conversion to wet AMD. The features used included volume, height and reflectivity of drusen. In the case where the advanced AMD was geographic atrophy (GA) as opposed to neovascular, the same lab has developed similarly crafted features that were predictive of GA progression (Niu et al., 2016). In this study, the best feature was thinning and loss of reflectivity of the inner/outer segment junction, a structural measure derived from the OCT data. A similar combination of OCT-based structural features and visual acuity were used temporally across an initiation phase to characterize response to anti-VEGF treatment using a random forest classifier (Bogunovic et al., 2017). With areas under the curves (AUCs) between 0.7 and 0.8, the resulting predictive model had comparable performance with an expert human grader in predicting both low and high anti-VEGF treatment requirements. Interestingly, they found that temporally differential features were not found to play an important, discriminatory role in their model's predictions, and that a cross sectional analysis, as is presented here, achieved the same performance. More recently, Schmidt-Erfurth et al., (2018) used machine learning methods to assimilate various imaging, demographic and genetic features to predict the likelihood of conversion from intermediate to advanced AMD. In a study of 495 eyes, they had separate models for conversion to wet AMD (N=114) and geographic atrophy (N=45), and reported AUCs of 0.68 and 0.80, respectively, using 10-fold cross validation. The deep learning component used segmented hyperreflective foci in the OCT data producing an en face map of their location that generated nine separate numerical features based on location and distribution that was included in the final 71 features used. The "predictive hallmarks" for CNV were reported as "mostly drusen-centric".

7.2 Aims

In this work we look to derive OCT-based biomarkers based on a deep learning classifier to help predict which patients will progress from early/intermediate AMD to wet AMD using OCT imaging data alone. For context, we also present the performance of more traditional machine learning classifiers using features akin to those of de Sisternes et al., (2014) and Schmidt-Erfurth et al., (2018).

7.3 Methods

The participant demographics of this study has been discussed in chapter 3 and summarized Table 5.

7.3.1 Traditional image processing

Following earlier work (de Sisternes et al., 2014, Schmidt-Erfurth et al., 2018), we first assayed to perform the prediction using traditional image processing and machine learning techniques. All datasets were analyzed using patient data and layer-based biomarkers from OCT analysis software (Orion, Voxeleron LLC, Pleasanton, CA). The software automatically segments the OCT volumes into 8 retinal layers allowing analysis of various metrics such as average thicknesses and volumes of the different layers (and of the drusen) within the ETDRS zones (1991b) based on an automatic foveal centration. All segmentations were verified to be error-free (AL and JDO), and then analyzed for separation using a state-of-the-art machine learning classifier. Example segmentations for both progressors and non-progressors are shown in Figures 20 and 21, where we highlight more normal looking retinas and also those with some obvious drusen. Multiple layer segmentation offers multiple parameters that can be analyzed in an effort to

separate the two groups. An ETDRS grid has 9 zones, and with 7 average thicknesses being reported in each of these zones we can use any combination of thicknesses, or volumes over different regions to train a classifier to predict the class.

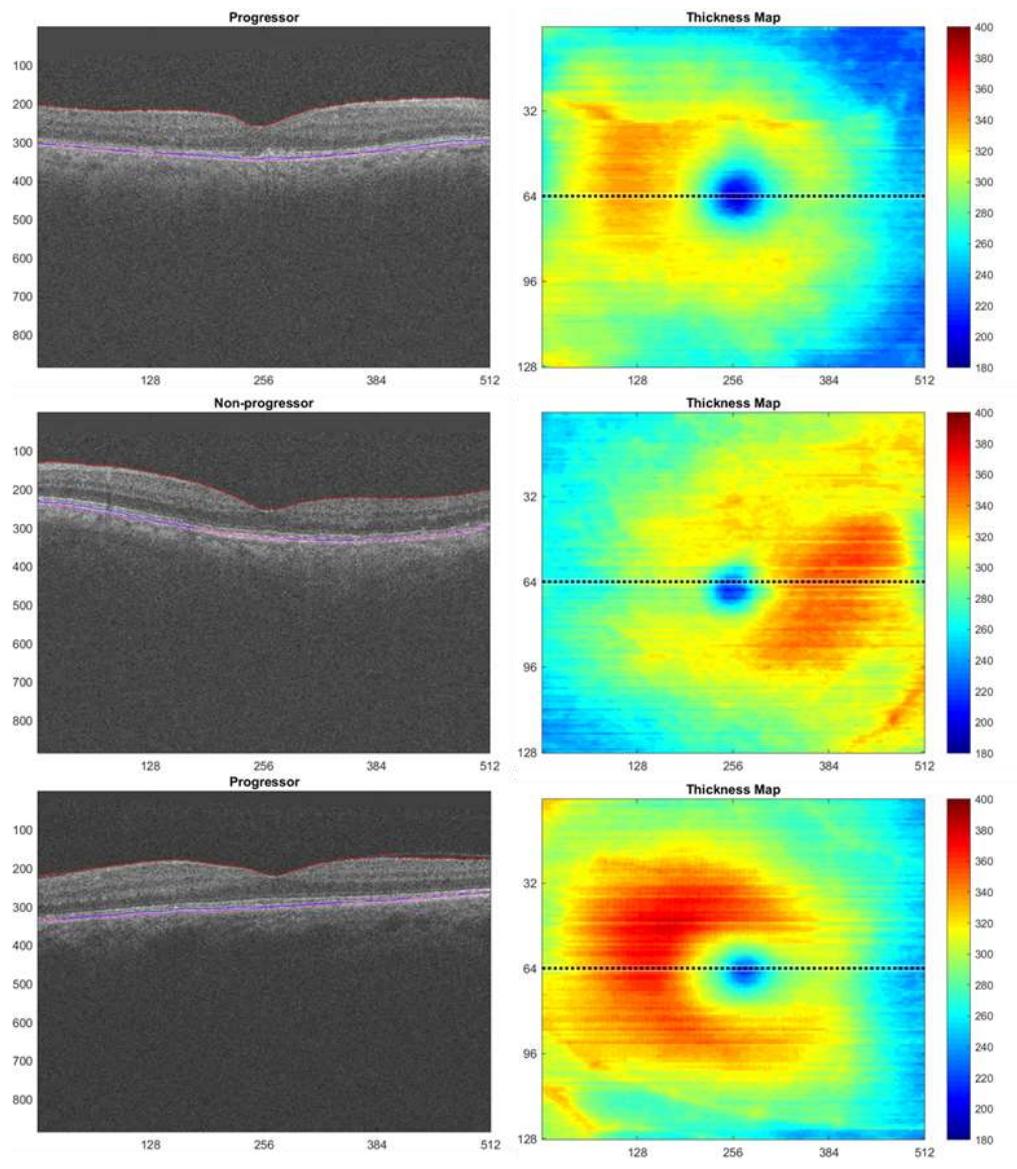


Figure 20. The left-hand side shows segmentations in both the progressor (top, bottom) and non-progressor (middle) groups. The right hand side shows their corresponding total retinal thickness maps in microns.

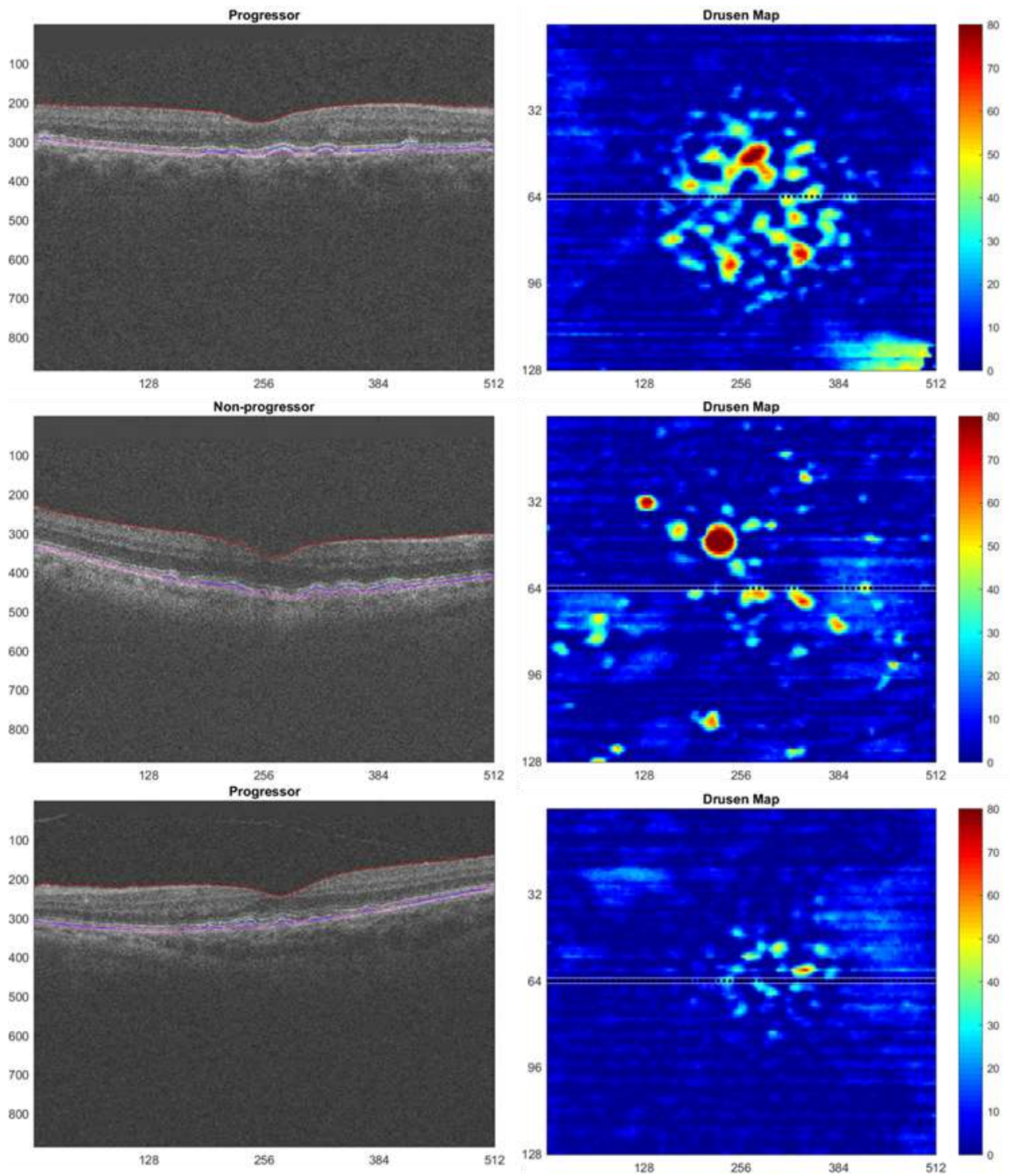


Figure 21. The left-hand side shows segmentations in both the progressor (top, bottom) and non-progressor (middle) groups. The right hand side shows their corresponding drusen thickness maps in microns.

We used a 32-dimensional feature vector that comprised biomarkers from the segmentation as well as patient information (Table 20). We used a support vector machine (SVM), a well-defined, state-of-the-art machine learning classifier to perform the prediction (Boser et al., 1992). The SVM was trained with radial basis functions for the kernel and the free parameters (box constraint, kernel scale) were chosen empirically. We evaluated the SVM using 5-fold cross validation taking care that the splits were made at the volume level so that no one patient's data ever appeared in both the training and testing sets. We report both the receiver operating characteristic (ROC) curve as well as its AUC in Figure 22.

Table 20. The 32 features used to train the SVM classifier. The thicknesses were taken as averages with the fovea-centered ETDRS grid, where: IA=inner annulus (circle of 3mm diameter, less the central 1mm subfield), OA=outer annulus (circle of 6mm diameter, less the central 1mm subfield and the IA), TA= IA+OA, D=entire 6mm diameter circle. The layer names follow the APOSTEL recommendations (Cruz-Herranz et al., 2016), and are: retinal nerve fiber layer (RNFL), ganglion-cell + inner plexiform layer (GC-IPL), inner nuclear layer (INL), outer plexiform layer (OPL), outer nuclear layer (ONL), photo receptor complex (PR), as well as RPE to Bruch's and the total retinal thickness (TRT). Foveal thicknesses of the RNFL and GC-IPL were excluded.

Layer	RNFL	GC-IPL	INL	OPL	ONL	PR	RPE to Bruch's	TRT	Patient-based
Zones	IA,OA,TA	IA,OA,TA	IA,OA,TA,D	IA,OA,TA,D	IA,OA,TA,D	IA,OA,TA,D	IA,OA,TA,D	IA,OA,TA,D	Age, Sex
Features	3	3	4	4	4	4	4	4	2

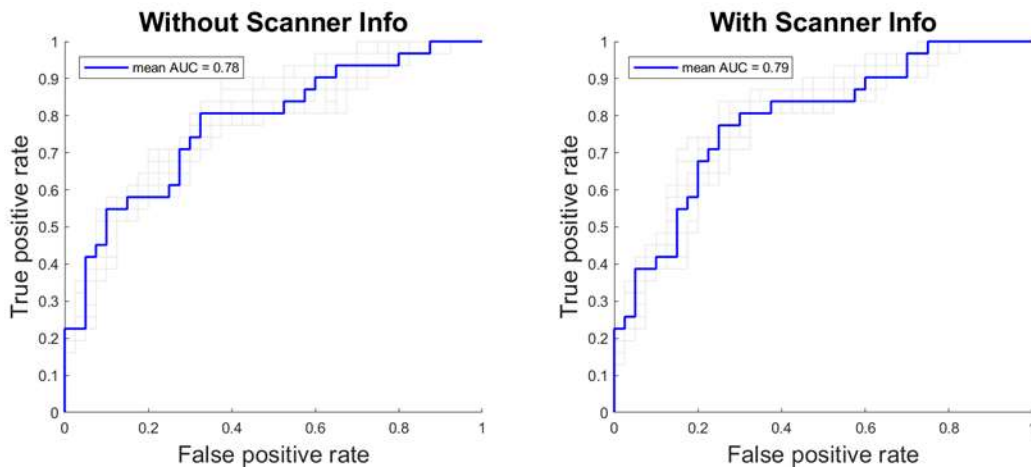


Figure 22. The above compares the performance of the SVM classifier (left) with the same data + instrument type added as a feature (right). This information appears to offer very little improvement in the classification.

7.3.2 Deep Learning-based Analysis

Our deep learning approach consists of a two-step process decoupling the image segmentation step from the classification step. This has the effect of allowing the classifier to focus specifically on the regions of interest. After the segmentation step, we tried two different CNNs:

1. Transfer learning using the popular VGG16 network (Simonyan and Zisserman, 2014)
2. AMDnet, a novel, simplified architecture trained from scratch

7.3.2.1 Segmentation-based Preprocessing

The 71 volumes were decomposed into 9088 B-scans which were preprocessed using the aforementioned layer segmentation software, to identify the inner limiting membrane (ILM) and Bruch's membrane (Figure 23). Each B-scan was then cropped from the ILM to a fixed offset (390 microns) below Bruch's membrane and resampled to a uniform size (Figure 24). The offset used was designed to capture choroidal

information over a fixed area beneath the choriocapillaris. It was chosen based on work from Manjunath et al. (2011) to represent 2 standard deviations above the mean subfoveal choroidal thickness in a population with AMD. This preprocessing was performed to reduce the variance of the training set and create some invariance to scale.

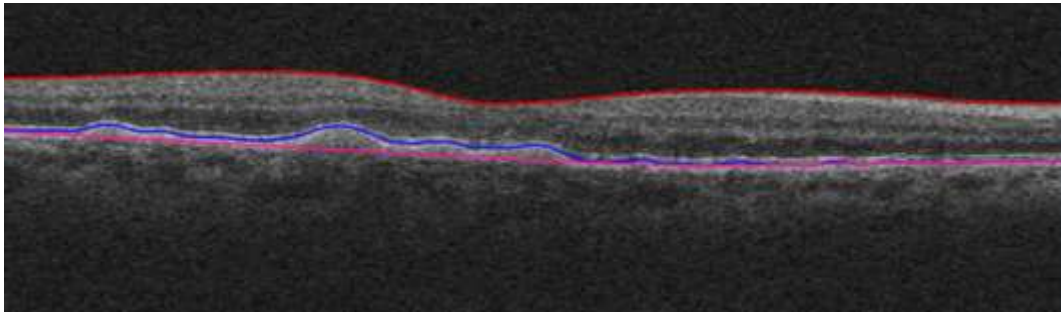


Figure 23. Example B-scan showing the automated segmentation (ILM in red, RPE in blue, and Bruch's membrane in magenta) used for the pre-processing. In this example, we clearly see signal in the choroid, albeit diminished below the drusen.

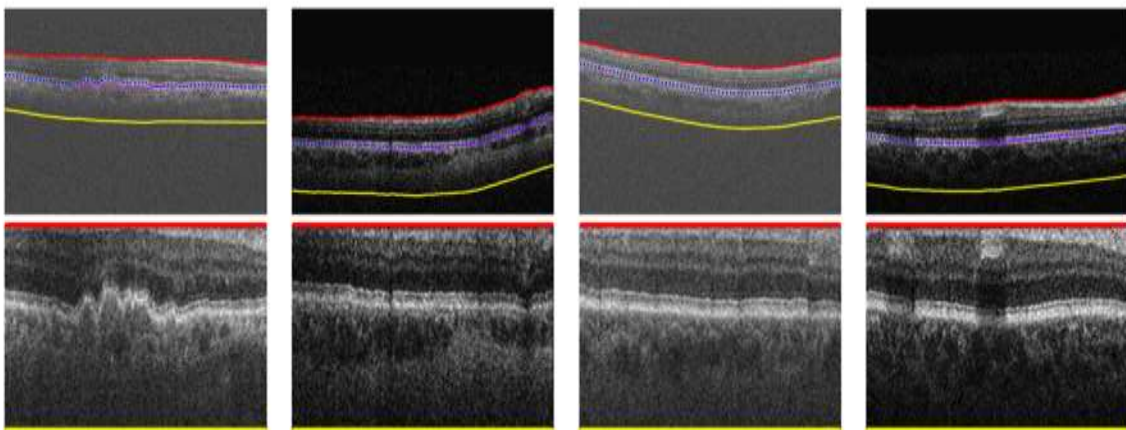


Figure 24 . An example of the preprocessing used to normalize the B-scans. The top row shows B-scans from a Topcon OCT scanner and the bottom row shows the corresponding images with normalization applied. The data is cropped between the ILM (red) and a fixed offset (390 μm) from Bruch's membrane (magenta-solid), which is itself estimated as a baseline (magenta-dashed) to the retinal pigment epithelium (RPE) (blue). Normalization in this way greatly reduces the variance in the training set and allows for robust training of smaller data sets as well as better generalizability. Note that, despite this being an SD-OCT device, the signal in the choroid is apparent and strong in each case.

7.3.2.2 A Transfer Learning Model

To evaluate the preprocessing, an existing, well-established deep convolutional neural network (CNN) (VGG16) (Simonyan and Zisserman, 2014) was fine-tuned using transfer learning based on the standard strategy of retraining only the fully-connected layers of the model (Rattani and Derakhshani, 2017). We used the original paper's fully-connected layer sizes (4096 neurons each) changing only the final layer from 1000 neurons to 2 neurons to fit our problem. Similar to Rattani and Derakhshani (2017), we experimented with simpler versions with a smaller number of neurons, settling on 512 and 128 neurons for the first two fully-connected layers, respectively. This process was applied to both the raw and preprocessed B-scans. The raw and preprocessed B-scans were resized to 224x224 to match VGG16's expected input. The training was run for 2500 epochs using stochastic gradient descent with Nesterov momentum and a learning rate of 5e-5. To avoid overtraining, we used early stopping with a patience of 20. The resulting classifiers were evaluated using the same 5-fold cross validation splits from the prior, traditional image processing analysis.

7.3.2.3 The AMDnet Model

Alternate architectures were explored in an effort to further improve the results. We tried both deeper, more complex networks as well as shallower, simpler ones and eventually settled on the latter. AMDnet (Figures 25 & 26) consists of just 3 convolutional layers with varying amounts of pooling. The number of parameters for this model is just over 2 million vs. more than 27 million (12 million trainable) for

VGG16. Given the relatively small size of the dataset, we took care to regularize this model in three specific ways:

1. We used dropout regularization with a percentage of 45% at the end of all but one of the convolutional and fully-connected layers. Dropout essentially acts during training on each batch to randomly remove a percentage of the previous layer's neurons. Dropout has the effect of averaging an ensemble of classifiers which produces more robust results and resists overtraining (Hinton et al., 2012).
2. We used L2 regularization for each of the convolutional layers which penalizes very large weights and has the effect of simplifying the model.
3. We used *maxnorm* regularization for the dense layers which also works to simplify the model by requiring the norm of a given layer's weights to be less than a pre-specified value.

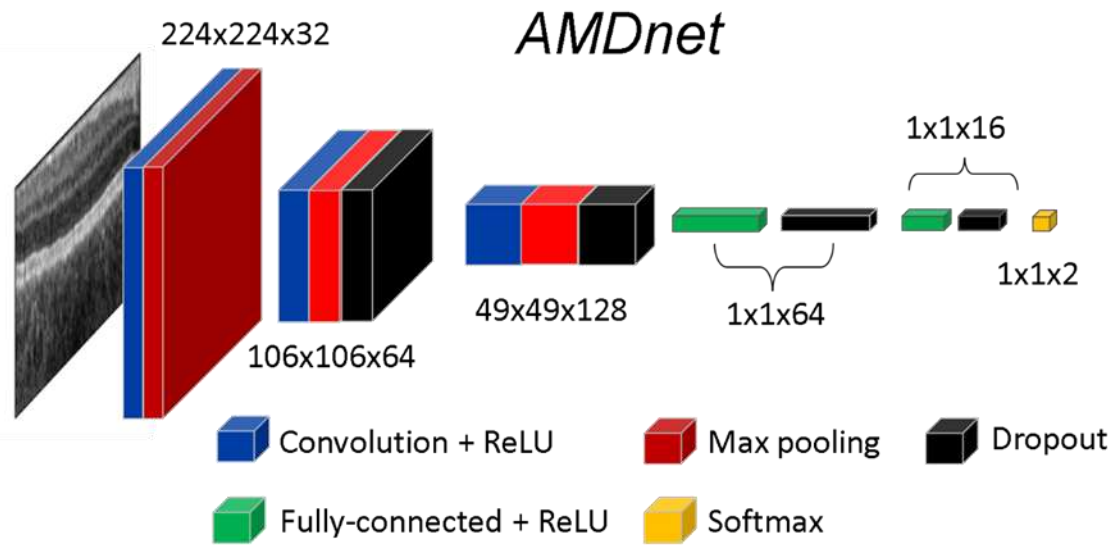


Figure 25. A schematic of the architecture of AMDnet.

Figure 26 has a detailed breakdown of the architecture of AMDnet. We evaluated AMDnet using the exact same 5-fold cross validation and splits as described above.

Layer	Input	Size	Stride	Padding	Regularization	Activation	Output	No. parameters
Conv1	224x224	5x5x32	1	Valid	L2 (l=1E-3)	ReLU	220x220x32	832
MaxPool1	220x220x32	2x2	1	-	-	-	110x110x32	0
Conv2	110x110x32	5x5x64	1	Valid	L2 (l=1E-3)	ReLU	106x106x64	51,264
MaxPool2	106x106x64	2x2	1	-	-	-	53x53x64	0
Dropout1 (45%)	-	-	-	-	-	-	-	0
Conv3	53x53x64	5x5x128	1	Valid	L2 (l=1E-3)	ReLU	49x49x128	204,928
MaxPool3	49x49x128	3x3	1	-	-	-	16x16x128	0
Dropout2 (45%)	-	-	-	-	-	-	-	0
Flatten1	16x16x128	-	-	-	-	-	32768x1	0
Dense1	32768x1	-	-	-	maxnorm (m=2)	ReLU	64x1	2,097,216
BatchNorm1	64x1	-	-	-	-	-	64x1	256
Dropout3 (45%)	-	-	-	-	-	-	-	0
Dense2	64x1	-	-	-	maxnorm (m=2)	ReLU	16x1	1,040
BatchNorm2	16x1	-	-	-	-	-	16x1	64
Dropout4 (45%)	-	-	-	-	-	-	-	0
Dense3	16x1	-	-	-	-	Softmax	2x1	34

Figure 26. A detailed breakdown of AMDnet.

7.3.3 Feature analysis

In an effort to tease out what latent features the classifier is relying on, and perhaps learn something about disease process itself, we also performed an occlusion sensitivity analysis (Zeiler and Fergus, 2013) of the outputs of the neural network. The occlusion analysis shows the regions of the image that are most discriminative with respect to a specific class. Such visualizations help interpret the overall results, especially in asking whether the method makes basic sense and whether artifacts or irrelevant features are driving the performance. This we revisit more thoroughly in the discussion.

7.4 Results

7.4.1 Traditional image processing

The summary results of the SVM analysis are shown in Figure 22 on the left. With AUC's in the range of 0.74-0.82 (mean = 0.78), these results are consistent with what has been previously reported by for this type of approach (de Sisternes et al., 2014, Schmidt-Erfurth et al., 2018).

Another consideration was given to potential bias introduced based on machine type as the two Topcon devices use different spectrometers, resulting in different axial resolutions. To investigate this, we added the dimensionality of the scan's axial resolution (either 480 or 885 pixels) as a feature, acting as an instrument flag. All features were scaled to zero mean and unit variance as part of the training process (test features being scaled based on the learned ranges). We reran the best performing SVM from the previous experiment using this new feature set and report the results in Figure 22 on the right. The mean AUC for this experiment of 0.79

suggests that having knowledge of the instrument appears to add little to no additional information to the classifier's performance.

Finally, we explore the potential bias of the follow-up interval on the performance of the classifier. Following the experiments above, we chose an operating point with false positive rate of 0.25 and looked at the true positives, true negatives, false positives and false negatives with respect to follow-up interval. We conclude, based on Figure 27, that small variations in the follow-up interval do not introduce a large bias into the results.

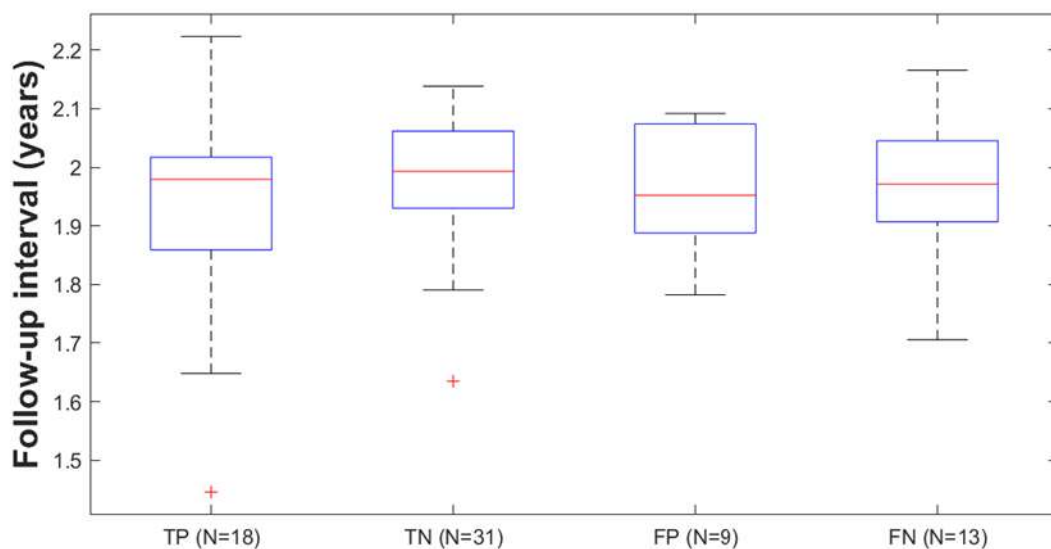


Figure 27. An analysis of the SVM results for a specific operating point (FP rate = 0.25). The follow-up interval does not seem to have a marked effect on the results.

7.4.2 Deep Learning

The results comparing the effect of the preprocessing (Figure 28) are presented at both the B-scan and volume levels. The prediction value for the volume-level analysis was calculating by taking the mean of each volume's individual B-scan predictions. For VGG16 with preprocessing, the AUC was 0.82 at the B-scan level

and 0.87 at the volume level while the same run without preprocessing (only scaling to match the VGG16 input) had AUC's of 0.67 and 0.69, respectively. The results for the same 5-fold validation for AMDnet are shown in Figure 29. We achieve a marked improvement with AMDnet at the B-scan level (0.89) and at the volume level (0.91). Interestingly, we also performed simple augmentation of the data (adding small rotations plus noise) but were unable to improve the algorithm's performance. This very clearly demonstrates the benefits of preprocessing as, regardless of network and evaluation metric, the performance improves each time.

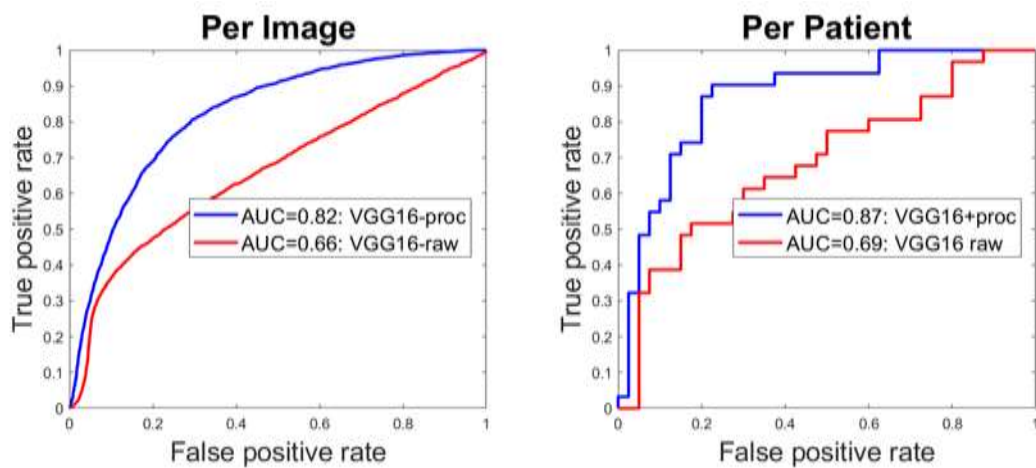


Figure 28. Per-B-scan (left) and per-patient (right) ROC and AUC results for the fine-tuned VGG16 CNN using segmentation-based preprocessing (blue) and just simple resizing (red). As expected, preprocessing to reduce the variance of the input data dramatically improves the results.

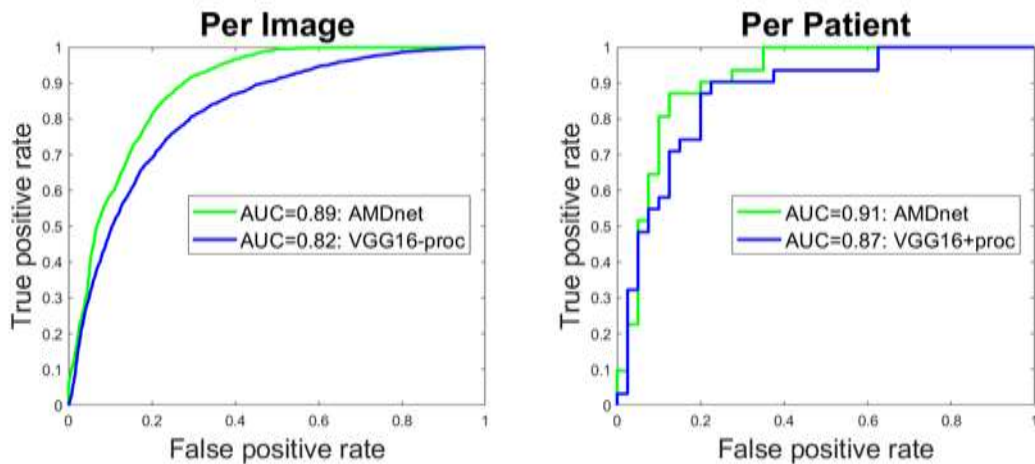


Figure 29 . Per-B-scan (left) and per-patient (right) ROC and AUC results for AMDnet (green) and VGG16 with preprocessing (blue). The simplified AMDnet architecture shows improvements across both sets.

The results of the feature analysis, shown in Figure 30, illustrate that the areas around the retinal pigment epithelium (RPE) and choroid seem to be the most useful to the classifier in making its predictions. In particular, this analysis shows that pixels around the RPE have the largest impact on the final score of the classifier in the case of non-progressors while progressors seem to have more sub-RPE choroidal involvement. In addition, we stacked the class activation maps into volumes looking for a pattern in the en face direction (Figure 31). These results suggest a stronger response nasally for non-progressors while the temporal area relies more on the temporal region. Further investigation is needed, but this difference could potentially be due to the presence of more photoreceptors nasally or large arterioles nasally skewing the choroidal density.

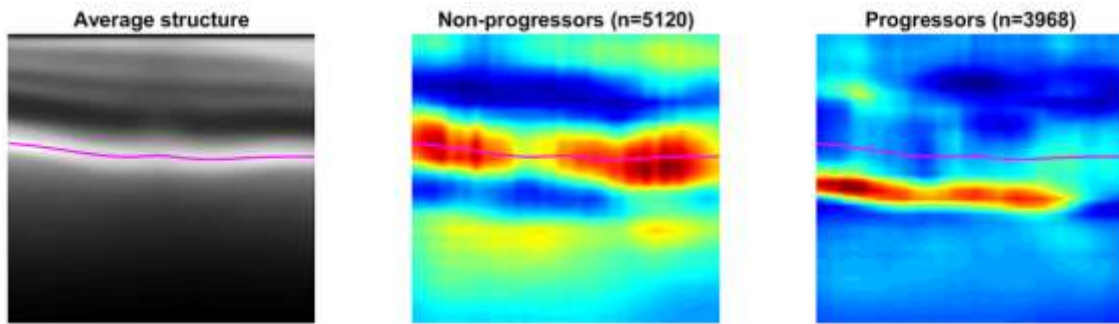


Figure 30 . Occlusion sensitivity analysis for progressors (right) and non-progressors (middle). These images were derived by averaging the occlusion analysis outputs for all B-scans in their respective groups. The average structure for all B-scans is shown on the left and the mean location of Bruch's membrane in all scans is plotted in magenta. This analysis shows that, in particular, pixels around the RPE have the largest impact on the final score of the classifier for non-progressors. It also suggests more sub-RPE or choroidal involvement for progressors.

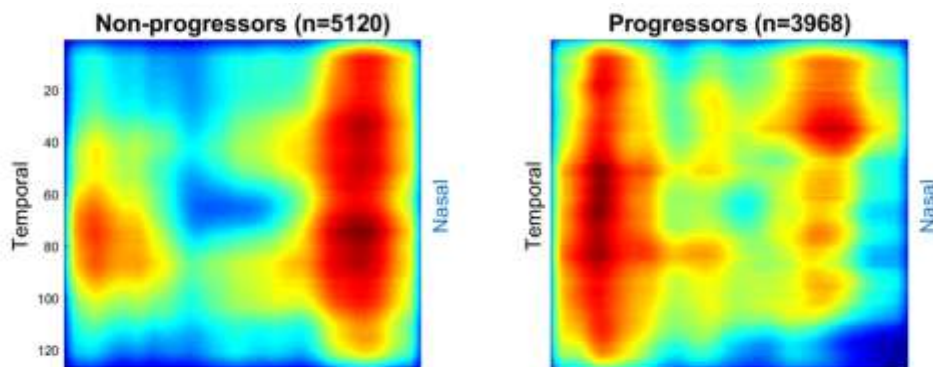


Figure 31 . En face visualization of occlusion sensitivity analysis. The results from each B-scan's occlusion analyses were stacked into a volume and all of these volumes were averaged. An en face image of the average volume is displayed for non-progressors (left) and progressors (right). The non-progressors seems to have more relevant features in the nasal side of the volumes while the progressors show the opposite effect.

7.5 Discussion

We have reported on a use of deep learning to predict conversion to wet AMD using OCT imaging. The results show clear separation between the progressors and the non-progressors and the occlusion sensitivity analysis indicates that relevant features are brought to bear by the technique. In the following we add context to these findings, discuss their clinical relevance, present some limitations of the study, and close with some conclusions.

One of the major challenges in the clinical management of patients with early/intermediate AMD is the assessment of risk of conversion and any metrics supportive of this assessment are welcome. Structural OCT data have been used to create anatomical biomarkers such as thickness and volumetric measures, but despite being researched for several years now, compelling indicators of conversion have yet to emerge. Instead, interest has turned to OCTA where subclinical neovascularization is being observed and studies are being carried out on how to quantify these observations such that they can be deployed clinically. OCTA instrumentation is, however, less widely used, and longitudinal data less readily available. In addition, OCTA data has greater dependence on variations in signal strength across different systems and is vulnerable to projection artifacts that makes it difficult to assess flow as a reliable bio-marker, especially in the case of neovascularization underneath the RPE (Type 1) (Novais et al., 2016). With the advent of more advanced feature extractors and classifiers facilitated through deep learning, we have revisited and further mined the OCT data sets for signal that, akin to OCTA, might be supportive of the subclinical assessment of non-exudative neovascularization.

An immediate interpretation of the findings is that the neural network has discovered specific patterns indicative of pathological change. OCT-based features identified in early CNV have been previously reported (Mukkamala et al., 2012, Querques et al., 2014, Sato et al., 2007, Spaide, 2009). The analysis we report on, however, looks at data before any clinically observable signs of conversion, so consideration must be given to more subtle features including textural changes that are perhaps occurring as a direct result of early physiological changes. Pathology detection using OCT texture analysis has itself been previously researched (Gossage et al., 2003). Such approaches failed to gain traction, but in the advent of better computational resources and the more sophisticated learning approaches, we envisage a resurgence in such work. The texture descriptors were examples of hand-crafted features, a technique that has been superseded by the ability to instead learn the features through deep learning. Similarly, in the work from de Sisternes (2014), Niu (2016) and Schmidt-Erfurth (2018), the features were manually crafted, and, through extensive use of regression, applied to temporal data in their final models. Through learning the features in a systematic way afforded by deep neural networks, more powerful and better regularized solutions are now possible. Very important to the method, however, is the pre-processing of the input data via a segmentation step that 1) gives us some invariance to instrumentation and 2) allows the network to concentrate on tissue of interest. This is somewhat akin to the recent work by De Fauw (2018) where their classification scheme uses a separate segmentation step, here using a U-Net deep learning architecture (Ronneberger O., 2015) and then classifying the homogenous tissue regions into referral classes using a second deep learning architecture, one that is very similar in composition to that used in this study.

In our work, however, we do not disregard the image intensities and distributions as they are critical to our method in differentiating the classes.

The results show that the signals are localised at the RPE level extending to the choroid. This finding paves our way to concentrating research to these layers. There has been significant confusion as to which outer layer is primarily involved – is it the photoreceptors and the hypoxia induced mainly by the rod function or is it the lipofuscin loaded RPE cells that interfere with the metabolic transfer of nutrients and the visual cycle or is it the atherosclerosis and slowing of blood flow of the choriocapillaris that is not involved. The study results cannot be used to conclude a inciting layer but it shows that in eyes that are at risk of conversion to neovascular AMD, the choroidal signals increase significantly while those that do not progress show significant signals around the RPE layer. This mirrors our findings on increasing thickness of the outer retina before conversion. However, the choroidal signals are very important as it suggests subclinical neovascularisation that is not detectable on OCT. Our study needs to be validated in a larger cohort but is definitely showing a clear distinction between progressors and non-progressors.

This study is not without some limitations. Although this is not a large and balanced data set, more data would help better support our conclusions. To address this, unbiased estimates of performance are reported including the cross-validation approach given in the method section, where care was taken to evenly balance the cohorts in the test and training sets, ensuring same subject data was not used across data sets. As a pilot study, however, the findings are compelling.

A second limitation could perhaps also be considered a strength of the method given the positive results and the indication that information in the choroid is of importance

to the performance. This is namely the SDOCT scanner used (Topcon 3d OCT) has a light source of 840nm which offers limited depth penetration given its relatively short wavelength. Longer wavelengths are preferred for resolving detail in the choroid even if these lose some axial resolution. However, through simple review of the B-scans (see Figures 20 and 21, for example), one can see clear choroidal signal in the OCT data. And conversely, this speaks to the strength of the method as even with this limited penetration, there is clearly information in the choroidal regions of the data that is being used to discriminate progressors from non-progressors (Figure 30). We are currently collecting data to test the method using other devices, including SS OCT as well as depth enhanced imaging (EDI), a spectral domain approach that puts the focal plane (point of greatest signal) lower in the image. In addition, no adjustments were made for age or risk factors such as smoking.

This study is on a population of unilateral neovascular AMD eyes, who have a high risk of conversion. Therefore, studying the non-progressors and progressors in this enriched cohort allowed us to target the pathological area better. As this is the case, however, it is not known how the models and results would generalize to patients with bilateral early/intermediate AMD, who constitute the majority of the at-risk population. Again, this is an interesting avenue of research that we would also like to look at in more detail.

To conclude, we report that a deep learning CNN with layer segmentation-based preprocessing shows strong predictive power with respect to the progression of early/intermediate AMD to advanced AMD. Such adjunct analysis could be useful in, for example, setting the frequency of patient visits and guiding interventions.

8 Chapter 8: Summary, conclusion and future directions

Identifying biomarkers that can predict the progression to wet AMD is an unmet need, in order to allow early intervention before permanent damage. There are a numbers of clinical trials that have failed to prevent progression to advanced AMD. Although these failures have been attributed to the drugs not being effective, a fundamental flaw is that the end-points that mark disease progression are limited and require measurement over years. AMD is also a heterogeneous disease. This thesis aimed to study various aspects of disease progression to wet AMD including the study of heritability and imaging characteristics. I studied cohorts of normal eyes with aging, eyes with early/intermediate AMD and fellow eyes of patients with unilateral wet AMD to predict the rate of conversion to wet AMD.

The thesis is divided into 5 parts, first a study on measurement of retinal layer volumes of healthy and AMD patients. Second, the heritability of retinal layer volumes. Third, the drusen measurements and their associations with wet AMD progression. Fourth, the difference between occult and classic CNVs in terms of drusen load and retinal layer volumes. Finally, the use of deep learning to predict AMD progression.

8.1 Changes in volume of various retinal layers over time in early and intermediate AMD

This part of the thesis aimed to evaluate volume changes longitudinally in inner and outer retinal layers in early and intermediate AMD and compare the results to age

matched control population using OCT. Moreover, a sub-analysis of the AMD eyes that progressed to wet AMD and other that did not progress were performed. The rationale for conducting this study was to identify changes in retinal layer volumes in AMD eyes, which might be used as biomarkers for disease conversion.

The emergence of software that have the ability to segment the retina into layers akin to its histological structure influenced us to conduct the study. We used Orion segmentation software, which has been shown by many previous studies to be able to measure thicknesses and volumes of retinal layers with distinct boundaries. It is designed to accurately and rapidly segmenting macular OCT images into 7 layers (excluding TRV) including Retinal Nerve Fiber Layer (RNFL), Ganglion Cell-Inner Plexiform Layer (GCIPL), Inner Nuclear Layer (INL), Outer Plexiform Layer (OPL), Outer Nuclear Layer (ONL), Photoreceptors (PR), and Retinal Pigment Epithelium-Bruch's Membrane complex (RPE-BM).

Our results of a longitudinal study of 102 participants over 2 years showed that inner and outer retina layer volumes may differentiate AMD eyes from healthy eyes. When comparing progressors to non-progressors eyes, we found that baseline volume of GCIPL may differentiate between the 2 groups.

Firstly, we compared baseline and year 2 volume measurements of AMD with controls and found that some inner retinal layer volumes (GCIPL and INL) were thinner and some outer retinal volumes (PR and RPE-BM) were thicker in eyes with AMD compared to healthy eyes. We then explored longitudinal changes over 2 years follow-up. OPL and RPE-BM volumes were found to increase, whereas the volume of ONL was found to decrease during the 2-year follow-up in AMD eyes.

Secondly, we performed a sub-analysis in the AMD eyes, aiming to differentiate between eyes that progressed to wet AMD and others that did not. There were significant difference between the progressors and non-progressors in mean volumes of GCIPL and OPL at baseline, and RPE-BM at year 2. GCIPL and OPL volumes were less in progressors than non-progressors at baseline. Conversely, RPE-BM volume was greater in the progressing group than non-progressing one at year 2. When looking at the progressors during the 2-year follow-up, there was a progressive reduction in the volume of INL and ONL, and a significant expansion in the volume of RPE-BM. The GCIPL volume remained unchanged in progressors over the 2 years. The thinning of GCIPL volume at baseline may be used as a biomarker for disease conversion.

By looking at outer retinal layer volumes, we know that the expansion of RPE-BM and PR volume is likely to be a consequence of RPE function failure, resulting in drusen formation (RPE-BM expansion) and decline in phagocytosis of photoreceptor outer segments (PR expansion) (Bonilha, 2008). In addition, the expansion in OPL volume might represent remodelling or might also be a consequence of mechanical factors, including expansion as neighbouring cellular layers might reduce in volume. Of note, the volume of ONL did not show any difference between AMD and control eyes as well as between the progressors and non-progressors but during the follow-up period there was a noticeable reduction in ONL volume in AMD eyes regardless of the disease subgroup (progressors or non-progressors). Histological study demonstrated that rods are more vulnerable to damage than cones in AMD eyes, suggesting rods loss begin first then cones in more advanced form of the disease (Curcio et al., 1996). This may explain the huge reduction of ONL volume in more advanced dry AMD as there are significantly more rods in the macular area than

cones. This also explains that cone related visual function remains normal until advanced AMD involves the fovea but rod related dark adaptation reduces in eyes with intermediate early long before disease progresses to advanced AMD. Thus, we conclude that ONL thinning may be an early sign of AMD eyes. Large cohorts need to be tested on this to validate my findings.

Moving to the inner retina, the thinning of GCIPL and INL that we found in our study is already established in recent studies using OCT, and thought to be a consequence of either ischemia or transsynaptic issue (Villegas-Perez et al., 1998, Feigl et al., 2007, Toto et al., 2016, Toto et al., 2017, Strettoi et al., 2002), although these have not been confirmed in histopathological studies. RNFL also decreased in volume but in slower rate compared to other inner retinal layers. Thus, we conclude that all inner retinal layers decrease in AMD eyes. These changes are unlikely just related to compression from outer retinal thickening and suggest that AMD may in fact affect all layers of the retina because the reduction in GCIPL and INL volume precede the reduction in ONL volume as the disease progresses. This finding gives clues that inner retina may be markedly damaged before outer retina. Our finding of chapter 4 (heritability of retinal layer volumes study) showed that genetic predisposition play a role in variance in inner retinal layer volumes might partly explain the early degeneration of the inner retinal layers in the present study. However, the theory on inner retinal ischaemia and dysfunction of synaptic transmission suggested by other authors need to be investigated further.

8.2 Retinal layers volumes: age association and heritability

This section of the thesis aimed to investigate segmented macular layer volumes from macular OCT scans from a healthy adult twin cohort (TwinsUK), exploring heritability and changes with age of each layer separately. The rationale for conducting this study was to evaluate whether heritability was responsible for ageing changes of the retinal layer volumes.

Twin studies allow investigation of relative genetic and environmental contributions to phenotypic traits. A higher correlation in MZ twin pairs indicates that genetic factors are important in determining variance in retinal layer volumes and this can be performed by comparing intra-pair correlation of retinal layer volumes in MZ and DZ twin pairs. Estimation of the proportion of the variance in a trait that is attributable to genetic factors can therefore be formally calculated by twin modelling, defined as heritability.

Our results of this cross sectional study of 184 (92 pair) twins showed significant heritability of the majority of segmented layer volumes. We also found that TRV, and volume of some inner retinal layers, decreased with age, while outer layer volumes increased with age.

Firstly, we explored heritability of retinal layer volumes using the twin study paradigm and found that intra-pair correlation was greater for MZ than DZ for all layers.

Heritability estimates were highest (>80%) for TRV and GCIPL volume, and lowest for RPE-BM volume. High heritability of inner retinal volumes represents greater importance of genetic factors in the volumes variance of inner retinal layers, whereas

low heritability of outer retinal layer volumes could represent a greater influence of environmental factors on these outer retinal layers.

Secondly, we examined age-associated changes in retinal layer volumes and found that TRV and volumes of inner retinal layers (RNFL, GCIPL, and INL) decreased with age; increasing volume with age was observed for most outer retinal layers (PR, RPE and OPL), though not the ONL. Our findings of thinning in inner retinal layer volumes with increasing age are completely consistent with findings of previous studies in the literature (Ooto et al., 2011, Demirkaya et al., 2013, Nieves-Moreno et al., 2018). However, the finding in the present study of thickening in some outer retinal layers with increasing age is not consistent completely with other studies. Outer retinal layer thicknesses have been shown to be either increase, decrease or do not change with age; it is possible that methodological differences explain the disagreement between studies.

By interpreting the data of the present study together with the previous study (chapter 3), we can conclude that the high heritability of inner retinal layers might explain the early degeneration of inner retinal layers in AMD eyes. Moreover, changes in retinal layer volumes with age are exactly similar to that seen in AMD eyes. However, the rate of change over time was significantly greater in AMD eyes compared to age-matched control healthy eyes.

8.3 Changes in numbers, area and volume of drusen in fellow eye of patients with neovascular AMD

This part of the thesis aimed to explore the rate of change in drusen morphology based on OCT images in fellow eyes of patients with unilateral wet AMD. The

rationale for conducting this study was to evaluate whether any of drusen parameters (count, area, volume) would predict AMD progression to CNV; then can be used as a biomarker for disease conversion.

Recently, drusen measurements such as number and area have been established as risk factors of AMD progression. They are routinely measured on colour fundus photograph but this is prone to errors and reader variability, and is time consuming. The advance in OCT and the development of automated drusen segmentation algorithms have allowed us to detect and quantify drusen more accurately and easily. Topcon OCT is widely used in daily practice and it has its own in-built drusen software, which makes drusen measurement more convenient for the research as well as clinical purpose. Therefore, taking this opportunity forward by studying drusen, using Topcon, was one of the reasons for conducting the present study, in order to be applied to clinical practice. As a result, patients can be counselled more accurately about the time to second eye involvement

Our results of this longitudinal study of 248 participants demonstrated a significant change in drusen parameters occur in AMD eyes in the preceding 12 months prior to conversion to wet AMD. Changes in drusen volume were the most sensitive predictor of conversion to wet AMD.

Firstly, we compared baseline drusen count, area and volume between fellow eyes that developed CNV (CNV-developed) by year 2 and those that did not (non CNV-developed), and found that the mean measurements were larger in CNV-developed eyes than non CNV-developed ones. We also analysed the baseline measurements as predictors of progression to CNV by year 2 and found that baseline drusen volume was a significant predictor for developing CNV.

Secondly, we also compared the rate of change of drusen parameters between CNV-developed eyes and non CNV-developed eyes over the 2-year follow-up in terms of 2 time points; year 1 (from baseline to year) and year 2 (year 1 to year 2). While there was no difference in the rate of change between the two groups at year 1, there was a statistically significant difference at year 2, particularly drusen volume and area. Drusen volume and area increased significantly in CNV-developed eyes in the year preceding conversion, indicating the importance of these OCT drusen measurements as biomarkers for disease progression.

Taken together, this study has shown that drusen volume growth rate across a 6 mm macula cube using the automatic Topcon drusen analysis software may be used as a predictor for conversion to CNV.

By interpreting findings of the present study together with chapter 3 findings, we can conclude that increase in RPE-BM volume correlates with increase in drusen volume/area over time in eyes with early/intermediate AMD. However, as some eyes have very few drusen especially in eyes with classic CNV, I investigated further as to whether this change applies to all CNV.

8.4 Predictor of CNV type based on drusen load and retinal layer volumes

This part of the thesis aimed to evaluate whether any correlation existed between prior drusen and/or retinal layer quantification measurements and the subsequent CNV type. The rationale for conducting this study was to identify biomarkers that can predict CNV type (occult or classic).

Distinguishing between classic and occult CNV types based on identified predictive biomarkers might aid in separating these CNV lesions in future trials of novel therapies. Although CNV classification is not required in the current treatment of wet AMD with anti-VEGF, recent trials of novel therapies have included CNV type as a part in their inclusion criteria (Danis et al., 2014, Jaffe et al., 2017). This indicates the significance of classifying CNV as the natural history of wet AMD varied between CNV types. Classic lesions are aggressive and associated with severe vision loss and scar formation (Daniel et al., 2018), whereas occult CNVs are often stable and associated with overall a better visual acuity than other CNVs (Invernizzi et al., 2019). Therefore, predicting the CNV type will allow for more individualised patients care and more effective trials because prognosis and treatment may vary based on CNV type.

Our results of this longitudinal study of 51 participants demonstrated a significant increase in drusen area and volume in the preceding 12 months prior to develop occult CNV. We also found that baseline volume of ONL may differentiate between the 2 CNV groups.

Firstly, we compared means of drusen count, area and volume at baseline, year 1 and year 2 between eyes that developed occult and classic CNVs, and there were no statistical differences between the 2 CNV types. We also compared the rate of change of drusen area and volume between the 2 groups over the 2-year follow-up in terms of 2 time points; year 1 (from baseline to year 1) and year 2 (year 1 to year 2). The rate of change of drusen area and volume was higher in occult CNV types than in classic CNV types in year 2.

Secondly, we compared means of retinal layer volumes at baseline, year 1 and year 2 and found that only volume of ONL at baseline and year 1 was thinner in classic CNVs than occult CNVs. We then explored longitudinal changes over 2 years follow-up in terms of 2 time points; year 1 and year 2. In year 1, no differences were found between the 2 CNV groups or within each CNV group. In year 2, significant differences in change volumes of ONL (3 mm and 6 mm) and OPL (3 mm) were found between the 2 CNV groups. There was a progressive reduction in the volume of ONL, and an expansion in the volume of OPL. In occult CNVs, OPL (3 mm and 6 mm) and RPE-BM (3 mm) volumes were found to be expand, whereas the volumes of ONL (3 mm and 6 mm) and INL (3 mm) were found to be reduced. In classic CNVs, only RPE-BM (6 mm) volume increased and no other changes were found.

Taken together, this study has shown that increase in drusen area and volume, and reduction in volume of ONL in the preceding year prior to conversion to wet AMD are associated with developing of occult type CNV in particular. The ONL volume showed a reduction two years prior to development of classic CNV and remained unchanged over the 2-year follow-up, indicating that this layer degenerated earlier in the classic CNV type.

8.5 Deep learning for prediction of AMD progression

This part of the thesis aimed to evaluate whether artificial intelligence such as deep learning methods using OCT imaging data can predict the likelihood of progression from early/intermediate AMD to wet AMD.

Our results of this study of 71 participants demonstrated the ability of our deep learning model to identify those who progressed to wet AMD (progressors) than those who did not (non-progressors). The quantitative feature for progression was

the area around the retinal pigment epithelium (RPE) and choroid, suggesting more sub-RPE choroidal involvement for progressors versus non-progressors.

Two deep convolutional neural networks (CNN) were trained using the OCT data: (1) a novel, simplified CNN architecture was trained from scratch and (2) VGG16, a popular CNN for large scale image recognition (Simonyan and Zisserman, 2014). Preprocessing was added in the form of a segmentation-based normalization to reduce variance in the data and improve performance.

Our predictive model with preprocessing achieved an area under the ROC curve (AUC) of 0.89 for B-scans and 0.91 for volumes. Results for VGG16 with preprocessing were 0.82 for B-scans and 0.87 for volumes.

In summary, a deep learning CNN with layer segmentation-based preprocessing shows strong predictive power for the progression of early/intermediate AMD to wet AMD. Regardless of the network architecture, using the segmentation-based preprocessing has shown to improve overall performance. Predictive hallmark for CNV progression was significant involvement of sub-RPE choroidal region.

8.6 Conclusion

This thesis has identified imaging biomarkers that can be used in predicting AMD progression from early and intermediate stages to wet AMD. This could allow us to identify patients who are likely to progress to advanced stage, and thereby permit making the appropriate management and follow-up.

Our approach was based on computational analysis of patients' images only. This technology based approach may be used in future clinical trials to predict the risk of disease progression.

To sum up, drusen load increases and retinal layer volumes changes before conversion to wet AMD and automated drusen and retinal layer volumes measurement tools may be used as useful biomarkers to monitor eyes for conversion to wet AMD. The deep learning technique also suggests the choroid may indeed be involved early before conversion and we need to validate this finding in large cohorts. This thesis indicates that there are multiple ways by which our known markers of AMD can be used to refine conversion rates more accurately. Other findings such as inner retinal heritability and choroidal changes preceding conversion add new dimensions to our understanding of conversion to wet AMD. These may allow earlier detection of AMD progression, enabling earlier treatment and better clinical outcomes.

8.7 Future directions

My thesis adds valuable information to AMD literature, the findings have thrown light to novel areas of investigations to better phenotype this heterogeneous disease.

Firstly, the OCT finding of inner layer volumes thinning in early AMD stages suggests pathological process affecting particularly ganglion cell-inner plexiform layer and inner nuclear layer very early in the AMD disease process. I also show that heritability may account for these changes. Therefore, researchers can now focus their attention on complement genotype changes on inner retina.

Secondly, outer nuclear layer thinning at early AMD stage may occur mainly in eyes that convert to CNV type. This concept better explains why dark adaptation is affected early in AMD. Further structure-function studies should be directed to this field.

Thirdly, the deep learning predictive model shows that the predictive hallmark for CNV conversion is at the sub-RPE choroidal region in eyes that progressed to wet AMD. Although imaging of the choroid remains challenging, this thesis directs the focus of future research to the choroid. Interestingly, this study has shown that the non-progressors seem to have more relevant features in the nasal side of the volumes while the progressors show the opposite effect. This hypothesis might be tested by further studies on larger cohorts of patients.

Finally, we would like to use the same methodology to look at geographic atrophy development/progression in AMD patients.

9 References from websites

1. OCT SCANS

<http://www.octscans.com>

2. Voxeleron

<https://www.voxeleron.com/orion/>

3. Topcon

https://www.topcon.co.jp/en/eyecare/products/product/ diagnostic/oct/3DOCT-2000_E.html

4. TOPCON 3D OCT Series Normative Database

http://www.topconmedical.com/_assets/cf/downloadFile.cfm?section=productLit&file=3D-OCT-Series-Normative-Summary.pdf&parentUUID=55E1DBB5-CB99-9BF1-88CBBBE970ECAB77.

10 References

- 1991a. Laser photocoagulation of subfoveal neovascular lesions in age-related macular degeneration. Results of a randomized clinical trial. Macular Photocoagulation Study Group. *Arch Ophthalmol*, 109, 1220-31.
- 1991b. Subfoveal neovascular lesions in age-related macular degeneration. Guidelines for evaluation and treatment in the macular photocoagulation study. Macular Photocoagulation Study Group. *Arch Ophthalmol*, 109, 1242-57.
1992. Risk factors for neovascular age-related macular degeneration. The Eye Disease Case-Control Study Group. *Arch Ophthalmol*, 110, 1701-8.
1993. Five-year follow-up of fellow eyes of patients with age-related macular degeneration and unilateral extrafoveal choroidal neovascularization. Macular Photocoagulation Study Group. *Arch Ophthalmol*, 111, 1189-99.
1996. Occult choroidal neovascularization. Influence on visual outcome in patients with age-related macular degeneration. Macular Photocoagulation Study Group. *Arch Ophthalmol*, 114, 400-12.
1997. Risk factors for choroidal neovascularization in the second eye of patients with juxtafoveal or subfoveal choroidal neovascularization secondary to age-related macular degeneration. Macular Photocoagulation Study Group. *Arch Ophthalmol*, 115, 741-7.
1999. Photodynamic therapy of subfoveal choroidal neovascularization in age-related macular degeneration with verteporfin: one-year results of 2 randomized clinical trials--TAP report. Treatment of age-related macular degeneration with photodynamic therapy (TAP) Study Group. *Arch Ophthalmol*, 117, 1329-45.
2001. A randomized, placebo-controlled, clinical trial of high-dose supplementation with vitamins C and E, beta carotene, and zinc for age-related macular degeneration and vision loss: AREDS report no. 8. *Arch Ophthalmol*, 119, 1417-36.
2013. Lutein + zeaxanthin and omega-3 fatty acids for age-related macular degeneration: the Age-Related Eye Disease Study 2 (AREDS2) randomized clinical trial. *Jama*, 309, 2005-15.
- ABDELFATTAH, N. S., ZHANG, H., BOYER, D. S., ROSENFELD, P. J., FEUER, W. J., GREGORI, G. & SADDA, S. R. 2016. Drusen Volume as a Predictor of Disease Progression in Patients With Late Age-Related Macular Degeneration in the Fellow Eye. *Invest Ophthalmol Vis Sci*, 57, 1839-46.
- ABDELSALAM, A., DEL PRIORE, L. & ZARBIN, M. A. 1999. Drusen in age-related macular degeneration: pathogenesis, natural course, and laser photocoagulation-induced regression. *Surv Ophthalmol*, 44, 1-29.
- ABUGREEN, S., MULDREW, K. A., STEVENSON, M. R., VANLEEUEWEN, R., DEJONG, P. T. & CHAKRAVARTHY, U. 2003. CNV subtype in first eyes predicts severity of ARM in fellow eyes. *Br J Ophthalmol*, 87, 307-11.
- AGAWA, T., MIURA, M., IKUNO, Y., MAKITA, S., FABRITIUS, T., IWASAKI, T., GOTO, H., NISHIDA, K. & YASUNO, Y. 2011. Choroidal thickness measurement in healthy Japanese subjects by three-dimensional high-penetration optical coherence tomography. *Graefes Arch Clin Exp Ophthalmol*, 249, 1485-92.
- ALAMOUTI, B. & FUNK, J. 2003. Retinal thickness decreases with age: an OCT study. *Br J Ophthalmol*, 87, 899-901.
- ANDERSON, D. H., MULLINS, R. F., HAGEMAN, G. S. & JOHNSON, L. V. 2002. A role for local inflammation in the formation of drusen in the aging eye. *Am J Ophthalmol*, 134, 411-31.
- APPUKUTTAN, B., GIRIDHAR, A., GOPALAKRISHNAN, M. & SIVAPRASAD, S. 2014. Normative spectral domain optical coherence tomography data on macular and retinal nerve fiber layer thickness in Indians. *Indian J Ophthalmol*, 62, 316-21.

- ARDELJAN, D. & CHAN, C. C. 2013. Aging is not a disease: distinguishing age-related macular degeneration from aging. *Prog Retin Eye Res*, 37, 68-89.
- BARTLETT, H. & EPERJESI, F. 2007. Use of Fundus Imaging in Quantification of Age-related Macular Change. *Survey of Ophthalmology*, 52, 655-671.
- BAYNES, J. W. 2001. The role of AGEs in aging: causation or correlation. *Exp Gerontol*, 36, 1527-37.
- BEHBEHANI, R., ABU AL-HASSAN, A., AL-SALAHAT, A., SRIRAMAN, D., OAKLEY, J. D. & ALROUGHANI, R. 2017. Optical coherence tomography segmentation analysis in relapsing remitting versus progressive multiple sclerosis. *PLoS One*, 12, e0172120.
- BERENDSCHOT, T. T. & VAN NORREN, D. 2006. Macular pigment shows ringlike structures. *Invest Ophthalmol Vis Sci*, 47, 709-14.
- BERRA, A., FERREIRA, S., STANGA, P. & LLESUY, S. 2002. Age-related antioxidant capacity of the vitreous and its possible relationship with simultaneous changes in photoreceptors, retinal pigment epithelium and Bruchs' membrane in human donors' eyes. *Arch Gerontol Geriatr*, 34, 371-7.
- BHATTI, T., TARIQ, A., SHEN, T., WILLIAMS, K. M., HAMMOND, C. J. & MAHROO, O. A. 2017. Relative Genetic and Environmental Contributions to Variations in Human Retinal Electrical Responses Quantified in a Twin Study. *Ophthalmology*, 124, 1175-1185.
- BHENDE, M., SHETTY, S., PARTHASARATHY, M. K. & RAMYA, S. 2018. Optical coherence tomography: A guide to interpretation of common macular diseases. *Indian J Ophthalmol*, 66, 20-35.
- BHUACHALLA, B. N., MCGARRIGLE, C. A., O'LEARY, N., AKUFFO, K. O., PETO, T., BEATTY, S. & KENNY, R. A. 2018. Orthostatic hypertension as a risk factor for age-related macular degeneration: Evidence from the Irish longitudinal study on ageing. *Exp Gerontol*, 106, 80-87.
- BIRD, A. C., BRESSLER, N. M., BRESSLER, S. B., CHISHOLM, I. H., COSCAS, G., DAVIS, M. D., DE JONG, P. T., KLAVER, C. C., KLEIN, B. E., KLEIN, R. & ET AL. 1995. An international classification and grading system for age-related maculopathy and age-related macular degeneration. The International ARM Epidemiological Study Group. *Surv Ophthalmol*, 39, 367-74.
- BLANKS, J. C., ADINOLFI, A. M. & LOLLEY, R. N. 1974. Photoreceptor degeneration and synaptogenesis in retinal-degenerative (rd) mice. *J Comp Neurol*, 156, 95-106.
- BOGUNOVIC, H., WALDSTEIN, S. M., SCHLEGL, T., LANGS, G., SADEGHIPOUR, A., LIU, X., GERENDAS, B. S., OSBORNE, A. & SCHMIDT-ERFURTH, U. 2017. Prediction of Anti-VEGF Treatment Requirements in Neovascular AMD Using a Machine Learning Approach. *Invest Ophthalmol Vis Sci*, 58, 3240-3248.
- BONILHA, V. L. 2008. Age and disease-related structural changes in the retinal pigment epithelium. *Clin Ophthalmol*, 2, 413-24.
- BONNEL, S., MOHAND-SAID, S. & SAHEL, J. A. 2003. The aging of the retina. *Exp Gerontol*, 38, 825-31.
- BORA, P. S., SOHN, J. H., CRUZ, J. M., JHA, P., NISHIHORI, H., WANG, Y., KALIAPPAN, S., KAPLAN, H. J. & BORA, N. S. 2005. Role of complement and complement membrane attack complex in laser-induced choroidal neovascularization. *J Immunol*, 174, 491-7.
- BORRELLI, E., ABDELFATTAH, N. S., UJI, A., NITTALA, M. G., BOYER, D. S. & SADDA, S. R. 2017. Postreceptor Neuronal Loss in Intermediate Age-related Macular Degeneration. *Am J Ophthalmol*, 181, 1-11.
- BOSER, B. E., GUYON, I. M. & VAPNIK, V. N. A training algorithm for optimal margin classifiers. Proceedings of the fifth annual workshop on Computational learning theory, 1992. ACM, 144-152.
- BRANDL, C., BRUCKLMAYER, C., GUNTHER, F., ZIMMERMANN, M. E., KUCHENHOFF, H., HELBIG, H., WEBER, B. H. F., HEID, I. M. & STARK, K. J. 2019. Retinal Layer Thicknesses in Early Age-Related Macular Degeneration: Results From the German AugUR Study. *Invest Ophthalmol Vis Sci*, 60, 1581-1594.
- BRESSLER, N. M., BRESSLER, S. B. & FINE, S. L. 1988a. Age-related macular degeneration. *Survey of ophthalmology*, 32, 375-413.

- BRESSLER, N. M., BRESSLER, S. B. & FINE, S. L. 1988b. Age-related macular degeneration. *Surv Ophthalmol*, 32, 375-413.
- BRESSLER, N. M., FINKLESTEIN, D., SUNNESS, J. S., MAGUIRE, A. M. & YARIAN, D. 1990a. Retinal pigment epithelial tears through the fovea with preservation of good visual acuity. *Arch Ophthalmol*, 108, 1694-7.
- BRESSLER, N. M., MUNOZ, B., MAGUIRE, M. G. & ET AL. 1995. Five-year incidence and disappearance of drusen and retinal pigment epithelial abnormalities: Waterman study. *Archives of Ophthalmology*, 113, 301-308.
- BRESSLER, S. B., MAGUIRE, M. G., BRESSLER, N. M. & FINE, S. L. 1990b. Relationship of drusen and abnormalities of the retinal pigment epithelium to the prognosis of neovascular macular degeneration. The Macular Photocoagulation Study Group. *Arch Ophthalmol*, 108, 1442-7.
- BREW, K. & NAGASE, H. 2010. The tissue inhibitors of metalloproteinases (TIMPs): an ancient family with structural and functional diversity. *Biochim Biophys Acta*, 1803, 55-71.
- BROE, R., RASMUSSEN, M. L., FRYDKJAER-OLSEN, U., OLSEN, B. S., MORTENSEN, H. B., PETO, T. & GRAUSLUND, J. 2014. Retinal vascular fractals predict long-term microvascular complications in type 1 diabetes mellitus: the Danish Cohort of Pediatric Diabetes 1987 (DCPD1987). *Diabetologia*, 57, 2215-21.
- BROWN, D. M., KAISER, P. K., MICHELS, M., SOUBRANE, G., HEIER, J. S., KIM, R. Y., SY, J. P. & SCHNEIDER, S. 2006. Ranibizumab versus verteporfin for neovascular age-related macular degeneration. *N Engl J Med*, 355, 1432-44.
- BUCH, H., NIELSEN, N. V., VINDING, T., JENSEN, G. B., PRAUSE, J. U. & LA COUR, M. 2005. 14-year incidence, progression, and visual morbidity of age-related maculopathy: the Copenhagen City Eye Study. *Ophthalmology*, 112, 787-98.
- CAMACHO, P., DUTRA-MEDEIROS, M. & PARIS, L. 2017. Ganglion Cell Complex in Early and Intermediate Age-Related Macular Degeneration: Evidence by SD-OCT Manual Segmentation. *Ophthalmologica*, 238, 31-43.
- CAMPOCHIARO, P. A., SOLOWAY, P., RYAN, S. J. & MILLER, J. W. 1999. The pathogenesis of choroidal neovascularization in patients with age-related macular degeneration. *Mol Vis*, 5, 34.
- CHAMBERLAIN, M. D., GUYMER, R. H., DIRANI, M., HOPPER, J. L. & BAIRD, P. N. 2006. Heritability of macular thickness determined by optical coherence tomography. *Invest Ophthalmol Vis Sci*, 47, 336-40.
- CHANG, B., YANNUZZI, L. A., LADAS, I. D., GUYER, D. R., SLAKTER, J. S. & SORENSON, J. A. 1995. Choroidal neovascularization in second eyes of patients with unilateral exudative age-related macular degeneration. *Ophthalmology*, 102, 1380-6.
- CHANG, T. S., BRESSLER, N. M., FINE, J. T., DOLAN, C. M., WARD, J. & KLESERT, T. R. 2007. Improved vision-related function after ranibizumab treatment of neovascular age-related macular degeneration: results of a randomized clinical trial. *Arch Ophthalmol*, 125, 1460-9.
- CHEN, Q., LENG, T., ZHENG, L., KUTZSCHER, L., MA, J., DE SISTERNES, L. & RUBIN, D. L. 2013. Automated drusen segmentation and quantification in SD-OCT images. *Med Image Anal*, 17, 1058-72.
- CHEN, W., STAMBOLIAN, D., EDWARDS, A. O., BRANHAM, K. E., OTHMAN, M., JAKOBSDOTTIR, J., TOSAKULWONG, N., PERICAK-VANCE, M. A., CAMPOCHIARO, P. A., KLEIN, M. L., TAN, P. L., CONLEY, Y. P., KANDA, A., KOPPLIN, L., LI, Y., AUGUSTAITIS, K. J., KAROUKIS, A. J., SCOTT, W. K., AGARWAL, A., KOVACH, J. L., SCHWARTZ, S. G., POSTEL, E. A., BROOKS, M., BARATZ, K. H., BROWN, W. L., BRUCKER, A. J., ORLIN, A., BROWN, G., HO, A., REGILLO, C., DONOSO, L., TIAN, L., KADERLI, B., HADLEY, D., HAGSTROM, S. A., PEACHEY, N. S., KLEIN, R., KLEIN, B. E., GOTOH, N., YAMASHIRO, K., FERRIS III, F., FAGERNESS, J. A., REYNOLDS, R., FARRER, L. A., KIM, I. K., MILLER, J. W., CORTON, M., CARRACEDO, A., SANCHEZ-SALORIO, M., PUGH, E. W., DOHENY, K. F., BRION, M., DEANGELIS, M. M., WEEKS, D. E., ZACK, D. J., CHEW, E. Y., HECKENLIVELY, J. R., YOSHIMURA, N., IYENGAR, S. K., FRANCIS, P. J., KATSANIS, N., SEDDON, J. M., HAINES, J. L., GORIN, M. B., ABECASIS, G. R. & SWAROOP, A. 2010. Genetic variants

- near TIMP3 and high-density lipoprotein-associated loci influence susceptibility to age-related macular degeneration. *Proc Natl Acad Sci U S A*, 107, 7401-6.
- CHIU, S. J., IZATT, J. A., O'CONNELL, R. V., WINTER, K. P., TOTH, C. A. & FARSIU, S. 2012. Validated automatic segmentation of AMD pathology including drusen and geographic atrophy in SD-OCT images. *Invest Ophthalmol Vis Sci*, 53, 53-61.
- CHOI, W., MOULT, E. M., WAHEED, N. K., ADHI, M., LEE, B., LU, C. D., DE CARLO, T. E., JAYARAMAN, V., ROSENFELD, P. J., DUKER, J. S. & FUJIMOTO, J. G. 2015. Ultrahigh-Speed, Swept-Source Optical Coherence Tomography Angiography in Nonexudative Age-Related Macular Degeneration with Geographic Atrophy. *Ophthalmology*, 122, 2532-44.
- CHOMA, M., SARUNIC, M., YANG, C. & IZATT, J. 2003. Sensitivity advantage of swept source and Fourier domain optical coherence tomography. *Opt Express*, 11, 2183-9.
- CHRISTEN, W. G., GLYNN, R. J., MANSON, J. E., AJANI, U. A. & BURING, J. E. 1996. A prospective study of cigarette smoking and risk of age-related macular degeneration in men. *Jama*, 276, 1147-51.
- CHUNG, C. Y., TANG, H. H. Y., LI, S. H. & LI, K. K. W. 2018. Differential microvascular assessment of retinal vein occlusion with coherence tomography angiography and fluorescein angiography: a blinded comparative study. *Int Ophthalmol*, 38, 1119-1128.
- CRINGLE, S. J., YU, D. Y., YU, P. K. & SU, E. N. 2002. Intraretinal oxygen consumption in the rat in vivo. *Invest Ophthalmol Vis Sci*, 43, 1922-7.
- CRUICKSHANKS, K. J., KLEIN, R., KLEIN, B. E. & NONDAHL, D. M. 2001. Sunlight and the 5-year incidence of early age-related maculopathy: the beaver dam eye study. *Arch Ophthalmol*, 119, 246-50.
- CRUZ-HERRANZ, A., BALK, L. J., OBERWAHRENBROCK, T., SAIDHA, S., MARTINEZ-LAPISCINA, E. H., LAGREZE, W. A., SCHUMAN, J. S., VILLOSLADA, P., CALABRESI, P., BALCER, L., PETZOLD, A., GREEN, A. J., PAUL, F., BRANDT, A. U. & ALBRECHT, P. 2016. The APOSTEL recommendations for reporting quantitative optical coherence tomography studies. *Neurology*, 86, 2303-9.
- CUENCA, N., ORTUNO-LIZARAN, I. & PINILLA, I. 2018. Cellular Characterization of OCT and Outer Retinal Bands Using Specific Immunohistochemistry Markers and Clinical Implications. *Ophthalmology*, 125, 407-422.
- CURCIO, C. A., MEDEIROS, N. E. & MILLICAN, C. L. 1996. Photoreceptor loss in age-related macular degeneration. *Invest Ophthalmol Vis Sci*, 37, 1236-49.
- CURCIO, C. A., MILLICAN, C. L., ALLEN, K. A. & KALINA, R. E. 1993. Aging of the human photoreceptor mosaic: evidence for selective vulnerability of rods in central retina. *Invest Ophthalmol Vis Sci*, 34, 3278-96.
- CURCIO, C. A., MILLICAN, C. L., BAILEY, T. & KRUTH, H. S. 2001. Accumulation of cholesterol with age in human Bruch's membrane. *Invest Ophthalmol Vis Sci*, 42, 265-74.
- CURRAN-CELENTANO, J., HAMMOND, B. R., JR., CIULLA, T. A., COOPER, D. A., PRATT, L. M. & DANIS, R. B. 2001. Relation between dietary intake, serum concentrations, and retinal concentrations of lutein and zeaxanthin in adults in a Midwest population. *Am J Clin Nutr*, 74, 796-802.
- DANIEL, E., PAN, W., YING, G. S., KIM, B. J., GRUNWALD, J. E., FERRIS, F. L., 3RD, JAFFE, G. J., TOTH, C. A., MARTIN, D. F., FINE, S. L. & MAGUIRE, M. G. 2018. Development and Course of Scars in the Comparison of Age-Related Macular Degeneration Treatments Trials. *Ophthalmology*, 125, 1037-1046.
- DANIS, R., MCLAUGHLIN, M. M., TOLENTINO, M., STAURENGHI, G., YE, L., XU, C. F., KIM, R. Y. & JOHNSON, M. W. 2014. Pazopanib eye drops: a randomised trial in neovascular age-related macular degeneration. *Br J Ophthalmol*, 98, 172-8.
- DE BOER, J. F., CENSE, B., PARK, B. H., PIERCE, M. C., TEARNEY, G. J. & BOUMA, B. E. 2003. Improved signal-to-noise ratio in spectral-domain compared with time-domain optical coherence tomography. *Opt Lett*, 28, 2067-9.

- DE FAUW, J., KEANE, P., TOMASEV, N., VISENTIN, D., VAN DEN DRIESSCHE, G., JOHNSON, M., HUGHES, C. O., CHU, C., LEDSAM, J., BACK, T., PETO, T., REES, G., MONTGOMERY, H., RAINE, R., RONNEBERGER, O. & CORNEBISE, J. 2016. Automated analysis of retinal imaging using machine learning techniques for computer vision. *F1000Res*, 5, 1573.
- DE FAUW, J., LEDSAM, J. R., ROMERA-PAREDES, B., NIKOLOV, S., TOMASEV, N., BLACKWELL, S., ASKHAM, H., GLOROT, X., O'DONOGHUE, B., VISENTIN, D., VAN DEN DRIESSCHE, G., LAKSHMINARAYANAN, B., MEYER, C., MACKINDER, F., BOUTON, S., AYOUB, K., CHOPRA, R., KING, D., KARTHIKESALINGAM, A., HUGHES, C. O., RAINE, R., HUGHES, J., SIM, D. A., EGAN, C., TUFAIL, A., MONTGOMERY, H., HASSABIS, D., REES, G., BACK, T., KHAW, P. T., SULEYMAN, M., CORNEBISE, J., KEANE, P. A. & RONNEBERGER, O. 2018. Clinically applicable deep learning for diagnosis and referral in retinal disease. *Nature Medicine*, 24, 1342-1350.
- DE OLIVEIRA DIAS, J. R., ZHANG, Q., GARCIA, J. M. B., ZHENG, F., MOTULSKY, E. H., ROISMAN, L., MILLER, A., CHEN, C. L., KUBACH, S., DE SISTERNES, L., DURBIN, M. K., FEUER, W., WANG, R. K., GREGORI, G. & ROSENFELD, P. J. 2018. Natural History of Subclinical Neovascularization in Nonexudative Age-Related Macular Degeneration Using Swept-Source OCT Angiography. *Ophthalmology*, 125, 255-266.
- DE SISTERNES, L., SIMON, N., TIBSHIRANI, R., LENG, T. & RUBIN, D. L. 2014. Quantitative SD-OCT imaging biomarkers as indicators of age-related macular degeneration progression. *Invest Ophthalmol Vis Sci*, 55, 7093-103.
- DEGROOT, J., VERZIJL, N., WENTING-VAN WIJK, M. J., BANK, R. A., LAFEBER, F. P., BIJLSMA, J. W. & TEKOPPELE, J. M. 2001. Age-related decrease in susceptibility of human articular cartilage to matrix metalloproteinase-mediated degradation: the role of advanced glycation end products. *Arthritis Rheum*, 44, 2562-71.
- DELORI, F. C., GOGGER, D. G. & DOREY, C. K. 2001. Age-related accumulation and spatial distribution of lipofuscin in RPE of normal subjects. *Invest Ophthalmol Vis Sci*, 42, 1855-66.
- DEMIRKAYA, N., VAN DIJK, H. W., VAN SCHUPPEN, S. M., ABRAMOFF, M. D., GARVIN, M. K., SONKA, M., SCHLINGEMANN, R. O. & VERBRAAK, F. D. 2013. Effect of age on individual retinal layer thickness in normal eyes as measured with spectral-domain optical coherence tomography. *Invest Ophthalmol Vis Sci*, 54, 4934-40.
- DIETZEL, M., ZEIMER, M., HEIMES, B., PAULEIKHOFF, D. & HENSE, H. W. 2011. The ringlike structure of macular pigment in age-related maculopathy: results from the Muenster Aging and Retina Study (MARS). *Invest Ophthalmol Vis Sci*, 52, 8016-24.
- DINIZ, B., RIBEIRO, R., HEUSSEN, F. M., MAIA, M. & SADDA, S. 2014. Drusen measurements comparison by fundus photograph manual delineation versus optical coherence tomography retinal pigment epithelial segmentation automated analysis. *Retina*, 34, 55-62.
- DREXLER, W., SATTMANN, H., HERMANN, B., KO, T. H., STUR, M., UNTERHUBER, A., SCHOLDA, C., FINDL, O., WIRTITSCH, M., FUJIMOTO, J. G. & FERCHER, A. F. 2003. Enhanced visualization of macular pathology with the use of ultrahigh-resolution optical coherence tomography. *Arch Ophthalmol*, 121, 695-706.
- DUAN, X. R., LIANG, Y. B., FRIEDMAN, D. S., SUN, L. P., WONG, T. Y., TAO, Q. S., BAO, L., WANG, N. L. & WANG, J. J. 2010. Normal macular thickness measurements using optical coherence tomography in healthy eyes of adult Chinese persons: the Handan Eye Study. *Ophthalmology*, 117, 1585-94.
- EDWARDS, A. O., RITTER, R., 3RD, ABEL, K. J., MANNING, A., PANHUYSSEN, C. & FARRER, L. A. 2005. Complement factor H polymorphism and age-related macular degeneration. *Science*, 308, 421-4.
- ELIASIEH, K., LIETS, L. C. & CHALUPA, L. M. 2007. Cellular reorganization in the human retina during normal aging. *Invest Ophthalmol Vis Sci*, 48, 2824-30.
- ERIKSSON, U. & ALM, A. 2009. Macular thickness decreases with age in normal eyes: a study on the macular thickness map protocol in the Stratus OCT. *Br J Ophthalmol*, 93, 1448-52.

- EVANS, J. R., FLETCHER, A. E. & WORMALD, R. P. 2004. Age-related macular degeneration causing visual impairment in people 75 years or older in Britain: an add-on study to the Medical Research Council Trial of Assessment and Management of Older People in the Community. *Ophthalmology*, 111, 513-7.
- EVANS, J. R. & LAWRENSON, J. G. 2017a. Antioxidant vitamin and mineral supplements for preventing age-related macular degeneration. *Cochrane Database Syst Rev*, 7, Cd000253.
- EVANS, J. R. & LAWRENSON, J. G. 2017b. Antioxidant vitamin and mineral supplements for slowing the progression of age-related macular degeneration. *Cochrane Database Syst Rev*, 7, Cd000254.
- FARSIU, S., CHIU, S. J., IZATT, J. A. & TOTH, C. A. Fast detection and segmentation of drusen in retinal optical coherence tomography images. Biomedical Optics (BiOS) 2008, 2008. International Society for Optics and Photonics, 68440D-68440D-12.
- FARSIU, S., CHIU, S. J., O'CONNELL, R. V., FOLGAR, F. A., YUAN, E., IZATT, J. A. & TOTH, C. A. 2014. Quantitative classification of eyes with and without intermediate age-related macular degeneration using optical coherence tomography. *Ophthalmology*, 121, 162-172.
- FEIGL, B., BROWN, B., LOVIE-KITCHIN, J. & SWANN, P. 2007. Functional loss in early age-related maculopathy: the ischaemia postreceptor hypothesis. *Eye (Lond)*, 21, 689-96.
- FERRARA, D., SILVER, R. E., LOUZADA, R. N., NOVAIS, E. A., COLLINS, G. K. & SEDDON, J. M. 2017. Optical Coherence Tomography Features Preceding the Onset of Advanced Age-Related Macular Degeneration. *Invest Ophthalmol Vis Sci*, 58, 3519-3529.
- FERRIS, F. L., 3RD, FINE, S. L. & HYMAN, L. 1984. Age-related macular degeneration and blindness due to neovascular maculopathy. *Arch Ophthalmol*, 102, 1640-2.
- FERRIS, F. L., 3RD, WILKINSON, C. P., BIRD, A., CHAKRAVARTHY, U., CHEW, E., CSAKY, K. & SADDA, S. R. 2013. Clinical classification of age-related macular degeneration. *Ophthalmology*, 120, 844-51.
- FERRIS, F. L., DAVIS, M. D., CLEMONS, T. E., LEE, L. Y., CHEW, E. Y., LINDBLAD, A. S., MILTON, R. C., BRESSLER, S. B. & KLEIN, R. 2005. A simplified severity scale for age-related macular degeneration: AREDS Report No. 18. *Arch Ophthalmol*, 123, 1570-4.
- FOLGAR, F. A., YUAN, E. L., SEVILLA, M. B., CHIU, S. J., FARSIU, S., CHEW, E. Y. & TOTH, C. A. 2016. Drusen Volume and Retinal Pigment Epithelium Abnormal Thinning Volume Predict 2-Year Progression of Age-Related Macular Degeneration. *Ophthalmology*, 123, 39-50 e1.
- FREUND, K. B., ZWEIFEL, S. A. & ENGELBERT, M. 2010. Do we need a new classification for choroidal neovascularization in age-related macular degeneration? *Retina*, 30, 1333-49.
- FRIBERG, T. R., HUANG, L., PALAIOU, M. & BREMER, R. 2007. Computerized detection and measurement of drusen in age-related macular degeneration. *Ophthalmic Surgery Lasers and Imaging*, 38, 126-134.
- FRIEDMAN, D. S., KATZ, J., BRESSLER, N. M., RAHMANI, B. & TIELSCH, J. M. 1999. Racial differences in the prevalence of age-related macular degeneration: the Baltimore Eye Survey. *Ophthalmology*, 106, 1049-55.
- FRIEDMAN, D. S., O'COLMAIN, B. J., MUNOZ, B., TOMANY, S. C., MCCARTY, C., DE JONG, P. T., NEMESURE, B., MITCHELL, P. & KEMPEN, J. 2004. Prevalence of age-related macular degeneration in the United States. *Arch Ophthalmol*, 122, 564-72.
- FUJIMOTO, J. & SWANSON, E. 2016. The Development, Commercialization, and Impact of Optical Coherence Tomography. *Invest Ophthalmol Vis Sci*, 57, Oct1-oct13.
- GABRIELE, M. L., WOLLSTEIN, G., ISHIKAWA, H., KAGEMANN, L., XU, J., FOLIO, L. S. & SCHUMAN, J. S. 2011. Optical coherence tomography: history, current status, and laboratory work. *Invest Ophthalmol Vis Sci*, 52, 2425-36.
- GAO, H. & HOLLYFIELD, J. G. 1992. Aging of the human retina. Differential loss of neurons and retinal pigment epithelial cells. *Invest Ophthalmol Vis Sci*, 33, 1-17.
- GARCIA FILHO, C. A. D. A., YEHOSHUA, Z., GREGORI, G., NUNES, R. P., PENHA, F. M., MOSHFEGHI, A. A., ZHANG, K., FEUER, W. & ROSENFELD, P. J. 2014. Change in drusen volume as a novel

- clinical trial endpoint for the study of complement inhibition in age-related macular degeneration. *Ophthalmic Surgery Lasers and Imaging*, 45, 18-31.
- GARTNER, S. & HENKIND, P. 1981. Aging and degeneration of the human macula. 1. Outer nuclear layer and photoreceptors. *Br J Ophthalmol*, 65, 23-8.
- GASS, J. D. 1994. Biomicroscopic and histopathologic considerations regarding the feasibility of surgical excision of subfoveal neovascular membranes. *Am J Ophthalmol*, 118, 285-98.
- GIRKIN, C. A., MCGWIN, G., JR., SINAI, M. J., SEKHAR, G. C., FINGERET, M., WOLLSTEIN, G., VARMA, R., GREENFIELD, D., LIEBMANN, J., ARAIE, M., TOMITA, G., MAEDA, N. & GARWAY-HEATH, D. F. 2011. Variation in optic nerve and macular structure with age and race with spectral-domain optical coherence tomography. *Ophthalmology*, 118, 2403-8.
- GLENN, J. V., MAHAFFY, H., DASARI, S., OLIVER, M., CHEN, M., BOULTON, M. E., XU, H., CURRY, W. J. & STITT, A. W. 2012. Proteomic profiling of human retinal pigment epithelium exposed to an advanced glycation-modified substrate. *Graefes Arch Clin Exp Ophthalmol*, 250, 349-59.
- GOLDBERG, J., FLOWERDEW, G., SMITH, E., BRODY, J. A. & TSO, M. O. 1988. Factors associated with age-related macular degeneration. An analysis of data from the first National Health and Nutrition Examination Survey. *Am J Epidemiol*, 128, 700-10.
- GOSSAGE, K. W., TKACZYK, T. S., RODRIGUEZ, J. J. & BARTON, J. K. 2003. Texture analysis of optical coherence tomography images: feasibility for tissue classification. *J Biomed Opt*, 8, 570-5.
- GOTTFREDSOTTIR, M. S., SVERRISSON, T., MUSCH, D. C. & STEFANSSON, E. 1999. Age related macular degeneration in monozygotic twins and their spouses in Iceland. *Acta Ophthalmol Scand*, 77, 422-5.
- GRASSI, M. A., FINGERT, J. H., SCHEETZ, T. E., ROOS, B. R., RITCH, R., WEST, S. K., KAWASE, K., SHIRE, A. M., MULLINS, R. F. & STONE, E. M. 2006. Ethnic variation in AMD-associated complement factor H polymorphism p.Tyr402His. *Hum Mutat*, 27, 921-5.
- GREEN, W. R. 1999. Histopathology of age-related macular degeneration. *Mol Vis*, 5, 27.
- GREEN, W. R. & ENGER, C. 1993a. Age-related macular degeneration histopathologic studies. The 1992 Lorenz E. Zimmerman Lecture. *Ophthalmology*, 100, 1519-35.
- GREEN, W. R. & ENGER, C. 1993b. Age-related macular degeneration histopathologic studies: the 1992 Lorenz E. Zimmerman Lecture. *Ophthalmology*, 100, 1519-1535.
- GREGORI, G., WANG, F., ROSENFELD, P. J., YEHOSHUA, Z., GREGORI, N. Z., LUJAN, B. J., PULIAFITO, C. A. & FEUER, W. J. 2011. Spectral domain optical coherence tomography imaging of drusen in nonexudative age-related macular degeneration. *Ophthalmology*, 118, 1373-9.
- GREGORI, G., YEHOSHUA, Z., GARCIA FILHO, C. A., SADDA, S. R., PORTELLA NUNES, R., FEUER, W. J. & ROSENFELD, P. J. 2014. Change in drusen area over time compared using spectral-domain optical coherence tomography and color fundus imaging. *Invest Ophthalmol Vis Sci*, 55, 7662-8.
- GRIZZARD, S. W., ARNETT, D. & HAAG, S. L. 2003. Twin study of age-related macular degeneration. *Ophthalmic Epidemiol*, 10, 315-22.
- GU, X., NERIC, N. J., CRABB, J. S., CRABB, J. W., BHATTACHARYA, S. K., RAYBORN, M. E., HOLLYFIELD, J. G. & BONILHA, V. L. 2012. Age-related changes in the retinal pigment epithelium (RPE). *PLoS One*, 7, e38673.
- GULCAN, H. G., ALVAREZ, R. A., MAUDE, M. B. & ANDERSON, R. E. 1993. Lipids of human retina, retinal pigment epithelium, and Bruch's membrane/choroid: comparison of macular and peripheral regions. *Invest Ophthalmol Vis Sci*, 34, 3187-93.
- GULMEZ SEVIM, D., UNLU, M., GULTEKIN, M. & KARACA, C. 2019. Retinal single-layer analysis with optical coherence tomography shows inner retinal layer thinning in Huntington's disease as a potential biomarker. *Int Ophthalmol*, 39, 611-621.
- HAM, W. T., JR., MUELLER, H. A., RUFFOLO, J. J., JR., GUERRY, D., 3RD & GUERRY, R. K. 1982. Action spectrum for retinal injury from near-ultraviolet radiation in the aphakic monkey. *Am J Ophthalmol*, 93, 299-306.

- HAMMES, H. P., HOERAUF, H., ALT, A., SCHLEICHER, E., CLAUSEN, J. T., BRETZEL, R. G. & LAQUA, H. 1999. N(epsilon)(carboxymethyl)lysine and the AGE receptor RAGE colocalize in age-related macular degeneration. *Invest Ophthalmol Vis Sci*, 40, 1855-9.
- HAMMOND, C. J., WEBSTER, A. R., SNIEDER, H., BIRD, A. C., GILBERT, C. E. & SPECTOR, T. D. 2002. Genetic influence on early age-related maculopathy: a twin study. *Ophthalmology*, 109, 730-6.
- HANDELMAN, G. J., DRATZ, E. A., REAY, C. C. & VAN KUIJK, J. G. 1988. Carotenoids in the human macula and whole retina. *Invest Ophthalmol Vis Sci*, 29, 850-5.
- HANUTSAHA, P., GUYER, D. R., YANNUZZI, L. A., NAING, A., SLAKTER, J. S., SORENSON, J. S., SPAIDE, R. F., FREUND, K. B., FEINSOD, M. & ORLOCK, D. A. 1998. Indocyanine-green videoangiography of drusen as a possible predictive indicator of exudative maculopathy. *Ophthalmology*, 105, 1632-6.
- HARTMANN, K. I., GOMEZ, M. L., BARTSCH, D. U., SCHUSTER, A. K. & FREEMAN, W. R. 2012. Effect of change in drusen evolution on photoreceptor inner segment/outer segment junction. *Retina*, 32, 1492-9.
- HEIN, G., WIEGAND, R., LEHMANN, G., STEIN, G. & FRANKE, S. 2003. Advanced glycation end-products pentosidine and N epsilon-carboxymethyllysine are elevated in serum of patients with osteoporosis. *Rheumatology (Oxford)*, 42, 1242-6.
- HERNOWO, A. T., BOUCARD, C. C., JANSONIUS, N. M., HOOYMANS, J. M. & CORNELISSEN, F. W. 2011. Automated morphometry of the visual pathway in primary open-angle glaucoma. *Invest Ophthalmol Vis Sci*, 52, 2758-66.
- HERNOWO, A. T., PRINS, D., BASELER, H. A., PLANK, T., GOUWS, A. D., HOOYMANS, J. M., MORLAND, A. B., GREENLEE, M. W. & CORNELISSEN, F. W. 2014. Morphometric analyses of the visual pathways in macular degeneration. *Cortex*, 56, 99-110.
- HINTON, G. E., SRIVASTAVA, N., KRIZHEVSKY, A., SUTSKEVER, I. & SALAKHUTDINOV, R. R. 2012. Improving neural networks by preventing co-adaptation of feature detectors. *arXiv preprint arXiv:1207.0580*.
- HIRANO, T., KAKIHARA, S., TORIYAMA, Y., NITTALA, M. G., MURATA, T. & SADDA, S. 2018. Wide-field en face swept-source optical coherence tomography angiography using extended field imaging in diabetic retinopathy. *Br J Ophthalmol*, 102, 1199-1203.
- HOGG, R. E., ONG, E. L., CHAMBERLAIN, M., DIRANI, M., BAIRD, P. N., GUYMER, R. H. & FITZKE, F. 2012. Heritability of the spatial distribution and peak density of macular pigment: a classical twin study. *Eye (Lond)*, 26, 1217-25.
- HOUGAARD, J. L., KESSEL, L., SANDER, B., KYVIK, K. O., SORENSEN, T. I. & LARSEN, M. 2003. Evaluation of heredity as a determinant of retinal nerve fiber layer thickness as measured by optical coherence tomography. *Invest Ophthalmol Vis Sci*, 44, 3011-6.
- HUANG, D., SWANSON, E. A., LIN, C. P., SCHUMAN, J. S., STINSON, W. G., CHANG, W., HEE, M. R., FLOTTE, T., GREGORY, K., PULIAFITO, C. A. & ET AL. 1991. Optical coherence tomography. *Science*, 254, 1178-81.
- HUANG, J. D., AMARAL, J., LEE, J. W., LARRAYOZ, I. M. & RODRIGUEZ, I. R. 2012. Sterculic acid antagonizes 7-ketocholesterol-mediated inflammation and inhibits choroidal neovascularization. *Biochim Biophys Acta*, 1821, 637-46.
- HUSSAIN, A. A., LEE, Y. & MARSHALL, J. 2010. High molecular-weight gelatinase species of human Bruch's membrane: compositional analyses and age-related changes. *Invest Ophthalmol Vis Sci*, 51, 2363-71.
- HUSSAIN, A. A., LEE, Y., ZHANG, J.-J. & MARSHALL, J. 2011. Disturbed Matrix Metalloproteinase Activity of Bruch's Membrane in Age-Related Macular Degeneration. *Investigative Ophthalmology & Visual Science*, 52, 4459-4466.
- HYMAN, L. & NEBORSKY, R. 2002. Risk factors for age-related macular degeneration: an update. *Curr Opin Ophthalmol*, 13, 171-5.

- INVERNIZZI, A., NGUYEN, V., TEO, K., BARTHELMES, D., FUNG, A., VINCENT, A. & GILLIES, M. 2019. Five-Year Real-World Outcomes of Occult and Classic Choroidal Neovascularization: Data From the Fight Retinal Blindness! Project. *Am J Ophthalmol*, 204, 105-112.
- IWAMA, D., HANGAI, M., OOTO, S., SAKAMOTO, A., NAKANISHI, H., FUJIMURA, T., DOMALPALLY, A., DANIS, R. P. & YOSHIMURA, N. 2012. Automated assessment of drusen using three-dimensional spectral-domain optical coherence tomography. *Invest Ophthalmol Vis Sci*, 53, 1576-83.
- JACKSON, G. R., OWSLEY, C. & CURCIO, C. A. 2002. Photoreceptor degeneration and dysfunction in aging and age-related maculopathy. *Ageing Res Rev*, 1, 381-96.
- JAFFE, G. J., CIULLA, T. A., CIARDELLA, A. P., DEVIN, F., DUGEL, P. U., EANDI, C. M., MASONSON, H., MONES, J., PEARLMAN, J. A., QUARANTA-EL MAFTOUHI, M., RICCI, F., WESTBY, K. & PATEL, S. C. 2017. Dual Antagonism of PDGF and VEGF in Neovascular Age-Related Macular Degeneration: A Phase IIb, Multicenter, Randomized Controlled Trial. *Ophthalmology*, 124, 224-234.
- JAIN, N., FARSIU, S., KHANIFAR, A. A., BEARELLY, S., SMITH, R. T., IZATT, J. A. & TOTH, C. A. 2010. Quantitative comparison of drusen segmented on SD-OCT versus drusen delineated on color fundus photographs. *Invest Ophthalmol Vis Sci*, 51, 4875-83.
- JAKOBSDOTTIR, J., CONLEY, Y. P., WEEKS, D. E., MAH, T. S., FERRELL, R. E. & GORIN, M. B. 2005. Susceptibility genes for age-related maculopathy on chromosome 10q26. *Am J Hum Genet*, 77, 389-407.
- JHA, P., BORA, P. S. & BORA, N. S. 2007. The role of complement system in ocular diseases including uveitis and macular degeneration. *Mol Immunol*, 44, 3901-8.
- JOBLING, A. I., GUYMER, R. H., VESSEY, K. A., GREFERATH, U., MILLS, S. A., BRASSINGTON, K. H., LUU, C. D., AUNG, K. Z., TROGRIC, L., PLUNKETT, M. & FLETCHER, E. L. 2015. Nanosecond laser therapy reverses pathologic and molecular changes in age-related macular degeneration without retinal damage. *The FASEB Journal*, 29, 696-710.
- JONAS, J. B., XU, L., WEI, W. B., PAN, Z., YANG, H., HOLBACH, L., PANDA-JONAS, S. & WANG, Y. X. 2016. Retinal Thickness and Axial Length. *Invest Ophthalmol Vis Sci*, 57, 1791-7.
- KAHN, H. A., LEIBOWITZ, H. M., GANLEY, J. P., KINI, M. M., COLTON, T., NICKERSON, R. S. & DAWBER, T. R. 1977. The Framingham Eye Study. II. Association of ophthalmic pathology with single variables previously measured in the Framingham Heart Study. *Am J Epidemiol*, 106, 33-41.
- KAMEI, M. & HOLLYFIELD, J. G. 1999. TIMP-3 in Bruch's membrane: changes during aging and in age-related macular degeneration. *Invest Ophthalmol Vis Sci*, 40, 2367-75.
- KASHANI, A. H., ZIMMER-GALLER, I. E., SHAH, S. M., DUSTIN, L., DO, D. V., ELIOTT, D., HALLER, J. A. & NGUYEN, Q. D. 2010. Retinal thickness analysis by race, gender, and age using Stratus OCT. *Am J Ophthalmol*, 149, 496-502.e1.
- KAWASAKI, R., WANG, J. J., AUNG, T., TAN, D. T., MITCHELL, P., SANDAR, M., SAW, S. M. & WONG, T. Y. 2008. Prevalence of age-related macular degeneration in a Malay population: the Singapore Malay Eye Study. *Ophthalmology*, 115, 1735-41.
- KERNT, M., WALCH, A., NEUBAUER, A. S., HIRNEISS, C., HARITOGLOU, C., ULBIG, M. W. & KAMPIK, A. 2012. Filtering blue light reduces light-induced oxidative stress, senescence and accumulation of extracellular matrix proteins in human retinal pigment epithelium cells. *Clin Exp Ophthalmol*, 40, e87-97.
- KHAN, J. C., THURLBY, D. A., SHAHID, H., CLAYTON, D. G., YATES, J. R., BRADLEY, M., MOORE, A. T. & BIRD, A. C. 2006. Smoking and age related macular degeneration: the number of pack years of cigarette smoking is a major determinant of risk for both geographic atrophy and choroidal neovascularisation. *Br J Ophthalmol*, 90, 75-80.
- KHANIFAR, A. A., KOREISHI, A. F., IZATT, J. A. & TOTH, C. A. 2008. Drusen ultrastructure imaging with spectral domain optical coherence tomography in age-related macular degeneration. *Ophthalmology*, 115, 1883-90.

- KHAWAJA, A. P., CHAN, M. P., YIP, J. L., BROADWAY, D. C., GARWAY-HEATH, D. F., LUBEN, R., HAYAT, S., MATTHEWS, F. E., BRAYNE, C., KHAW, K. T. & FOSTER, P. J. 2016. Retinal Nerve Fiber Layer Measures and Cognitive Function in the EPIC-Norfolk Cohort Study. *Invest Ophthalmol Vis Sci*, 57, 1921-6.
- KIRBY, M. L., BEATTY, S., LOANE, E., AKKALI, M. C., CONNOLLY, E. E., STACK, J. & NOLAN, J. M. 2010. A central dip in the macular pigment spatial profile is associated with age and smoking. *Invest Ophthalmol Vis Sci*, 51, 6722-8.
- KLAVER, C. C., WOLFS, R. C., ASSINK, J. J., VAN DUIJN, C. M., HOFMAN, A. & DE JONG, P. T. 1998a. Genetic risk of age-related maculopathy. Population-based familial aggregation study. *Arch Ophthalmol*, 116, 1646-51.
- KLAVER, C. C., WOLFS, R. C., VINGERLING, J. R., HOFMAN, A. & DE JONG, P. T. 1998b. Age-specific prevalence and causes of blindness and visual impairment in an older population: the Rotterdam Study. *Arch Ophthalmol*, 116, 653-8.
- KLEIN, M. L., MAULDIN, W. M. & STOUMBOS, V. D. 1994. Heredity and age-related macular degeneration. Observations in monozygotic twins. *Arch Ophthalmol*, 112, 932-7.
- KLEIN, R., CLEGG, L., COOPER, L. S., HUBBARD, L. D., KLEIN, B. E., KING, W. N. & FOLSOM, A. R. 1999. Prevalence of age-related maculopathy in the Atherosclerosis Risk in Communities Study. *Arch Ophthalmol*, 117, 1203-10.
- KLEIN, R., CRUICKSHANKS, K. J., NASH, S. D., KRANTZ, E. M., NIETO, F. J., HUANG, G. H., PANKOW, J. S. & KLEIN, B. E. 2010. The prevalence of age-related macular degeneration and associated risk factors. *Arch Ophthalmol*, 128, 750-8.
- KLEIN, R., DAVIS, M. D., MAGLI, Y. L., SEGAL, P., KLEIN, B. E. & HUBBARD, L. 1991. The Wisconsin age-related maculopathy grading system. *Ophthalmology*, 98, 1128-34.
- KLEIN, R., KLEIN, B. E. & JENSEN, S. C. 1997a. The relation of cardiovascular disease and its risk factors to the 5-year incidence of age-related maculopathy: the Beaver Dam Eye Study. *Ophthalmology*, 104, 1804-12.
- KLEIN, R., KLEIN, B. E., JENSEN, S. C. & CRUICKSHANKS, K. J. 1998. The relationship of ocular factors to the incidence and progression of age-related maculopathy. *Arch Ophthalmol*, 116, 506-13.
- KLEIN, R., KLEIN, B. E., JENSEN, S. C., CRUICKSHANKS, K. J., LEE, K. E., DANFORTH, L. G. & TOMANY, S. C. 2001. Medication use and the 5-year incidence of early age-related maculopathy: the Beaver Dam Eye Study. *Arch Ophthalmol*, 119, 1354-9.
- KLEIN, R., KLEIN, B. E., JENSEN, S. C. & MEUER, S. M. 1997b. The five-year incidence and progression of age-related maculopathy: the Beaver Dam Eye Study. *Ophthalmology*, 104, 7-21.
- KLEIN, R., KLEIN, B. E., KNUDTSON, M. D., MEUER, S. M., SWIFT, M. & GANGNON, R. E. 2007. Fifteen-year cumulative incidence of age-related macular degeneration: the Beaver Dam Eye Study. *Ophthalmology*, 114, 253-62.
- KLEIN, R., KLEIN, B. E., KNUDTSON, M. D., WONG, T. Y., COTCH, M. F., LIU, K., BURKE, G., SAAD, M. F. & JACOBS, D. R., JR. 2006. Prevalence of age-related macular degeneration in 4 racial/ethnic groups in the multi-ethnic study of atherosclerosis. *Ophthalmology*, 113, 373-80.
- KLEIN, R., KLEIN, B. E. & LINTON, K. L. 1992. Prevalence of age-related maculopathy. The Beaver Dam Eye Study. *Ophthalmology*, 99, 933-43.
- KLEIN, R., KLEIN, B. E., LINTON, K. L. & DEMETS, D. L. 1993. The Beaver Dam Eye Study: the relation of age-related maculopathy to smoking. *Am J Epidemiol*, 137, 190-200.
- KLEIN, R., KLEIN, B. E., MARINO, E. K., KULLER, L. H., FURBERG, C., BURKE, G. L. & HUBBARD, L. D. 2003. Early age-related maculopathy in the cardiovascular health study. *Ophthalmology*, 110, 25-33.
- KLEIN, R., KLEIN, B. E., TOMANY, S. C., MEUER, S. M. & HUANG, G. H. 2002. Ten-year incidence and progression of age-related maculopathy: The Beaver Dam eye study. *Ophthalmology*, 109, 1767-79.
- KLEIN, R., MEUER, S. M., KNUDTSON, M. D., IYENGAR, S. K. & KLEIN, B. E. 2008. The epidemiology of retinal reticular drusen. *Am J Ophthalmol*, 145, 317-326.

- KO, F., FOSTER, P. J., STROUTHIDIS, N. G., SHWEIKH, Y., YANG, Q., REISMAN, C. A., MUTHY, Z. A., CHAKRAVARTHY, U., LOTERY, A. J., KEANE, P. A., TUFAIL, A., GROSSI, C. M. & PATEL, P. J. 2017. Associations with Retinal Pigment Epithelium Thickness Measures in a Large Cohort: Results from the UK Biobank. *Ophthalmology*, 124, 105-117.
- KO, F., MUTHY, Z. A., GALLACHER, J., SUDLOW, C., REES, G., YANG, Q., KEANE, P. A., PETZOLD, A., KHAW, P. T., REISMAN, C., STROUTHIDIS, N. G., FOSTER, P. J. & PATEL, P. J. 2018. Association of Retinal Nerve Fiber Layer Thinning With Current and Future Cognitive Decline: A Study Using Optical Coherence Tomography. *JAMA Neurol*, 75, 1198-1205.
- KRISHNAIAH, S., DAS, T., NIRMALAN, P. K., NUTHETI, R., SHAMANNA, B. R., RAO, G. N. & THOMAS, R. 2005. Risk factors for age-related macular degeneration: findings from the Andhra Pradesh eye disease study in South India. *Invest Ophthalmol Vis Sci*, 46, 4442-9.
- LAMIN, A., DUBIS, A. M. & SIVAPRASAD, S. 2019a. Changes in macular drusen parameters preceding the development of neovascular age-related macular degeneration. *Eye (Lond)*.
- LAMIN, A., OAKLEY, J. D., DUBIS, A. M., RUSSAKOFF, D. B. & SIVAPRASAD, S. 2019b. Changes in volume of various retinal layers over time in early and intermediate age-related macular degeneration. *Eye (Lond)*, 33, 428-434.
- LEE, E. K. & YU, H. G. 2015. Ganglion Cell-Inner Plexiform Layer and Peripapillary Retinal Nerve Fiber Layer Thicknesses in Age-Related Macular Degeneration. *Invest Ophthalmol Vis Sci*, 56, 3976-83.
- LEUSCHEN, J. N., SCHUMAN, S. G., WINTER, K. P., MCCALL, M. N., WONG, W. T., CHEW, E. Y., HWANG, T., SRIVASTAVA, S., SARIN, N., CLEMONS, T., HARRINGTON, M. & TOTH, C. A. 2013. Spectral-domain optical coherence tomography characteristics of intermediate age-related macular degeneration. *Ophthalmology*, 120, 140-50.
- LI, Y., WANG, J., ZHONG, X., TIAN, Z., WU, P., ZHAO, W. & JIN, C. 2014. Refractive error and risk of early or late age-related macular degeneration: a systematic review and meta-analysis. *PLoS One*, 9, e90897.
- LIEW, S. H., GILBERT, C. E., SPECTOR, T. D., MELLERIO, J., MARSHALL, J., VAN KUIJK, F. J., BEATTY, S., FITZKE, F. & HAMMOND, C. J. 2005. Heritability of macular pigment: a twin study. *Invest Ophthalmol Vis Sci*, 46, 4430-6.
- LIM, J. I., STERNBERG, P., JR., CAPONE, A., JR., AABERG, T. M., SR. & GILMAN, J. P. 1995. Selective use of indocyanine green angiography for occult choroidal neovascularization. *Am J Ophthalmol*, 120, 75-82.
- LIN, S. C., SINGH, K., CHAO, D. L. & LIN, S. C. 2016. Refractive Error and the Risk of Age-Related Macular Degeneration in the South Korean Population. *Asia Pac J Ophthalmol (Phila)*, 5, 115-21.
- LOANE, E., KELLIHER, C., BEATTY, S. & NOLAN, J. M. 2008. The rationale and evidence base for a protective role of macular pigment in age-related maculopathy. *Br J Ophthalmol*, 92, 1163-8.
- LUJAN, B. J., ROORDA, A., KNIGHTON, R. W. & CARROLL, J. 2011. Revealing Henle's fiber layer using spectral domain optical coherence tomography. *Invest Ophthalmol Vis Sci*, 52, 1486-92.
- MACHIDA, S., KONDO, M., JAMISON, J. A., KHAN, N. W., KONONEN, L. T., SUGAWARA, T., BUSH, R. A. & SIEVING, P. A. 2000. P23H rhodopsin transgenic rat: correlation of retinal function with histopathology. *Invest Ophthalmol Vis Sci*, 41, 3200-9.
- MAHROO, O. A., OOMERJEE, M., WILLIAMS, K. M., O'BRART, D. P. & HAMMOND, C. J. 2014. High heritability of posterior corneal tomography, as measured by Scheimpflug imaging, in a twin study. *Invest Ophthalmol Vis Sci*, 55, 8359-64.
- MANJUNATH, V., GOREN, J., FUJIMOTO, J. G. & DUKER, J. S. 2011. Analysis of choroidal thickness in age-related macular degeneration using spectral-domain optical coherence tomography. *Am J Ophthalmol*, 152, 663-8.
- MANN, S. S., RUTISHAUSER-ARNOLD, Y., PETO, T., JENKINS, S. A., LEUNG, I., XING, W., BIRD, A. C., BUNCE, C. & WEBSTER, A. R. 2011. The symmetry of phenotype between eyes of patients

- with early and late bilateral age-related macular degeneration (AMD). *Graefes Arch Clin Exp Ophthalmol*, 249, 209-14.
- MARES-PERLMAN, J. A., BRADY, W. E., KLEIN, R., VANDENLANGENBERG, G. M., KLEIN, B. E. & PALTA, M. 1995. Dietary fat and age-related maculopathy. *Arch Ophthalmol*, 113, 743-8.
- MARSIGLIA, M., BODDU, S., CHEN, C. Y., JUNG, J. J., MREJEN, S., GALLEGO-PINAZO, R. & FREUND, K. B. 2015. Correlation between neovascular lesion type and clinical characteristics of nonneovascular fellow eyes in patients with unilateral, neovascular age-related macular degeneration. *Retina*, 35, 966-74.
- MCGWIN, G., JR., MODJARRAD, K., HALL, T. A., XIE, A. & OWSLEY, C. 2006. 3-hydroxy-3-methylglutaryl coenzyme a reductase inhibitors and the presence of age-related macular degeneration in the Cardiovascular Health Study. *Arch Ophthalmol*, 124, 33-7.
- MCHUGH, K. J., LI, D., WANG, J. C., KWARK, L., LOO, J., MACHA, V., FARSIU, S., KIM, L. A. & SAINT-GENIEZ, M. 2019. Computational modeling of retinal hypoxia and photoreceptor degeneration in patients with age-related macular degeneration. *PLoS One*, 14, e0216215.
- MEDEIROS, N. E. & CURCIO, C. A. 2001. Preservation of ganglion cell layer neurons in age-related macular degeneration. *Invest Ophthalmol Vis Sci*, 42, 795-803.
- MEDZHITOV, R. 2008. Origin and physiological roles of inflammation. *Nature*, 454, 428-35.
- MEYERS, S. M., GREENE, T. & GUTMAN, F. A. 1995. A twin study of age-related macular degeneration. *Am J Ophthalmol*, 120, 757-66.
- MITCHELL, P., SMITH, W., ATTEBO, K. & WANG, J. J. 1995. Prevalence of age-related maculopathy in Australia. The Blue Mountains Eye Study. *Ophthalmology*, 102, 1450-60.
- MITCHELL, P., SMITH, W. & WANG, J. J. 1998. Iris color, skin sun sensitivity, and age-related maculopathy. The Blue Mountains Eye Study. *Ophthalmology*, 105, 1359-63.
- MITCHELL, P. & WANG, J. J. 1999. Diabetes, fasting blood glucose and age-related maculopathy: The Blue Mountains Eye Study. *Aust N Z J Ophthalmol*, 27, 197-9.
- MITCHELL, P., WANG, J. J., FORAN, S. & SMITH, W. 2002. Five-year incidence of age-related maculopathy lesions: the Blue Mountains Eye Study. *Ophthalmology*, 109, 1092-7.
- MOAYYERI, A., HAMMOND, C. J., HART, D. J. & SPECTOR, T. D. 2013. The UK Adult Twin Registry (TwinsUK Resource). *Twin Res Hum Genet*, 16, 144-9.
- MOHAND-SAID, S., HICKS, D., LEVEILLARD, T., PICAUD, S., PORTO, F. & SAHEL, J. A. 2001. Rod-cone interactions: developmental and clinical significance. *Prog Retin Eye Res*, 20, 451-67.
- MORGAN, W. H., COOPER, R. L., CONSTABLE, I. J. & EIKELBOOM, R. H. 1994. Automated extraction and quantification of macular drusen from fundal photographs. *Aust N Z J Ophthalmol*, 22, 7-12.
- MUFTUOGLU, I. K., RAMKUMAR, H. L., BARTSCH, D. U., MESHI, A., GABER, R. & FREEMAN, W. R. 2017. QUANTITATIVE ANALYSIS OF THE INNER RETINAL LAYER THICKNESSES IN AGE-RELATED MACULAR DEGENERATION USING CORRECTED OPTICAL COHERENCE TOMOGRAPHY SEGMENTATION. *Retina*.
- MUKKAMALA, S. K., COSTA, R. A., FUNG, A., SARRAF, D., GALLEGO-PINAZO, R. & FREUND, K. B. 2012. Optical coherence tomographic imaging of sub-retinal pigment epithelium lipid. *Arch Ophthalmol*, 130, 1547-53.
- MYERS, C. E., KLEIN, B. E., GANGNON, R., SIVAKUMARAN, T. A., IYENGAR, S. K. & KLEIN, R. 2014. Cigarette smoking and the natural history of age-related macular degeneration: the Beaver Dam Eye Study. *Ophthalmology*, 121, 1949-55.
- NATHOO, N. A., OR, C., YOUNG, M., CHUI, L., FALLAH, N., KIRKER, A. W., ALBIANI, D. A., MERKUR, A. B. & FOROOGHIAN, F. 2014. Optical coherence tomography-based measurement of drusen load predicts development of advanced age-related macular degeneration. *Am J Ophthalmol*, 158, 757-761.e1.
- NEUVILLE, J. M., BRONSON-CASTAIN, K., BEARSE, M. A., JR., NG, J. S., HARRISON, W. W., SCHNECK, M. E. & ADAMS, A. J. 2009. OCT reveals regional differences in macular thickness with age. *Optom Vis Sci*, 86, E810-6.

- NIEVES-MORENO, M., MARTINEZ-DE-LA-CASA, J. M., MORALES-FERNANDEZ, L., SANCHEZ-JEAN, R., SAENZ-FRANCES, F. & GARCIA-FEIJOO, J. 2018. Impacts of age and sex on retinal layer thicknesses measured by spectral domain optical coherence tomography with Spectralis. *PLoS One*, 13, e0194169.
- NITTALA, M. G., HOGG, R. E., LUO, Y., VELAGA, S. B., SILVA, R., ALVES, D., STAURENGHI, G., CHAKRAVARTHY, U. & SADDA, S. R. 2019. Changes in Retinal Layer Thickness in the Contralateral Eye of Patients with Unilateral Neovascular Age-Related Macular Degeneration. *Ophthalmol Retina*, 3, 112-121.
- NITTALA, M. G., RUIZ-GARCIA, H. & SADDA, S. R. 2012. Accuracy and reproducibility of automated drusen segmentation in eyes with non-neovascular age-related macular degeneration. *Invest Ophthalmol Vis Sci*, 53, 8319-24.
- NIU, S., DE SISTERNES, L., CHEN, Q., RUBIN, D. L. & LENG, T. 2016. Fully Automated Prediction of Geographic Atrophy Growth Using Quantitative Spectral-Domain Optical Coherence Tomography Biomarkers. *Ophthalmology*, 123, 1737-1750.
- NOLAN, J., O'DONOVAN, O., KAVANAGH, H., STACK, J., HARRISON, M., MULDOON, A., MELLERIO, J. & BEATTY, S. 2004. Macular pigment and percentage of body fat. *Invest Ophthalmol Vis Sci*, 45, 3940-50.
- NOLAN, J. M., STACK, J., O, O. D., LOANE, E. & BEATTY, S. 2007. Risk factors for age-related maculopathy are associated with a relative lack of macular pigment. *Exp Eye Res*, 84, 61-74.
- NOVAIS, E. A., ADHI, M., MOULT, E. M., LOUZADA, R. N., COLE, E. D., HUSVOGT, L., LEE, B., DANG, S., REGATIERI, C. V., WITKIN, A. J., BAUMAL, C. R., HORNEGGER, J., JAYARAMAN, V., FUJIMOTO, J. G., DUKER, J. S. & WAHEED, N. K. 2016. Choroidal Neovascularization Analyzed on Ultrahigh-Speed Swept-Source Optical Coherence Tomography Angiography Compared to Spectral-Domain Optical Coherence Tomography Angiography. *Am J Ophthalmol*, 164, 80-8.
- OOTO, S., HANGAI, M., TOMIDOKORO, A., SAITO, H., ARAIE, M., OTANI, T., KISHI, S., MATSUSHITA, K., MAEDA, N., SHIRAKASHI, M., ABE, H., OHKUBO, S., SUGIYAMA, K., IWASE, A. & YOSHIMURA, N. 2011. Effects of age, sex, and axial length on the three-dimensional profile of normal macular layer structures. *Invest Ophthalmol Vis Sci*, 52, 8769-79.
- OUYANG, Y., HEUSSEN, F. M., HARIRI, A., KEANE, P. A. & SADDA, S. R. 2013a. Optical coherence tomography-based observation of the natural history of drusenoid lesion in eyes with dry age-related macular degeneration. *Ophthalmology*, 120, 2656-2665.
- OUYANG, Y., HEUSSEN, F. M., HARIRI, A., KEANE, P. A. & SADDA, S. R. 2013b. Optical Coherence Tomography–Based Observation of the Natural History of Drusenoid Lesion in Eyes with Dry Age-related Macular Degeneration. *Ophthalmology*, 120, 2656-2665.
- OWEN, C. G., JARRAR, Z., WORMALD, R., COOK, D. G., FLETCHER, A. E. & RUDNICKA, A. R. 2012. The estimated prevalence and incidence of late stage age related macular degeneration in the UK. *Br J Ophthalmol*, 96, 752-6.
- PAKDEL, A. R., MAMMO, Z., LEE, S. & FOROOGHIAN, F. 2018. Normal Variation of Photoreceptor Outer Segment Volume With Age, Gender, Refractive Error, and Vitreomacular Adhesion. *Ophthalmic Surg Lasers Imaging Retina*, 49, 523-527.
- PAN, C. W., IKRAM, M. K., CHEUNG, C. Y., CHOI, H. W., CHEUNG, C. M., JONAS, J. B., SAW, S. M. & WONG, T. Y. 2013. Refractive errors and age-related macular degeneration: a systematic review and meta-analysis. *Ophthalmology*, 120, 2058-65.
- PARAPURAM, S. K., COJOCARU, R. I., CHANG, J. R., KHANNA, R., BROOKS, M., OTHMAN, M., ZAREPARSI, S., KHAN, N. W., GOTOH, N., COGLIATI, T. & SWAROOP, A. 2010. Distinct signature of altered homeostasis in aging rod photoreceptors: implications for retinal diseases. *PLoS One*, 5, e13885.
- PARODI, M. B., VIRGILI, G. & EVANS, J. R. 2009. Laser treatment of drusen to prevent progression to advanced age-related macular degeneration. *Cochrane database of systematic reviews (Online)*.

- PASCOLINI, D. & MARIOTTI, S. P. 2012. Global estimates of visual impairment: 2010. *Br J Ophthalmol*, 96, 614-8.
- PATEL, M. & CHAN, C. C. 2008. Immunopathological aspects of age-related macular degeneration. *Semin Immunopathol*, 30, 97-110.
- PATEL, P. J., FOSTER, P. J., GROSSI, C. M., KEANE, P. A., KO, F., LOTERY, A., PETO, T., REISMAN, C. A., STROUTHIDIS, N. G. & YANG, Q. 2016. Spectral-Domain Optical Coherence Tomography Imaging in 67 321 Adults: Associations with Macular Thickness in the UK Biobank Study. *Ophthalmology*, 123, 829-40.
- PAULEIKHOFF, D., BARONDES, M. J., MINASSIAN, D., CHISHOLM, I. H. & BIRD, A. C. 1990a. Drusen as risk factors in age-related macular disease. *Am J Ophthalmol*, 109, 38-43.
- PAULEIKHOFF, D., HARPER, C. A., MARSHALL, J. & BIRD, A. C. 1990b. Aging changes in Bruch's membrane. A histochemical and morphologic study. *Ophthalmology*, 97, 171-8.
- PENFOLD, P. L., MADIGAN, M. C., GILLIES, M. C. & PROVIS, J. M. 2001. Immunological and aetiological aspects of macular degeneration. *Prog Retin Eye Res*, 20, 385-414.
- PETZOLD, A., BALCER, L. J., CALABRESI, P. A., COSTELLO, F., FROHMAN, T. C., FROHMAN, E. M., MARTINEZ-LAPISCINA, E. H., GREEN, A. J., KARDON, R., OUTTERYCK, O., PAUL, F., SCHIPPLING, S., VERMERSCH, P., VILLOSLADA, P. & BALK, L. J. 2017. Retinal layer segmentation in multiple sclerosis: a systematic review and meta-analysis. *Lancet Neurol*, 16, 797-812.
- PIERAMICI, D. J. & BRESSLER, S. B. 1998. Age-related macular degeneration and risk factors for the development of choroidal neovascularization in the fellow eye. *Curr Opin Ophthalmol*, 9, 38-46.
- PIERRO, L., GIATSIDIS, S. M., MANTOVANI, E. & GAGLIARDI, M. 2010. Macular thickness interoperator and intraoperator reproducibility in healthy eyes using 7 optical coherence tomography instruments. *Am J Ophthalmol*, 150, 199-204.e1.
- PILAT, A. V., PROUDLOCK, F. A., MOHAMMAD, S. & GOTTLÖB, I. 2014. Normal macular structure measured with optical coherence tomography across ethnicity. *Br J Ophthalmol*, 98, 941-5.
- POSTEL, E. A., AGARWAL, A., CALDWELL, J., GALLINS, P., TOTH, C., SCHMIDT, S., SCOTT, W. K., HAUSER, M. A., HAINES, J. L. & PERICAK-VANCE, M. A. 2006. Complement factor H increases risk for atrophic age-related macular degeneration. *Ophthalmology*, 113, 1504-7.
- POTSAID, B., GORCZYNSKA, I., SRINIVASAN, V. J., CHEN, Y., JIANG, J., CABLE, A. & FUJIMOTO, J. G. 2008. Ultrahigh speed spectral / Fourier domain OCT ophthalmic imaging at 70,000 to 312,500 axial scans per second. *Opt Express*, 16, 15149-69.
- PULIAFITO, C. A., HEE, M. R., LIN, C. P., REICHEL, E., SCHUMAN, J. S., DUKER, J. S., IZATT, J. A., SWANSON, E. A. & FUJIMOTO, J. G. 1995. Imaging of macular diseases with optical coherence tomography. *Ophthalmology*, 102, 217-229.
- QUERQUES, G., CANOUI-POITRINE, F., COSCAS, F., MASSAMBA, N., QUERQUES, L., MIMOUN, G., BANDELLO, F. & SOUIED, E. H. 2012. Analysis of progression of reticular pseudodrusen by spectral domain-optical coherence tomography. *Invest Ophthalmol Vis Sci*, 53, 1264-70.
- QUERQUES, G., GEORGES, A., BEN MOUSSA, N., STERKERS, M. & SOUIED, E. H. 2014. Appearance of regressing drusen on optical coherence tomography in age-related macular degeneration. *Ophthalmology*, 121, 173-9.
- RATTANI, A. & DERAKHSHANI, R. On fine-tuning convolutional neural networks for smartphone based ocular recognition. Biometrics (IJCB), 2017 IEEE International Joint Conference on, 2017. IEEE, 762-767.
- REITER, G. S., TOLD, R., SCHLANITZ, F. G., BAUMANN, L., SCHMIDT-ERFURTH, U. & SACU, S. 2019. Longitudinal Association Between Drusen Volume and Retinal Capillary Perfusion in Intermediate Age-Related Macular Degeneration. *Invest Ophthalmol Vis Sci*, 60, 2503-2508.
- REPKA, M. X. & QUIGLEY, H. A. 1989. The effect of age on normal human optic nerve fiber number and diameter. *Ophthalmology*, 96, 26-32.

- RESNIKOFF, S., PASCOLINI, D., ETYA'ALE, D., KOCUR, I., PARARAJASEGARAM, R., POKHAREL, G. P. & MARIOTTI, S. P. 2004. Global data on visual impairment in the year 2002. *Bull World Health Organ*, 82, 844-51.
- RODRIGUEZ, I. R. & LARRAYOZ, I. M. 2010. Cholesterol oxidation in the retina: implications of 7KCh formation in chronic inflammation and age-related macular degeneration. *J Lipid Res*, 51, 2847-62.
- ROISMAN, L., ZHANG, Q., WANG, R. K., GREGORI, G., ZHANG, A., CHEN, C. L., DURBIN, M. K., AN, L., STETSON, P. F., ROBBINS, G., MILLER, A., ZHENG, F. & ROSENFELD, P. J. 2016. Optical Coherence Tomography Angiography of Asymptomatic Neovascularization in Intermediate Age-Related Macular Degeneration. *Ophthalmology*, 123, 1309-19.
- RONNEBERGER O., F. P., BROX T. . U-Net: Convolutional Networks for Biomedical Image Segmentation. MICCAI, 2015. Springer, 234-241.
- ROSENFELD, P. J. 2016. Optical Coherence Tomography and the Development of Antiangiogenic Therapies in Neovascular Age-Related Macular Degeneration. *Invest Ophthalmol Vis Sci*, 57, Oct14-26.
- ROSENFELD, P. J., BROWN, D. M., HEIER, J. S., BOYER, D. S., KAISER, P. K., CHUNG, C. Y. & KIM, R. Y. 2006. Ranibizumab for neovascular age-related macular degeneration. *N Engl J Med*, 355, 1419-31.
- ROY, M. & KAISER-KUPFER, M. 1990. Second eye involvement in age-related macular degeneration: a four-year prospective study. *Eye (Lond)*, 4 (Pt 6), 813-8.
- RUDOLF, M., CLARK, M. E., CHIMENTO, M. F., LI, C. M., MEDEIROS, N. E. & CURCIO, C. A. 2008. Prevalence and morphology of druse types in the macula and periphery of eyes with age-related maculopathy. *Invest Ophthalmol Vis Sci*, 49, 1200-9.
- SAADE, C. & SMITH, R. T. 2014. Reticular macular lesions: a review of the phenotypic hallmarks and their clinical significance. *Clin Exp Ophthalmol*, 42, 865-74.
- SADIGH, S., CIDECIYAN, A. V., SUMAROKA, A., HUANG, W. C., LUO, X., SWIDER, M., STEINBERG, J. D., STAMBOLIAN, D. & JACOBSON, S. G. 2013. Abnormal thickening as well as thinning of the photoreceptor layer in intermediate age-related macular degeneration. *Invest Ophthalmol Vis Sci*, 54, 1603-12.
- SADIGH, S., LUO, X., CIDECIYAN, A. V., SUMAROKA, A., BOXLEY, S. L., HALL, L. M., SHEPLOCK, R., FEUER, W. J., STAMBOLIAN, D. S. & JACOBSON, S. G. 2015. Drusen and photoreceptor abnormalities in African-Americans with intermediate non-neovascular age-related macular degeneration. *Curr Eye Res*, 40, 398-406.
- SANDBERG, M. A., WEINER, A., MILLER, S. & GAUDIO, A. R. 1998. High-risk characteristics of fellow eyes of patients with unilateral neovascular age-related macular degeneration. *Ophthalmology*, 105, 441-7.
- SARKS, J. P., SARKS, S. H. & KILLINGSWORTH, M. C. 1994. Evolution of soft drusen in age-related macular degeneration. *Eye (Lond)*, 8 (Pt 3), 269-83.
- SATO, T., KISHI, S., WATANABE, G., MATSUMOTO, H. & MUKAI, R. 2007. Tomographic features of branching vascular networks in polypoidal choroidal vasculopathy. *Retina*, 27, 589-94.
- SAVASTANO, M. C., MINNELLA, A. M., TAMBURRINO, A., GIOVINCO, G., VENTRE, S. & FALSINI, B. 2014. Differential vulnerability of retinal layers to early age-related macular degeneration: evidence by SD-OCT segmentation analysis. *Invest Ophthalmol Vis Sci*, 55, 560-6.
- SCHAAL, K. B., ROSENFELD, P. J., GREGORI, G., YEHOOSHUA, Z. & FEUER, W. J. 2016. Anatomic Clinical Trial Endpoints for Nonexudative Age-Related Macular Degeneration. *Ophthalmology*, 123, 1060-79.
- SCHACHAT, A. P., HYMAN, L., LESKE, M. C., CONNELL, A. M. & WU, S. Y. 1995. Features of age-related macular degeneration in a black population. The Barbados Eye Study Group. *Arch Ophthalmol*, 113, 728-35.

- SCHLANITZ, F. G., AHLERS, C., SACU, S., SCHUTZE, C., RODRIGUEZ, M., SCHRIEFL, S., GOLBAZ, I., SPALEK, T., STOCK, G. & SCHMIDT-ERFURTH, U. 2010. Performance of drusen detection by spectral-domain optical coherence tomography. *Invest Ophthalmol Vis Sci*, 51, 6715-21.
- SCHLANITZ, F. G., BAUMANN, B., KUNDI, M., SACU, S., BARATSITS, M., SCHESCHY, U., SHAHLAEE, A., MITTERMULLER, T. J., MONTUORO, A., ROBERTS, P., PIRCHER, M., HITZENBERGER, C. K. & SCHMIDT-ERFURTH, U. 2017. Drusen volume development over time and its relevance to the course of age-related macular degeneration. *Br J Ophthalmol*, 101, 198-203.
- SCHLANITZ, F. G., BAUMANN, B., SPALEK, T., SCHUTZE, C., AHLERS, C., PIRCHER, M., GOTZINGER, E., HITZENBERGER, C. K. & SCHMIDT-ERFURTH, U. 2011. Performance of automated drusen detection by polarization-sensitive optical coherence tomography. *Invest Ophthalmol Vis Sci*, 52, 4571-9.
- SCHMIDT-ERFURTH, U., WALDSTEIN, S. M., KLIMSCHA, S., SADEGHIPOUR, A., HU, X., GERENDAS, B. S., OSBORNE, A. & BOGUNOVIC, H. 2018. Prediction of Individual Disease Conversion in Early AMD Using Artificial Intelligence. *Invest Ophthalmol Vis Sci*, 59, 3199-3208.
- SCHNEIDER, U., GELISKEN, F., INHOFFEN, W. & KREISSIG, I. 1997. Indocyanine green angiographic findings in fellow eyes of patients with unilateral occult neovascular age-related macular degeneration. *Int Ophthalmol*, 21, 79-85.
- SCHUMAN, S. G., KOREISHI, A. F., FARSIU, S., JUNG, S. H., IZATT, J. A. & TOTH, C. A. 2009. Photoreceptor layer thinning over drusen in eyes with age-related macular degeneration imaged in vivo with spectral-domain optical coherence tomography. *Ophthalmology*, 116, 488-496.e2.
- SEDDON, J. M., AJANI, U. A. & MITCHELL, B. D. 1997. Familial aggregation of age-related maculopathy. *Am J Ophthalmol*, 123, 199-206.
- SEDDON, J. M., COTE, J., PAGE, W. F., AGGEN, S. H. & NEALE, M. C. 2005. The US twin study of age-related macular degeneration: relative roles of genetic and environmental influences. *Arch Ophthalmol*, 123, 321-7.
- SEDDON, J. M., REYNOLDS, R., SHAH, H. R. & ROSNER, B. 2011. Smoking, dietary betaine, methionine, and vitamin D in monozygotic twins with discordant macular degeneration: epigenetic implications. *Ophthalmology*, 118, 1386-94.
- SEDDON, J. M., SHARMA, S. & ADELMAN, R. A. 2006. Evaluation of the clinical age-related maculopathy staging system. *Ophthalmology*, 113, 260-6.
- SEDDON, J. M., WILLETT, W. C., SPEIZER, F. E. & HANKINSON, S. E. 1996. A prospective study of cigarette smoking and age-related macular degeneration in women. *Jama*, 276, 1141-6.
- SHELLEY, E. J., MADIGAN, M. C., NATOLI, R., PENFOLD, P. L. & PROVIS, J. M. 2009a. Cone degeneration in aging and age-related macular degeneration. *Arch Ophthalmol*, 127, 483-92.
- SHELLEY, E. J., MADIGAN, M. C., NATOLI, R., PENFOLD, P. L. & PROVIS, J. M. 2009b. Cone degeneration in aging and age-related macular degeneration. *Archives of Ophthalmology*, 127, 483-492.
- SHIN, D. S., JAVORNIK, N. B. & BERGER, J. W. 1999. Computer-assisted, interactive fundus image processing for macular drusen quantitation. *Ophthalmology*, 106, 1119-25.
- SILVA, R., CACHULO, M. L., FONSECA, P., BERNARDES, R., NUNES, S., VILHENA, N. & FARIA DE ABREU, J. R. 2011. Age-Related Macular Degeneration and Risk Factors for the Development of Choroidal Neovascularisation in the Fellow Eye: A 3-Year Follow-Up Study. *Ophthalmologica*, 226, 110-118.
- SIMONYAN, K. & ZISSERMAN, A. 2014. Very deep convolutional networks for large-scale image recognition. *arXiv preprint arXiv:1409.1556*.
- SIVAPRASAD, S., BIRD, A., NITIAHPAPAND, R., NICHOLSON, L., HYKIN, P. & CHATZIRALLI, I. 2016. Perspectives on reticular pseudodrusen in age-related macular degeneration. *Surv Ophthalmol*, 61, 521-37.

- SIVAPRASAD, S., MEMBREY, W. L., SIVAGNANAVEL, V., GONZALEZ, J. G., LIU, D. T., CHAN, W. M., LAM, D. S., JACKSON, H. & CHONG, N. V. 2006. Second eye of patients with unilateral neovascular age-related macular degeneration: Caucasians vs Chinese. *Eye (Lond)*, 20, 923-6.
- SKEIE, J. M. & MULLINS, R. F. 2009. Macrophages in neovascular age-related macular degeneration: friends or foes? *Eye (Lond)*, 23, 747-55.
- SMITH, R. T., CHAN, J. K., NAGASAKI, T., SPARROW, J. R. & BARBAZETTO, I. 2005. A method of drusen measurement based on reconstruction of fundus background reflectance. *British Journal of Ophthalmology*, 89, 87-91.
- SMITH, W., ASSINK, J., KLEIN, R., MITCHELL, P., KLAVER, C. C., KLEIN, B. E., HOFMAN, A., JENSEN, S., WANG, J. J. & DE JONG, P. T. 2001. Risk factors for age-related macular degeneration: Pooled findings from three continents. *Ophthalmology*, 108, 697-704.
- SMITH, W., MITCHELL, P. & LEEDER, S. R. 1996. Smoking and age-related maculopathy. The Blue Mountains Eye Study. *Arch Ophthalmol*, 114, 1518-23.
- SMITH, W., MITCHELL, P., LEEDER, S. R. & WANG, J. J. 1998. Plasma fibrinogen levels, other cardiovascular risk factors, and age-related maculopathy: the Blue Mountains Eye Study. *Arch Ophthalmol*, 116, 583-7.
- SMITH, W., MITCHELL, P. & WANG, J. J. 1997. Gender, oestrogen, hormone replacement and age-related macular degeneration: results from the Blue Mountains Eye Study. *Aust N Z J Ophthalmol*, 25 Suppl 1, S13-5.
- SOLOMON, S. D., JEFFERYS, J. L., HAWKINS, B. S. & BRESSLER, N. M. 2007. Incident choroidal neovascularization in fellow eyes of patients with unilateral subfoveal choroidal neovascularization secondary to age-related macular degeneration: SST report No. 20 from the Submacular Surgery Trials Research Group. *Arch Ophthalmol*, 125, 1323-30.
- SOMMER, A., TIELSCH, J. M., KATZ, J., QUIGLEY, H. A., GOTTSCH, J. D., JAVITT, J. C., MARTONE, J. F., ROYALL, R. M., WITT, K. A. & EZRINE, S. 1991. Racial differences in the cause-specific prevalence of blindness in east Baltimore. *N Engl J Med*, 325, 1412-7.
- SONG, W. K., LEE, S. C., LEE, E. S., KIM, C. Y. & KIM, S. S. 2010. Macular thickness variations with sex, age, and axial length in healthy subjects: a spectral domain-optical coherence tomography study. *Invest Ophthalmol Vis Sci*, 51, 3913-8.
- SPAIDE, R. F. 2004. Fundus Angiography. *Age-related macular degeneration*. Berlin, Heidelberg: Springer Berlin Heidelberg.
- SPAIDE, R. F. 2009. Enhanced depth imaging optical coherence tomography of retinal pigment epithelial detachment in age-related macular degeneration. *Am J Ophthalmol*, 147, 644-52.
- SPAIDE, R. F. 2013. Outer retinal atrophy after regression of subretinal drusenoid deposits as a newly recognized form of late age-related macular degeneration. *Retina*, 33, 1800-8.
- SPAIDE, R. F. & CURCIO, C. A. 2010. Drusen characterization with multimodal imaging. *Retina*, 30, 1441-54.
- SPERDUTO, R. D. & HILLER, R. 1986. Systemic hypertension and age-related maculopathy in the Framingham Study. *Arch Ophthalmol*, 104, 216-9.
- SPRAUL, C. W., LANG, G. E. & GROSSNIKLAUS, H. E. 1996. Morphometric analysis of the choroid, Bruch's membrane, and retinal pigment epithelium in eyes with age-related macular degeneration. *Invest Ophthalmol Vis Sci*, 37, 2724-35.
- SRINIVASAN, V. J., KO, T. H., WOJTKOWSKI, M., CARVALHO, M., CLERMONT, A., BURSELL, S.-E., SONG, Q. H., LEM, J., DUKER, J. S. & SCHUMAN, J. S. 2006a. Noninvasive volumetric imaging and morphometry of the rodent retina with high-speed, ultrahigh-resolution optical coherence tomography. *Investigative ophthalmology & visual science*, 47, 5522-5528.
- SRINIVASAN, V. J., MONSON, B. K., WOJTKOWSKI, M., BILONICK, R. A., GORCZYNSKA, I., CHEN, R., DUKER, J. S., SCHUMAN, J. S. & FUJIMOTO, J. G. 2008. Characterization of outer retinal morphology with high-speed, ultrahigh-resolution optical coherence tomography. *Invest Ophthalmol Vis Sci*, 49, 1571-9.

- SRINIVASAN, V. J., WOJTKOWSKI, M., WITKIN, A. J., DUKER, J. S., KO, T. H., CARVALHO, M., SCHUMAN, J. S., KOWALCZYK, A. & FUJIMOTO, J. G. 2006b. High-definition and 3-dimensional imaging of macular pathologies with high-speed ultrahigh-resolution optical coherence tomography. *Ophthalmology*, 113, 2054 e1-14.
- STAURENGHI, G., SADDA, S., CHAKRAVARTHY, U. & SPAIDE, R. F. 2014. Proposed lexicon for anatomic landmarks in normal posterior segment spectral-domain optical coherence tomography: the IN*OCT consensus. *Ophthalmology*, 121, 1572-8.
- STEVENS, T. S., BRESSLER, N. M., MAGUIRE, M. G., BRESSLER, S. B., FINE, S. L., ALEXANDER, J., PHILLIPS, D. A., MARGHERIO, R. R., MURPHY, P. L. & SCHACHAT, A. P. 1997. Occult choroidal neovascularization in age-related macular degeneration. A natural history study. *Arch Ophthalmol*, 115, 345-50.
- STRETTOI, E., PORCIATTI, V., FALSINI, B., PIGNATELLI, V. & ROSSI, C. 2002. Morphological and functional abnormalities in the inner retina of the rd/rd mouse. *J Neurosci*, 22, 5492-504.
- SUBHI, Y., FORSHAW, T. & SORENSEN, T. L. 2016. Macular thickness and volume in the elderly: A systematic review. *Ageing Res Rev*, 29, 42-9.
- SULLIVAN, R. K., WOLDEMUSSIE, E. & POW, D. V. 2007. Dendritic and synaptic plasticity of neurons in the human age-related macular degeneration retina. *Invest Ophthalmol Vis Sci*, 48, 2782-91.
- TAARNHOJ, N. C., MUNCH, I. C., SANDER, B., KESSEL, L., HOUGAARD, J. L., KYVIK, K., SORENSEN, T. I. & LARSEN, M. 2008. Straight versus tortuous retinal arteries in relation to blood pressure and genetics. *Br J Ophthalmol*, 92, 1055-60.
- TAN, J., YANG, Y., JIANG, H., LIU, C., DENG, Z., LAM, B. L., HU, L., OAKLEY, J. & WANG, J. 2016. The measurement repeatability using different partition methods of intraretinal tomographic thickness maps in healthy human subjects. *Clin Ophthalmol*, 10, 2403-2415.
- TARIQ, A., MAHROO, O. A., WILLIAMS, K. M., LIEW, S. H., BEATTY, S., GILBERT, C. E., VAN KUIJK, F. J. & HAMMOND, C. J. 2014. The heritability of the ring-like distribution of macular pigment assessed in a twin study. *Invest Ophthalmol Vis Sci*, 55, 2214-9.
- TAYLOR, H. R., MUNOZ, B., WEST, S., BRESSLER, N. M., BRESSLER, S. B. & ROSENTHAL, F. S. 1990. Visible light and risk of age-related macular degeneration. *Trans Am Ophthalmol Soc*, 88, 163-73; discussion 173-8.
- TERRY, L., CASSELS, N., LU, K., ACTON, J. H., MARGRAIN, T. H., NORTH, R. V., FERGUSON, J., WHITE, N. & WOOD, A. 2016. Automated Retinal Layer Segmentation Using Spectral Domain Optical Coherence Tomography: Evaluation of Inter-Session Repeatability and Agreement between Devices. *PLoS One*, 11, e0162001.
- THE AGE-RELATED EYE DISEASE STUDY RESEARCH, G. 2001. The age-related eye disease study system for classifying age-related macular degeneration from stereoscopic color fundus photographs: the age-related eye disease study report number 6. *American Journal of Ophthalmology*, 132, 668-681.
- TOMANY, S. C., CRUICKSHANKS, K. J., KLEIN, R., KLEIN, B. E. & KNUDTSON, M. D. 2004. Sunlight and the 10-year incidence of age-related maculopathy: the Beaver Dam Eye Study. *Arch Ophthalmol*, 122, 750-7.
- TOTAN, Y., YAGCI, R., BARDAK, Y., OZYURT, H., KENDIR, F., YILMAZ, G., SAHIN, S. & SAHIN TIG, U. 2009. Oxidative macromolecular damage in age-related macular degeneration. *Curr Eye Res*, 34, 1089-93.
- TOTH, C. A., NARAYAN, D. G., BOPPART, S. A., HEE, M. R., FUJIMOTO, J. G., BIRNGRUBER, R., CAIN, C. P., DICARLO, C. D. & ROACH, W. P. 1997. A comparison of retinal morphology viewed by optical coherence tomography and by light microscopy. *Arch Ophthalmol*, 115, 1425-8.
- TOTO, L., BORRELLI, E., DI ANTONIO, L., CARPINETO, P. & MASTROPASQUA, R. 2016. RETINAL VASCULAR PLEXUSES' CHANGES IN DRY AGE-RELATED MACULAR DEGENERATION, EVALUATED BY MEANS OF OPTICAL COHERENCE TOMOGRAPHY ANGIOGRAPHY. *Retina*, 36, 1566-72.

- TOTO, L., BORRELLI, E., MASTROPASQUA, R., DI ANTONIO, L., DORONZO, E., CARPINETO, P. & MASTROPASQUA, L. 2017. Association between outer retinal alterations and microvascular changes in intermediate stage age-related macular degeneration: an optical coherence tomography angiography study. *Br J Ophthalmol*, 101, 774-779.
- UGARTE, M., HUSSAIN, A. A. & MARSHALL, J. 2006. An experimental study of the elastic properties of the human Bruch's membrane-choroid complex: relevance to ageing. *Br J Ophthalmol*, 90, 621-6.
- VAN DEEMTER, M., PONSIOEN, T. L., BANK, R. A., SNABEL, J. M., VAN DER WORP, R. J., HOOYMANS, J. M. & LOS, L. I. 2009. Pentosidine accumulates in the aging vitreous body: a gender effect. *Exp Eye Res*, 88, 1043-50.
- VAN DER SCHAFT, T. L., MOOY, C. M., DE BRUIJN, W. C., ORON, F. G., MULDER, P. G. & DE JONG, P. T. 1992a. Histologic features of the early stages of age-related macular degeneration. A statistical analysis. *Ophthalmology*, 99, 278-86.
- VAN DER SCHAFT, T. L., MOOY, C. M., DE BRUIJN, W. C., ORON, F. G., MULDER, P. G. H. & DE JONG, P. T. V. M. 1992b. Histologic Features of the Early Stages of Age-related Macular Degeneration. *Ophthalmology*, 99, 278-286.
- VAN LEEUWEN, R., KLAVER, C. C., VINGERLING, J. R., HOFMAN, A. & DE JONG, P. T. 2003. Epidemiology of age-related maculopathy: a review. *Eur J Epidemiol*, 18, 845-54.
- VENZA, I., VISALLI, M., CUCINOTTA, M., TETI, D. & VENZA, M. 2012. Association between oxidative stress and macromolecular damage in elderly patients with age-related macular degeneration. *Ageing Clin Exp Res*, 24, 21-7.
- VERGMANN, A. S., BROE, R., KESSEL, L., HOUGAARD, J. L., MOLLER, S., KYVIK, K. O., LARSEN, M., MUNCH, I. C. & GRAUSLUND, J. 2017. Heritability of Retinal Vascular Fractals: A Twin Study. *Invest Ophthalmol Vis Sci*, 58, 3997-4002.
- VILLEGAS-PEREZ, M. P., LAWRENCE, J. M., VIDAL-SANZ, M., LAVAIL, M. M. & LUND, R. D. 1998. Ganglion cell loss in RCS rat retina: a result of compression of axons by contracting intraretinal vessels linked to the pigment epithelium. *J Comp Neurol*, 392, 58-77.
- VINDING, T. 1990. Pigmentation of the eye and hair in relation to age-related macular degeneration. An epidemiological study of 1000 aged individuals. *Acta Ophthalmol (Copenh)*, 68, 53-8.
- VISSCHER, P. M., HILL, W. G. & WRAY, N. R. 2008. Heritability in the genomics era--concepts and misconceptions. *Nat Rev Genet*, 9, 255-66.
- WAGNER-SCHUMAN, M., DUBIS, A. M., NORDGREN, R. N., LEI, Y., ODELL, D., CHIAO, H., WEH, E., FISCHER, W., SULAI, Y., DUBRA, A. & CARROLL, J. 2011. Race- and sex-related differences in retinal thickness and foveal pit morphology. *Invest Ophthalmol Vis Sci*, 52, 625-34.
- WANG, J., GAO, X., HUANG, W., WANG, W., CHEN, S., DU, S., LI, X. & ZHANG, X. 2015. Swept-source optical coherence tomography imaging of macular retinal and choroidal structures in healthy eyes. *BMC Ophthalmol*, 15, 122.
- WANG, J. J., FORAN, S., SMITH, W. & MITCHELL, P. 2003. Risk of age-related macular degeneration in eyes with macular drusen or hyperpigmentation: the Blue Mountains Eye Study cohort. *Arch Ophthalmol*, 121, 658-63.
- WANG, J. J., MITCHELL, P. & SMITH, W. 1998. Refractive error and age-related maculopathy: the Blue Mountains Eye Study. *Invest Ophthalmol Vis Sci*, 39, 2167-71.
- WANG, J. J., ROCHTCHINA, E., LEE, A. J., CHIA, E. M., SMITH, W., CUMMING, R. G. & MITCHELL, P. 2007. Ten-year incidence and progression of age-related maculopathy: the blue Mountains Eye Study. *Ophthalmology*, 114, 92-8.
- WASSELL, J., DAVIES, S., BARDSLEY, W. & BOULTON, M. 1999. The photoreactivity of the retinal age pigment lipofuscin. *J Biol Chem*, 274, 23828-32.
- WEITER, J. J., DELORI, F. C., WING, G. L. & FITCH, K. A. 1985. Relationship of senile macular degeneration to ocular pigmentation. *Am J Ophthalmol*, 99, 185-7.
- WINTERGERST, M. W. M., SCHULTZ, T., BIRTEL, J., SCHUSTER, A. K., PFEIFFER, N., SCHMITZ-VALCKENBERG, S., HOLZ, F. G. & FINGER, R. P. 2017. Algorithms for the Automated Analysis

- of Age-Related Macular Degeneration Biomarkers on Optical Coherence Tomography: A Systematic Review. *Transl Vis Sci Technol*, 6, 10.
- WOJTKOWSKI, M., LEITGEB, R., KOWALCZYK, A., BAJRASZEWSKI, T. & FERCHER, A. F. 2002. In vivo human retinal imaging by Fourier domain optical coherence tomography. *J Biomed Opt*, 7, 457-63.
- WOJTKOWSKI, M., SRINIVASAN, V., FUJIMOTO, J. G., KO, T., SCHUMAN, J. S., KOWALCZYK, A. & DUKER, J. S. 2005. Three-dimensional retinal imaging with high-speed ultrahigh-resolution optical coherence tomography. *Ophthalmology*, 112, 1734-46.
- WONG, R. W., RICHA, D. C., HAHN, P., GREEN, W. R. & DUNAIEF, J. L. 2007. Iron toxicity as a potential factor in AMD. *Retina*, 27, 997-1003.
- WONG, W. L., SU, X., LI, X., CHEUNG, C. M., KLEIN, R., CHENG, C. Y. & WONG, T. Y. 2014. Global prevalence of age-related macular degeneration and disease burden projection for 2020 and 2040: a systematic review and meta-analysis. *Lancet Glob Health*, 2, e106-16.
- WU, Z., LUU, C. D., AYTON, L. N., GOH, J. K., LUCCI, L. M., HUBBARD, W. C., HAGEMAN, J. L., HAGEMAN, G. S. & GUYMER, R. H. 2014. Optical Coherence Tomography-Defined Changes Preceding the Development of Drusen-Associated Atrophy in Age-Related Macular Degeneration. *Ophthalmology*, 121, 2415-2422.
- XU, H., CHEN, M. & FORRESTER, J. V. 2009. Para-inflammation in the aging retina. *Prog Retin Eye Res*, 28, 348-68.
- YAMADA, Y., ISHIBASHI, K., ISHIBASHI, K., BHUTTO, I. A., TIAN, J., LUTTY, G. A. & HANDA, J. T. 2006. The expression of advanced glycation endproduct receptors in rpe cells associated with basal deposits in human maculas. *Exp Eye Res*, 82, 840-8.
- YEHOOSHUA, Z., GREGORI, G., SADDA, S. R., PENHA, F. M., GOLDHARDT, R., NITTALA, M. G., KONDURU, R. K., FEUER, W. J., GUPTA, P., LI, Y. & ROSENFELD, P. J. 2013. Comparison of drusen area detected by spectral domain optical coherence tomography and color fundus imaging. *Invest Ophthalmol Vis Sci*, 54, 2429-34.
- YEHOOSHUA, Z., WANG, F., ROSENFELD, P. J., PENHA, F. M., FEUER, W. J. & GREGORI, G. 2011. Natural history of drusen morphology in age-related macular degeneration using spectral domain optical coherence tomography. *Ophthalmology*, 118, 2434-41.
- YENICE, E., SENGUN, A., SOYUGELLEN DEMIROK, G. & TURACLI, E. 2015. Ganglion cell complex thickness in nonexudative age-related macular degeneration. *Eye (Lond)*, 29, 1076-80.
- YI, K., MUJAT, M., PARK, B. H., SUN, W., MILLER, J. W., SEDDON, J. M., YOUNG, L. H., DE BOER, J. F. & CHEN, T. C. 2009. Spectral domain optical coherence tomography for quantitative evaluation of drusen and associated structural changes in non-neovascular age-related macular degeneration. *Br J Ophthalmol*, 93, 176-81.
- YOSHIMINE, S., OGAWA, S., HORIGUCHI, H., TERAOKA, M., MIYAZAKI, A., MATSUMOTO, K., TSUNEOKA, H., NAKANO, T., MASUDA, Y. & PESTILLI, F. 2018. Age-related macular degeneration affects the optic radiation white matter projecting to locations of retinal damage. *Brain Struct Funct*, 223, 3889-3900.
- YU, D. Y. & CRINGLE, S. J. 2001. Oxygen distribution and consumption within the retina in vascularised and avascular retinas and in animal models of retinal disease. *Prog Retin Eye Res*, 20, 175-208.
- ZAREPARSI, S., BRANHAM, K. E., LI, M., SHAH, S., KLEIN, R. J., OTT, J., HOH, J., ABECASIS, G. R. & SWAROOP, A. 2005a. Strong association of the Y402H variant in complement factor H at 1q32 with susceptibility to age-related macular degeneration. *Am J Hum Genet*, 77, 149-53.
- ZAREPARSI, S., BURACZYNSKA, M., BRANHAM, K. E., SHAH, S., ENG, D., LI, M., PAWAR, H., YASHAR, B. M., MOROI, S. E., LICHTER, P. R., PETTY, H. R., RICHARDS, J. E., ABECASIS, G. R., ELNER, V. M. & SWAROOP, A. 2005b. Toll-like receptor 4 variant D299G is associated with susceptibility to age-related macular degeneration. *Hum Mol Genet*, 14, 1449-55.
- ZAREPARSI, S., REDDICK, A. C., BRANHAM, K. E., MOORE, K. B., JESSUP, L., THOMS, S., SMITH-WHELOCK, M., YASHAR, B. M. & SWAROOP, A. 2004. Association of apolipoprotein E alleles

- with susceptibility to age-related macular degeneration in a large cohort from a single center. *Invest Ophthalmol Vis Sci*, 45, 1306-10.
- ZARUBINA, A. V., NEELY, D. C., CLARK, M. E., HUISINGH, C. E., SAMUELS, B. C., ZHANG, Y., MCGWIN, G., JR., OWSLEY, C. & CURCIO, C. A. 2016. Prevalence of Subretinal Drusenoid Deposits in Older Persons with and without Age-Related Macular Degeneration, by Multimodal Imaging. *Ophthalmology*, 123, 1090-100.
- ZEILER, M. D. & FERGUS, R. 2013. Visualizing and Understanding Convolutional Networks. *ArXiv e-prints* [Online]. Available: <https://ui.adsabs.harvard.edu/#abs/2013arXiv1311.2901Z> [Accessed November 01, 2013].
- ZEIMER, M., DIETZEL, M., HENSE, H. W., HEIMES, B., AUSTERMANN, U. & PAULEIKHOFF, D. 2012. Profiles of macular pigment optical density and their changes following supplemental lutein and zeaxanthin: new results from the LUNA study. *Invest Ophthalmol Vis Sci*, 53, 4852-9.
- ZUCCHIATTI, I., PARODI, M. B., PIERRO, L., CICINELLI, M. V., GAGLIARDI, M., CASTELLINO, N. & BANDELLO, F. 2015. Macular ganglion cell complex and retinal nerve fiber layer comparison in different stages of age-related macular degeneration. *Am J Ophthalmol*, 160, 602-607.e1.
- ZWEIFEL, S. A., IMAMURA, Y., SPAIDE, T. C., FUJIWARA, T. & SPAIDE, R. F. 2010a. Prevalence and significance of subretinal drusenoid deposits (reticular pseudodrusen) in age-related macular degeneration. *Ophthalmology*, 117, 1775-81.
- ZWEIFEL, S. A., SPAIDE, R. F., CURCIO, C. A., MALEK, G. & IMAMURA, Y. 2010b. Reticular pseudodrusen are subretinal drusenoid deposits. *Ophthalmology*, 117, 303-12.e1.

